Performance Evaluation of a Building Integrated Semi-Transparent Photovoltaic Thermal (BiSPVT) Facade

A Thesis

Submitted in Partial Fulfillment of the requirements for

The Award of the Degree of

DOCTOR OF PHILOSOPHY

By

PUJA HAZARIKA

(Registration number: 196151008)

School of Energy Science and Engineering

Indian Institute of Technology Guwahati

Guwahati-781039, Assam, India

March, 2026

Dedicated to my parents...

Mrs. Ila Hazarika

&

Mr. Jiten Hazarika

DECLARATION

I hereby certify that the work presented in this thesis entitled '***Performance Evaluation of a Building Integrated Semi-Transparent Photovoltaic Thermal (BiSPVT) Facade***' is entirely my own account of research performed under the guidance of Dr. Ankita Gaur and Dr. Pankaj Kalita. Any part of this work has not been submitted earlier for the award of any degree, diploma, fellowship or its equivalent to any University or Institution.

Date: 30 March 2026

Puja Hazarika

Registration number: 196151008

School of Energy Science and Engineering

Indian Institute of Technology Guwahati

School of Energy Science and Engineering

INDIAN INSTITUTE OF TECHNOLOGY GUWAHATI

भारतीय प्रौद्योगिकी संस्थान गुवाहाटी, गुवाहाटी- 781039

CERTIFICATE

This is to certify that the work contained in the thesis entitled '***Performance Evaluation of a Building Integrated Semi-Transparent Photovoltaic Thermal (BiSPVT) Facade***' submitted by **Puja Hazarika,** a student in the School of Energy Science and Engineering, Indian Institute of Technology Guwahati, India for the award of the degree of Doctor of Philosophy has been carried out under our supervision. She has fulfilled all the requirements according to the rules of the institute and the investigations embodied in her thesis have not been submitted elsewhere for the award of any other degree or diploma.

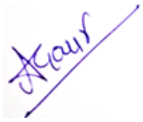

Dr. Ankita Gaur
Ramanujan Fellow
School of Energy Science and Engineering
Indian Institute of Technology Guwahati
Guwahati – 781039

Dr. Pankaj Kalita
Associate Professor
School of Energy Science and Engineering
Indian Institute of Technology Guwahati
Guwahati – 781039

Abstract

The 21st century is marked by unprecedented challenges including climate change, environmental degradation, and the widening gap between growing energy demand and its sustainable supply. Rapid urbanization, population growth, and accelerated economic development have placed immense strain on global energy systems, with the building sector emerging as a major contributor. Buildings currently account for 30% of global final energy use and about 34% of greenhouse gas emissions. This intensifies global warming and its consequences underscoring the urgent need for energy transition strategies centered on decarbonization. Renewable energy, particularly solar, offers a strong solution due to its abundance, inexhaustibility, and compatibility with decentralized building-scale applications.

Within this context, Building Integrated Photovoltaic Thermal (BIPVT) systems have gained prominence by embedding photovoltaics into building envelopes to provide on-site electricity while harvesting thermal energy. A key limitation of conventional PV modules is their temperature dependence: as cell temperature rises, resistive losses increase and voltage output decreases, reducing efficiency. To sustain performance, heat must be extracted when integrated into BIPVT facades, this recovered heat can be repurposed for services such as space heating. Semi-transparent facade-based BiSPVT systems address this dual challenge by improving PV efficiency and supplying usable thermal energy, making them highly suitable for cold climates. However, research to date has paid limited attention to the combined performance, lifecycle sustainability, and optimization of such systems under variable weather. This thesis responds through a comprehensive assessment of a ventilated semi-transparent BiSPVT facade for Srinagar, India.

The study employs a detailed numerical modeling and simulation framework to evaluate annual energy, exergy, and thermal performance. A one-dimensional thermal model was developed using geometric design parameters, meteorological data, and solar incidence calculations for a vertical south-facing surface via the Liu and Jordan method. Heat transfer coefficients and thermal balances were then estimated to determine module temperature profiles, outlet fluid temperature dynamics, and indoor room air temperature across four weather types: clear, hazy, hazy and cloudy, and cloudy, representative of real local climatic conditions.

Results show significant performance benefits of the BiSPVT system. Annual outputs included 121.22 kWh/m² of electricity, 366.23 kWh/m² of thermal energy, and 122.36 kWh/m²

of useful exergy. Seasonal variations highlighted October as the peak month due to favorable solar radiation and ambient conditions. The ventilated cavity reduced PV overheating while delivering heating benefits indoors, maintaining indoor–outdoor temperature differences up to 12.83°C. The overall effective optical efficiency was 78.3% with a heat loss coefficient of 1.422 W m^{-2} K^{-1}, demonstrating robust thermal management.

Exergoeconomic and enviroeconomic analyses confirmed long-term viability. Over a 30-year lifetime at 4% interest, the BiSPVT facade achieved minimal energy and exergy loss ratios, ensuring cost competitiveness against grid electricity. The uniform annualized cost (UAC) was 0.031 $/kWh for thermal and 0.09-0.16 $/kWh for exergy, competitive with current tariffs. Energy Payback Times were 3.2 years (thermal) and 9.8 years (exergy), while Greenhouse Gas Payback Time was 2.5 years, confirming both economic feasibility and sustainability.

From an environmental perspective, the system reduced CO_2 emissions by 2.81 tonnes annually, equivalent to over $40 in avoided costs. Life cycle assessment revealed PV modules and steel framing as major contributors, but total system impact was limited to 0.98 t CO_2-equivalent/m^2, aligning with international benchmarks. Sensitivity analysis further showed that amorphous-Si panels had the lowest overall environmental impact, while single-Si exhibited the highest. These results guide sustainable material choices for building-integrated applications.

The broader significance of this research extends beyond technical optimization. By demonstrating dual benefits of on-site electricity and thermal recovery in cold climates, it positions BiSPVT facades as multifunctional building skins for net-zero architecture. Methodologically, it establishes a replicable framework combining energy, exergy, economic, and life cycle assessment. More broadly, it contributes to global climate action by addressing one of the highest energy-consuming sectors. BiSPVT facades decentralize power generation, reduce grid dependency, enhance energy security in underserved regions, and directly support the United Nations Sustainable Development Goals (SDGs).

Keywords: BiSPVT; Thermal modeling; Energy; Exergy; Exergoeconomic; Enviroeconomic; Life Cycle Assessment (LCA)

Acknowledgment

The completion of this thesis stands not only as a personal endeavor but also as the outcome of the collective support, guidance, and encouragement I have been fortunate to receive along the way. Throughout this journey, I have been indebted to numerous individuals whether through their intellectual contributions, emotional support, or quiet encouragement, many of whom I cannot possibly name in full. Words are insufficient to capture the depth of my gratitude, yet it is with great joy and sincerity that I acknowledge the invaluable role each of them has played in bringing this work to fruition.

Firstly, I take this opportunity to express my sincere appreciation to the Indian Institute of Technology Guwahati for providing me with an excellent research environment. I am especially grateful to my supervisors, Dr. Ankita Gaur and Dr. Pankaj Kalita, for their constant support, encouragement, and active guidance throughout the entire research process. Thanks to their exceptional abilities in organization, planning, and management, I was able to pursue my research goal with utmost determination.

My sincere acknowledgement goes to Prof. Pratima Agarwal, Chairperson of Doctoral committee, for her unwavering encouragement, guidance, and support throughout all stages of my PhD research. I am also indebted to the members of Doctoral Committee, Prof. Sisir Kumar Nayak and Dr. Kuldeep Kumar for their invaluable suggestions about critical issues related to my work.

I express my profound gratitude to the Science and Engineering Research Board (SERB), Government of India, for their invaluable financial support provided through Project Grant number: SB/S2/RJN-055/2018.

I would like to thank Head, faculty members and all the staffs of School of Energy Science and Engineering for their wholehearted support and cooperation throughout my work. I extend my thanks to Dr. Lepakshi Barbora, Mr. Debarshi Baruah and Mr. Dhiren Huzuri for their resolute technical advice and constant support. I am also thankful to Mr. Nabajit Rajbongshi, Mr. Pranjal Bhuyan , Mr. Nayan Jyoti Das for their help in looking into all official documents during the course of my research work.

My gratitude extends to the Dr. Shyam, Assistant Professor, Kirori Mal College, Delhi University for guiding and assisting me at all stages of this research work. Without his time, support and encouragement, this work could not have been accomplished.

I would like to extend my profound appreciation to Dr. Dudul Das, Dr. Samar Das, Dr. Rabindra Kangsha Banik whose resolute support and valuable insights were instrumental in the success of my research. I would also like to express my gratitude to Mr. Biraj Das, Miss Urbashi Bordoloi, Mr. Akash

Dilip Kamble, Miss Priyanka Duarah, Miss Vijaya, Mr. Bitupon Das, for their support and encouragement throughout the doctoral research tenure. I am also grateful to Mr. Mukunda Madhab Khanikar for his encouragement and constant help. I also wish to acknowledge Mr. Gopinath Sengupta, Mr. Jyotisman Pathak, and Dr. Premeshwori Maibam for their kind assistance and motivation, which greatly enriched my research experience.

I am deeply grateful to my friends for their constant support and companionship throughout this journey. My heartfelt thanks to Dr. Sharfaa Hussain and Miss Winky Hazarika for standing by me, always offering reassurance and laughter. Grateful to Miss Pinaz Peemee Ahmed and Miss Ananya Saikia for being the best reminder of balance between effort and ease. I also wish to thank Miss Saswati Sarmah, Miss Sunondini Gogoi and Mr. Manas Pratim Baishya for bringing humor and perspective that made this path lighter and brighter.

I am sincerely thankful to Dr. Sarmistha Baruah and Miss Kakali Borah, who started this journey with me. We have grown together through every phase of our PhD, sharing both challenges and successes, which made the hardest times easier and the best moments more meaningful. They have seen every side of this experience, and I value our shared growth. I am also grateful to Dr. Angana Bhattacharya, a constant source of wisdom and humor, always ready with answers and a witty remark to lift our spirits.

All my love and gratitude go to my parents, Mrs. Ila Hazarika and Mr. Jiten Hazarika for all their unyielding patience and unrelenting support. My mother, who is no longer with us, remains an eternal source of strength and inspiration in everything I pursue. I carry her lessons in resilience and kindness with me always, and I hope I have made her proud through this work. To my father, whose endless patience, and occasional quirks have balanced my academic journey with warmth and perspective, I owe more than words can convey.

My heartfelt thanks go to my sister Mrs. Plabita Hazarika who has been both my fiercest critic and my most loving supporter, truly the best of both worlds and my brother-in-law Mr. Prabir Ranjan Gogoi for his unwavering support and belief. A special acknowledgment goes to my niece, Miss Atreyee Gogoi, whose playful reminders of calling me 'bossy and silly' kept me grounded through stressful days and reminded me of the joy beyond academic pursuits.

Finally, I express my deep sense of gratitude to God, the almighty who gave me patience and strength to complete this work.

Puja

Contents

Nomenclature

Abbreviations

AC	Alternative Current	IEA	International Energy Agency
AHU	Air Handling Unit	IGBC	Indian Green Building Council
ANN	Artificial Neural Network	INR	Indian Rupee
APOS	Allocation at the Point of Substitution	IPCC	Intergovernmental Panel on Climate Change
a-Si	Amorphous silicon	IREDA	Indian Renewable Energy Development Agency
BAPV	building-applied photovoltaic	ISCP	Impact Score of Construction Processes
BIPV	Building Integrated Photovoltaic	ISO	International Organization for Standardization
BIPVT	Building Integrated Photovoltaic Thermal	LCA	Life Cycle Assessment
BiSPVT	Building Integrated Semi-Transparent Photovoltaic	LCCE	Life cycle conversion efficiency
BOS	Balance of System	LCCE	Lifecycle Cost
CAGR	Compound Annual Growth Rate	LCIA	Life Cycle Impact Assessment
CdTe	Cadmium Telluride	LCOE	Levelized Cost of Energy
CED	Cumulative Energy Demand		
CFC - 11	Trichlorofluoromethane	MNRE	Ministry of New and Renewable Energy
CFD	computational fluid dynamics	N	Number of air change per hour
CIGS	Copper Indium Gallium Selenide	NEM	Net metering scheme
CIGS	Copper Indium Gallium Selenide	NER	Net Energy Ratio
CIS	Copper Indium Selenide	NPV	Net Present Value
c-si	Crystalline Silicon	NPV	Net Present Value
DALY	Disability adjusted Life years	NREL	National Renewable Energy Laboratory
DC	Direct current	PbA	Lead acid
DCB	Dichlorobenzene	PCM	Phase Change Material
DSF	Dynamic Shading Facade	PED	Primary Energy Demand
EAHE	Earth-to-Air Heat Exchangers	PV	Photovoltaic
ECBC	Energy Conservation Building Code	PV TSF	Photovoltaic Transparent Shading Facade
ECER	Environmental Cumulative Energy Requirement	PVC	Polyvinyl Chloride

Abbreviations

EI99	Eco-indicator 99	PVT	Photovoltaic thermal
EPBT	Energy Payback Time	ROW	Rest of World
FITs	Feed-in Tariffs	RSME	Root Mean Square Error
GaAs	Gallium Arsenide	RtSPV	Roof top solar photovoltaic system
GHG.	Greenhouse gases	SDGs	Sustainable Development Goals
GLO	Global	Si	Silicon
GPBT	Greenhouse payback time	SIDBI	Small Industries Development Bank of India
GRIHA	Green Rating for Integrated Habitat Assessment	STC	Standard Test Conditions
GST	Goods and Services Tax	UAC	uniform annualized cost
GWP	global warming potential	UN	United Nations
HIT	Heterojunction with Intrinsic Thin Layer	USD	United states dollar
HVAC	Heat Ventilation and Air-Conditioning	UV	Ultraviolet

Notations

T_a	Ambient Temperature (°C)	CH_4	Methane
A_m	Area of PV module (m²)	N	Number of air change per hour
A	Area, m²	V_{oc}	Open circuit voltage (V_{oc})
T_f	Average fluid temperature (°C)	T_{fo}	Outlet fluid temperature (°C)
T_b	Blackened absorber temperature (°C)	U_{bf}	Overall heat transfer coefficient from blackened absorber to fluid W/m²K
CO_2	Carbon dioxide	$U_{t,ma}$	Overall heat transfer coefficient from PV module to ambient W/m²K
h_{bf}	Convective heat transfer coefficient from blackened absorber to fluid	UA_r	Overall heat transfer coefficient from room to ambient air through walls and windows W/m²K
h_{mf}	Convective heat transfer coefficient from PV module to fluid	U	Overall heat transfer coefficient, W/m²K
h	Convective heat transfer coefficient, W/m²K	P	Power, W/m²
I	Current, Amp	P_r	Prandtl number
E_{in}	Embodied Energy	η_{PV}	PV module efficiency (%)
L_{en}	Energy Loss Rate (kWh/m2)	T_m	PV module temperature (°C)

Abbreviations

Z_{CO2}	Enviroeconomic parameter ($/annum)	R_e	Reynolds number
L_{ex}	Exergy loss rate (kWh/m2)	T_r	Room temperature(°C)
E_x	Exergy rate (kWh/m²)	I_{sc}	Short circuit current (I_{sc})
FF	Fill factor	I(t)	Solar radiation intensity (W/m²)
T_{fi}	Inlet fluid temperature	C_a	Specific heat of air, J/kg/K
z_{CO2}	International carbon price (14.5 dollar per ton of CO_2)	C_f	Specific heat of fluid
kg	kilo gram	C	Specific heat, J/kg K
kWh	kilowatt hour	T_o	Standard test condition temperature of PV (°C)
b	Length of air duct (m)	T	Temperature (°C)
$\dot{m}_f$	Mass flow rate of fluid(kg/s)	T_{pv}	Temperature of PV module (°C)
M_a	Mass of air, kg	TWh	Terawatt hour
I_{mp}	Maximum current (Amp)	K	Thermal conductivity (W/mK)
P_{max}	Maximum power (W/m²)	K	Thermal conductivity, W/mK
V_{mp}	Maximum voltage (Volt)	V	Voltage, Volt
MJ	Mega joule	V	Volume of room, m³
MW	Mega watt		
MWp	Megawatt peak		

Greek Symbols

α	Absorptivity	η	Efficiency (%)
β	Packing factor	ζ	Transmittivity
β_o	Temperature coefficient of PV module (%/°C)		

List of Figures

List of Tables

1

Introduction

Chapter Outline:

1.1. Motivation
1.2. Role of renewable energy technologies in the built environment
1.3. BIPV definition and its advantages
1.4. BIPVT and their relevant types
1.5. Performance of BIPVT systems
1.6. Alignment with SDGs
1.7. Objective of the thesis
1.8. Organization of the thesis

CHAPTER 1: INTRODUCTION

1.1 Motivation

Growing populations, expanding economies, and rapid urban development are placing increasing pressure on the planet's environmental and energy systems. These pressures intensify issues such as resource depletion, energy instability, and shifts in the global climate. [1]. Change of climate and global warming bring serious consequences, including higher sea levels, unpredictable rainfall, and more frequent natural disasters. A major driver of global warming is the buildup of greenhouse gases (GHs), and the construction sector is responsible for a substantial share of global energy use and GHG emissions [2]. According to International Energy Agency (IEA), buildings account for about 30% of final energy consumption globally and more than half of electricity consumption (**Fig. 1.1**). Overall, buildings saw the most dramatic increase in the energy consumption from 2023 to 2024, while industry and transport rose more modestly (**Fig. 1.2).** To combat this, various policies aim to transform high-energy-consuming buildings into net-zero energy structures, substituting fossil fuels with renewable sources.

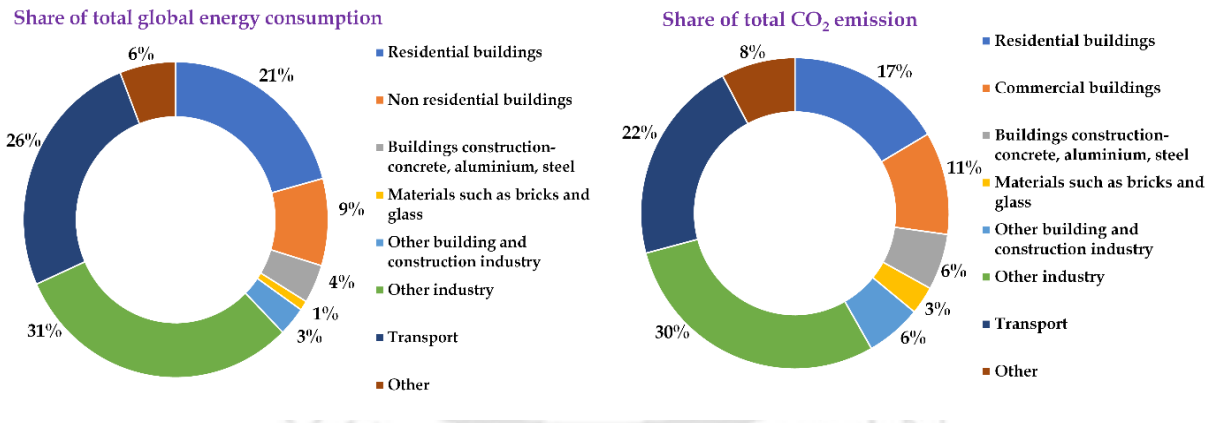

Fig. 1.1 Global energy consumption and emission by sector in 2023 [3]

This growth was driven largely by heightened air-conditioning needs due to extreme heatwaves in countries like India and China, as well as the rising power requirements of new data centres. Such high levels of energy use have a direct impact on greenhouse gas (GHG) emissions, with building operations responsible for about 34% of global GHG output [4]. As nations work toward limiting global warming and reducing carbon emissions, enhancing the energy efficiency of buildings and integrating renewable energy technologies have become essential strategies [5].

To meet this rapidly increasing energy demand, RE sources contributed the largest share to the totaled energy supply growth in 2024, accounting for 38%, followed by 28% for natural gas, 15% for coal at 15%, 11% for oil, and 8% for nuclear. Notably in 2024, the increase in CO_2 emissions related to energy was lowered to 0.8% from 1.2% in 2023, reflecting the growing role of cleaner energy sources in offsetting the carbon intensity of the building sector's escalating energy needs [5].

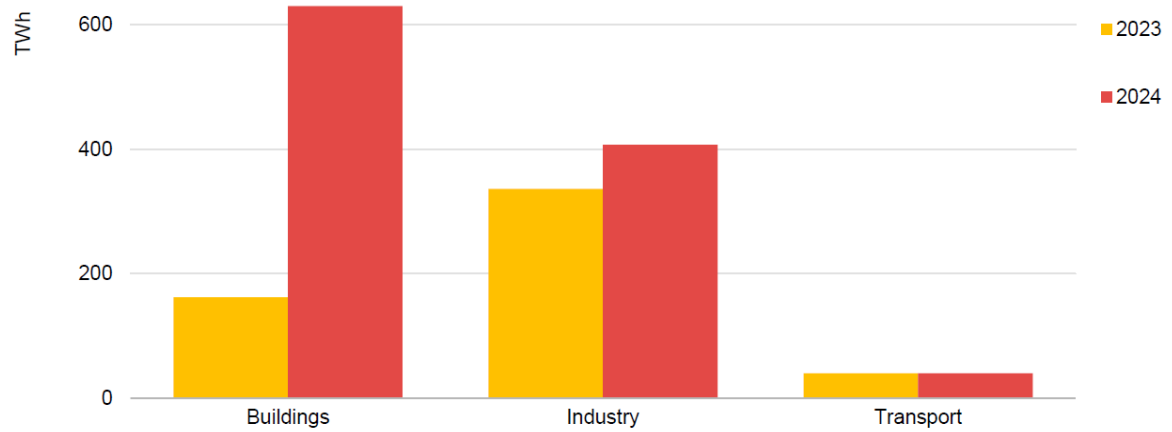

Fig. 1.2 Sector wise Annual consumption of electricity in 2023 and 2024

Over the past decade and a half, the share of renewables in global electricity production has grown substantially. Wind and solar, in particular, have experienced rapid expansion, with both sources collectively increasing their contribution far more than any other energy type. The most pronounced developments were observed in renewable energy sources: wind power increased more than sevenfold, rising from 346 TWh in 2010 to 2,497 TWh in 2024, while solar energy experienced an exceptional surge, expanding from just 32 TWh to 2,130 TWh over the same period - an increase of more than sixty times (**Fig. 1.3**).

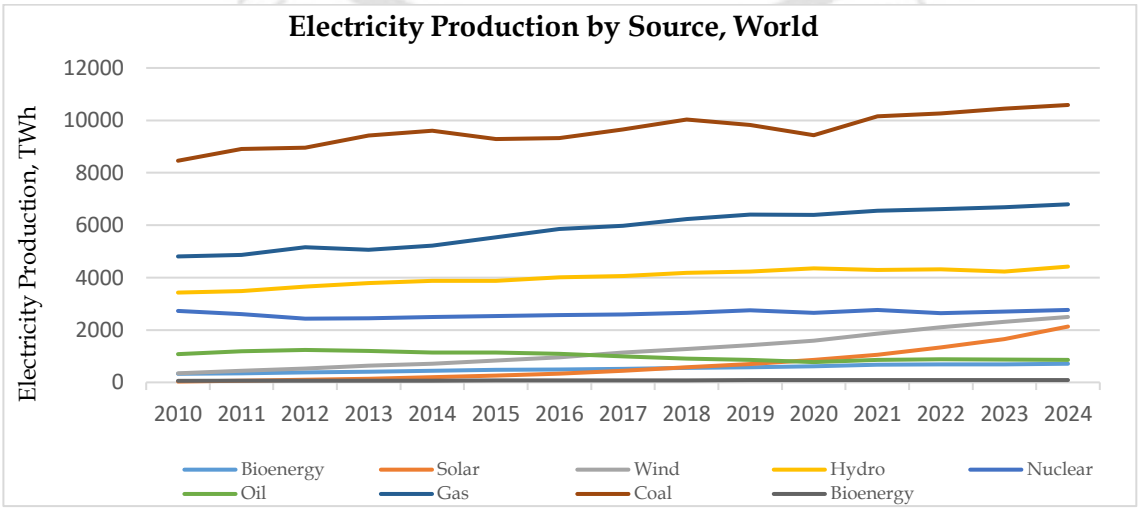

Fig. 1.3 World electricity production by source, 2024

Thus renewables now supported by significant technological advancements represent a much larger portion of the electricity mix compared to earlier years, marking an important step toward a more sustainable energy future [4].

1.2 Role of Renewable Energy technologies in the built environment

Among all earlier renewable technologies, solar power is widely regarded as an endless, extremely clean, and highly plentiful source of energy [6]. The amount of sunlight that reaches the Earth's surface is estimated to be nearly 1.8 × 101 MW, which far exceeds the total global energy needs by several orders of magnitude [7]. To capture and utilize this immense resource, many solar-based systems have been introduced, including solar lighting arrangements, solar-thermal collectors, solar-powered electricity plants, photovoltaic (PV) systems, and various solar-driven hydrogen production methods.

Solar PV technology has emerged as a major pathway for converting sunlight directly into usable electricity, as PV cells transform solar radiation into power through the photovoltaic effect. Over recent decades, PV deployment has expanded significantly progressing from small, individual photovoltaic units to large, grid-connected installations, which now represent over 90% of the world's PV capacity. A newer development within this field is building-integrated photovoltaics (BIPV), which has rapidly gained attention as a modern application of solar PV. BIPV incorporates solar modules directly into building components, replacing conventional materials in elements such as rooftops, windows, walls, balconies, and skylights. In contemporary building projects, PV panels are increasingly being adopted either as part of new construction, especially in facades and roofing or as retrofit elements for existing structures [7]. The primary benefit of BIPV systems, compared to mounted or stand-alone PV setups, is that the integrated components serve several functions at once. Besides generating on-site electricity, they also provide thermal insulation, acoustic protection, weather resistance, privacy benefits, and cost reduction by substituting other building materials. Due to these combined advantages, BIPV is considered one of the most promising renewable technologies for future urban energy solutions.

To promote adoption of BIPV, countries have come up with incentivizing their policies. Germany implemented "The Thousand Solar Roofs Program", the first of its kind scheme to support BIPV installations. The scheme resulted in increase of installed BIPV in the country[8]. The New York State Energy Research and Development Authority (NYSERDA) in 2022 came

up with a scheme to incorporate BIPV into the urban infrastructures, thereby with an aim to contribute to reducing greenhouse gas emissions by 85% by 2050 [9].

The Government of India supports the installation of solar PV, including building-integrated systems, through a mix of subsidies, regulatory measures, and enabling policies. Under the Rooftop Solar Programme Phase II, residential buildings receive central subsidies of up to 40% for systems up to 3 kW, with additional top-ups offered by some states [10]. Net-metering and gross-metering policies in most states allow building-mounted PV to offset on-site consumption and export surplus to the grid, while commercial and industrial owners benefit from 40% accelerated depreciation and a concessional 5% GST on modules [11]. Supportive frameworks such as the Energy Conservation Building Code, green building certifications (GRIHA, IGBC), and demonstration projects funded by Ministry of New and Renewable Energy (MNRE) encourage integration into new and existing structures [12]. Financing options, including low-interest loans under priority sector lending and green credit lines from Indian Renewable Energy Development Agency (IREDA) and Small Industries Development Bank of India (SIDBI), further facilitate adoption, making solar integration in buildings more financially and technically viable despite the absence of a dedicated BIPV-specific national programme [13].

The advancement in technology, policy incentives, and reduced cost of photovoltaic materials has made the adoption of BIPV and its future research viable at a much larger scale resulting in rapid development of the technology.

1.3 BIPV Definition and its advantages

BIPV involves embedding photovoltaic elements directly into a building's exterior so they can replace conventional materials while generating electricity on-site. These systems can be incorporated into roofs, balconies, facades, windows, and skylights during design, making them ideal for new construction. When PV panels are added later to existing structures, the approach is known as Building Applied Photovoltaic System (BAPV). Over time, BIPV has proven to be an efficient, multifunctional solution, providing clean power, improving energy self-sufficiency, reducing dependence on the grid, and lowering greenhouse-gas emissions. Because of these benefits, BIPV is considered a key technology for future low-carbon and net-zero energy buildings [14].

Fig. 1.4 Different form of BIPV application in buildings. (a) BIPV skylight system [15] (b) BIPV solar facades system [15] (c) BIPV rooftop system at Indian Green Business Centre (IGBC) – Hyderabad, India (d) Solar PV facades in NEW-Bauhaus Building, Germany [16] (e) PV as blinds integrated to building [17] (f) PV based windows at FLEXLAB, Solaria BIPV [18]

One of the notable advantages of BIPV, apart from its energy role, is its visual quality. Unlike standard construction materials, integrated PV systems can enhance both the appearance and performance of a building. Modern PV modules come in many forms - opaque, semi-transparent, flexible, or colored allowing architects to use them as roof panels, façades, shading devices, windows, or skylights. This variety gives designers more creative freedom while also supporting environmentally conscious design. **Fig. 1.4** shows the various forms of PV modules integration to a building.

BIPV systems also offer functional benefits. During summer, PV panels can block direct sunlight from hitting the building envelope, lowering heat gain and reducing the cooling load indoors. When an air gap is placed between the PV module and the external surface, air circulation in that space helps lower the module's operating temperature, which can enhance its energy output.

Overall, integrating PV technology into buildings does more than supply renewable electricity. It also enhances architectural aesthetics, improves natural lighting, increases thermal comfort, and reduces overall energy consumption. Compared to traditional building methods, PV-integrated designs provide visually appealing, energy-efficient, and environmentally responsible building solutions.

1.4 BIPVT and their relevant types

BIPV systems can be categorized in several ways depending on their power supply, integration mode, module type, and optical properties. From an energy supply perspective, they are either grid-connected, where the utility grid serves as the storage component ensuring stability and reliability, or stand-alone, which uses batteries to store surplus energy and may rely on backup generators during extreme weather.

In terms of integration, building-integrated systems replace conventional materials in new constructions, while building-applied systems are retrofitted onto existing structures without compromising functionality if removed. Integration options include roofs, which account for around 80% of the market, facades (20%), and other elements such as windows, sunshades, rain-screens, skylights, claddings, and railings [14].

Based on module type, rigid-module systems are made from materials like glass, plastic, or metal and can adopt any PV technology, whereas flexible-module systems, built on polymer films or metal sheets, often utilize emerging PV technologies.

Finally, according to optical properties, opaque systems are suited for non-transparent surfaces such as roofs and walls, while semi-transparent systems are integrated into glazing components like windows, facades, and skylights, producing electricity while maintaining daylighting functions.

1.5 Performance of BIPVT systems

Photovoltaic module fabrication can be done through wide range of PV technologies ranging from crystalline silicon, thin film technology to other emerging technologies. According to the National Renewable Energy Laboratory (NREL), efficiency records reported by laboratories, universities, and companies show notable advancements across these technologies. In the BIPV sector, silicon-based modules remain the most widely used, along with certain thin-film technologies such as Perovskite, CdTe and CIGS. By 2025, the highest recorded efficiencies

had reached 27.8% for single-crystalline silicon, 26.95% for perovskite cells, 21.2% for thin-film crystalline, 23.08% for CdTe, and 24.6% for CIGS (**Fig. 1.5**).

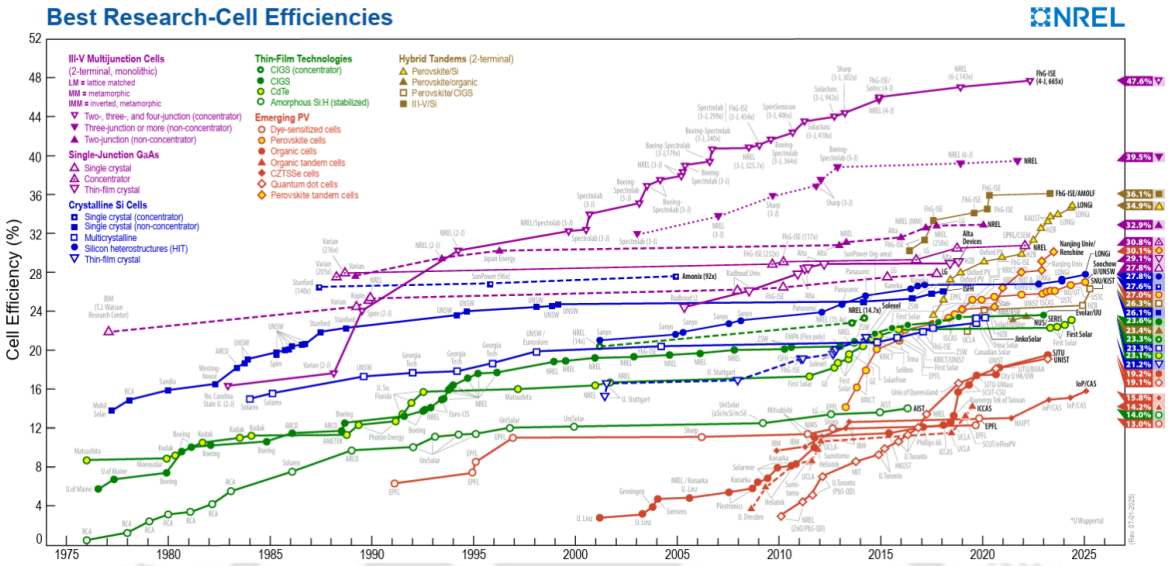

Fig. 1.5 Solar cell and their conversion efficiencies timeline, NREL

The amount of solar radiation that reaches a photovoltaic panel has direct impact on the electrical power generation. However, solar cells on absorbing the radiation experiences an increase in operating temperature, which in turn reduces electrical efficiency of PV module. As cell temperature increases, their electrical performance tends to decrease, as shown in **Fig. 1.7**. This decline is primarily due to several factors, including increased resistive losses within the cells and changes in the semiconductor material properties. PV modules are designed to absorb and convert sunlight into electricity, and they typically capture around 80% of the incident solar radiation [19]. Solar energy incident on a ground level constitutes of 47.4% of infrared radiation, 38.3% of visible light and 8.7% of ultraviolet rays [20]as shown in **Fig. 1.6** PV modules can only convert a certain percentage of the visible light spectrum into useful electric power. The infrared radiation of the solar spectrum which remains unutilized attributes to PV module heating, causing their temperature to increase. The heat, if not distributed effectively can lead to a rise in the cell temperature. This results in modules voltage output to decrease and electrical efficiency to decline. Therefore, it is crucial of thermal management of PV modules to maintain an optimal performance. Das et al., [19] reported that PV module efficiency decreases when they operate at temperatures higher than 80^{o}C. To mitigate the adverse effects of temperature on electrical efficiency, several cooling techniques are employed.

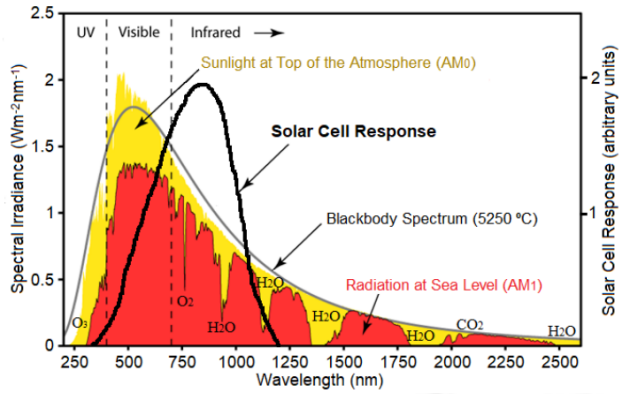

Fig. 1.6 Spectrum of Solar radiation and silicon solar cell spectral response [21]

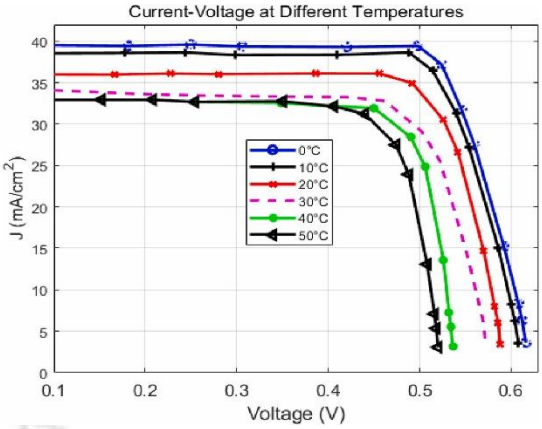

Fig. 1.7 The current-voltage (I-V) characteristics of a solar PV cell under different temperatures [21]

Active cooling mediums that includes air or liquid circulation, can dissipate the excess heat from the module's surface. This helps to maintain a lower operating temperature for the solar cells, which in turn improves their electrical performance and overall efficiency. The technological solutions based on various heat transfer process, forced and natural ventilated configurations, thermal storage wall has been widely described in the literature [7, 8, 9, 10]. \ PV module electrical efficiency which relies on cell temperature can be described mathematically using the expression given in equation 1.

$$\eta_{\mathrm{PV}} = \eta_{ref}[1 - \beta_o(T_{PV} - T_o)] \qquad (1.1)$$

Gaur et al. [26] experimental and theoretical investigation was carried out on a building-integrated semitransparent photovoltaic/thermal (BiSPVT) system, focusing on a roof-integrated monocrystalline silicon (c-Si) PV configuration with two design variations: (i) incorporating an air duct and (ii) without an air duct (**Fig. 1.8**). Analytical expressions were developed to determine the temperature-dependent electrical efficiencies of the system. A prototype BiSPVT setup was constructed at the Indian Institute of Technology, New Delhi, and tested under real conditions. Theoretical predictions obtained from the derived expressions were validated against experimentally measured thermal and electrical performance parameters for both configurations, showing close agreement. To enhance both electrical and thermal efficiencies, the system was optimized for key design parameters such as air duct cross-sectional area, duct height, airflow velocity, packing factor, and number of air changes. The study reported that, without an air duct, the system achieved an electrical

efficiency of 12% and an average room temperature of 25 °C, while with an air duct, efficiency improved to 13.11% and the average room temperature reduced to 10.1 °C (**Fig. 1.9**).

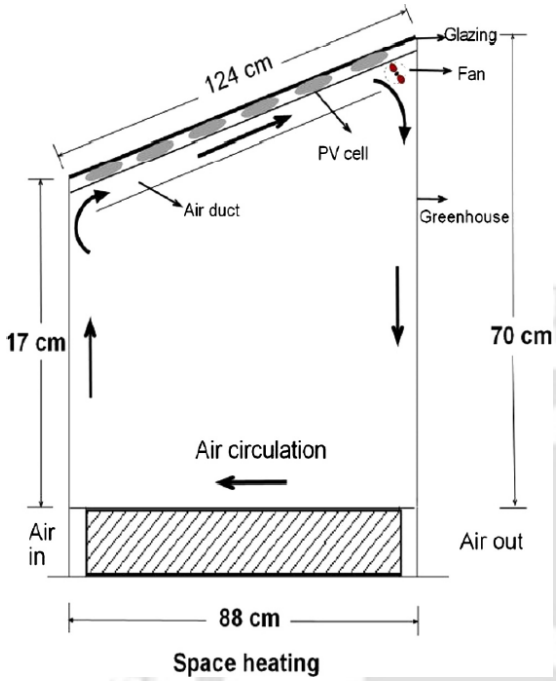

Fig. 1.8 Schematic of a BiSPVT rooftop system prototype used for space heating

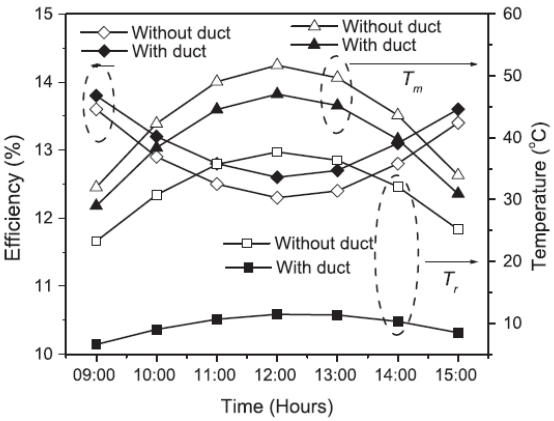

Fig. 1.9 c-Si BiSPVT system hourly electrical efficiency variation profile with and without duct

Park et al. [27] reported that for c-Si PV. modules, each 1°C rise in operating temperature reduced power output by 0.52% in outdoor environment conditions and 0.48% under STC. They also noted that the glass properties of PV modules significantly influenced its energy output and operating temperature. Yoon *et al.* [28] studied amorphous silicon windows at different inclinations, finding that vertical windows retained more heat in winter, while during summer the windows that were positioned horizontally and inclined windows were found to be cooler. Compared to conventional windows, during winter, BIPV windows had inner surface temperatures about 2°C higher at night and during summer a 1°C lower. Fossa *et al.* [29] experimentally determined that optimizing the thickness of air cavity and could lower surface temperatures, boost conversion efficiency, and enhance thermal energy recovery. Gan [30], through CFD simulations, found that a air gap width of 12-16 cm behind the PV module could reduce overheating and improved power generation. Similarly, Ritzen *et al.* [31] observed that ventilated PV rooftops in The Netherlands produced 2.6% more power than non-ventilated ones.

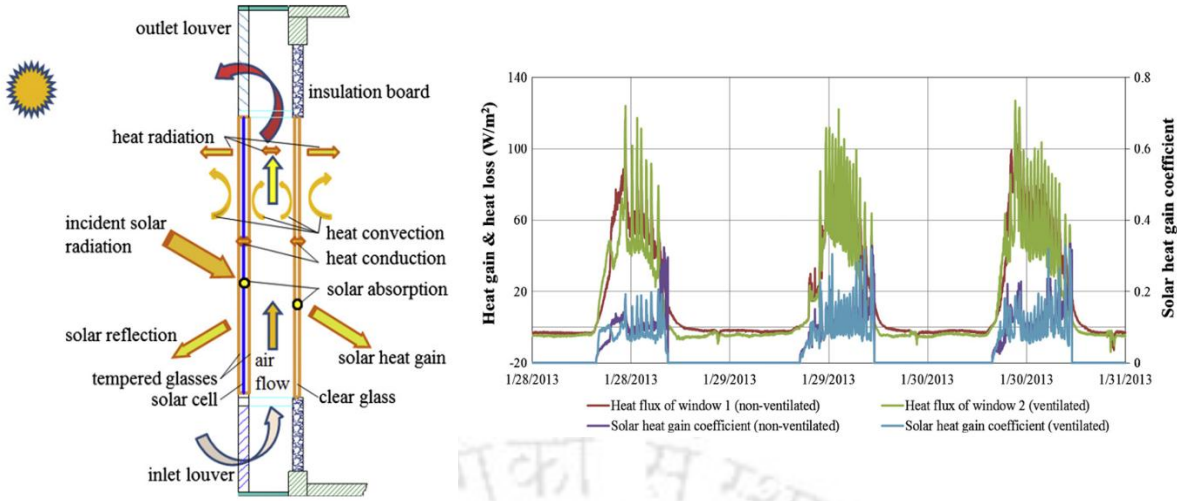

(a) **(b)**

Fig. 1.10 (a) Schematic of Photovoltaic Double Skin Facade (PV-DSF) (b) Analysis of thermal performance of the PV-DSF

Peng *et al.* [32] carried out experiments on a newly developed double-skin PV façade system, shown in **Fig. 1.10**. Their study found that when the facade operated in a ventilated mode, it produced the lowest solar heat-gain value, while the non-ventilated mode offered better resistance to heat loss. In another study, Peng *et al.* [33] analyzed the year-round thermal behavior of a multi-layer PV façade using numerical methods. The results showed that, during winter, the system reduced heat loss and heat gain by 32% and 69%, respectively, compared to a standard wall. During summer, the south-facing PV facade lowered heat gain by 51% relative to a conventional wall.

Studies related to analyzing the performance of BIPV systems that are semitransparent in nature are relatively limited. Lu and Law [34] introduced a novel approach to assess a single-glazed semitransparent PV window's energy performance in Hong Kong (**Fig. 1.11**). Their findings indicated that incorporating such a PV window could reduce building's heat gain in the selected location by 65%. Additionally, depending on the indoor HVAC system type, the annual electricity savings ranged from 900 to 1300 kWh compared to glass windows used conventionally (**Fig. 1.12 & Fig. 1.13**).

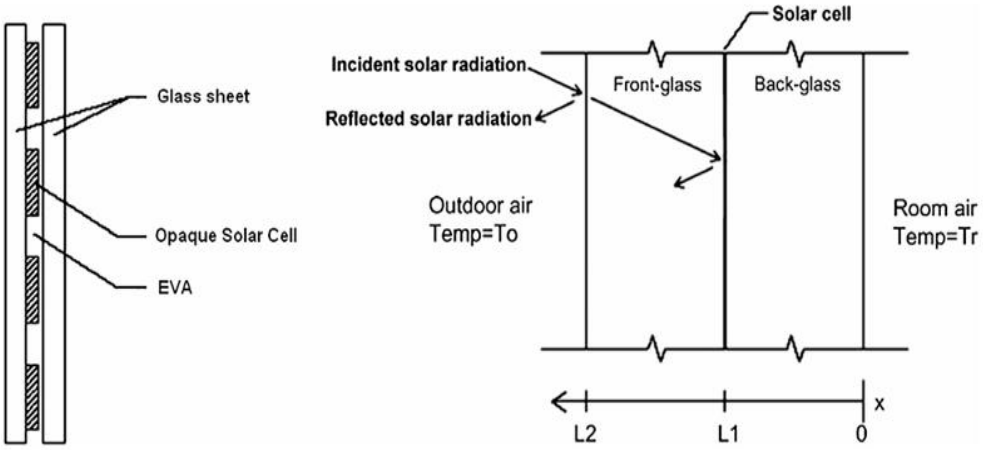

Fig. 1.11 Schematic of semitransparent BIPV module [34]

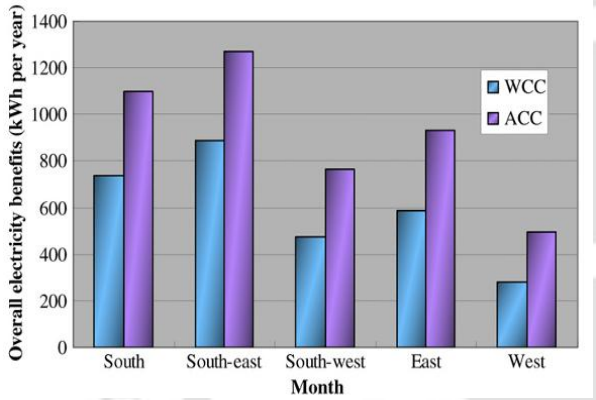

Fig. 1.12 PV window power generation profile annually [34]

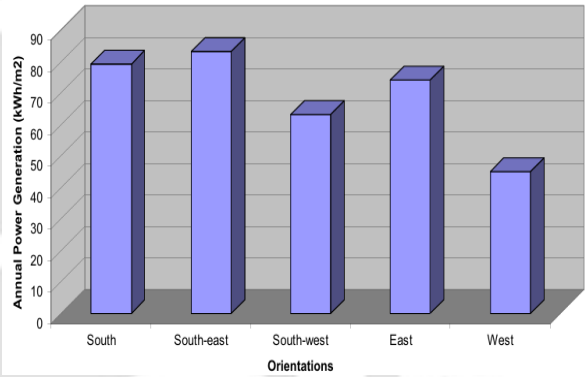

Fig. 1.13 Overall electricity gain profile annually for various PV orientation [34]

A summary of recently conducted studies in the year of 2019 - 2023 is presented in **Table 1.1**

Table 1.1 Studies based on BIPV relevant to the present research

Reference	Technology and Building integration	Location	PV module technology	Application	Remarks
Gao *et al.* [35]	Roof integrated AHU based BIPVT	Iran, Kermanshah	Opaque	Provided the benefit of HVAC unit	ANN and GP optimized equations were used for predicting systems performance
Shakouri *et al.* [36]	BIPVT-DSF	Tehran, Iran	Opaque	Thermal gain to building	Considerable cooling and thermal load reduction annually
Wajs *et al.* [37]	BIPV Roof Tile	Gdansk University of Technology	Opaque	Thermal energy gain	Maximum PV surface temperature reduction was by 6.3K
Shahsavar *et al.* [38]	Roof integrated EAHE	Iran, Kermanshah	Opaque	Electrical and thermal energy production	The hybrid system when compared with a BIPVT and EAHE

Reference	Technology and Building integration	Location	PV module technology	Application	Remarks
	assisted BIPVT system				system could generate greater useful energy by 10.1% and 935.6% respectively Hybrid system saved CO_2 by 3.2% less than BIPVT
Liang *et al.* [39]	Active solar building facade	China	Opaque	Hot water production, electrical power generation for domestic use	Active facade reduced heat flux to building by 40% making it superior than conventional wall in a building
Preet *et al.* [40]	PV-DSF system	India	CdTe PV module	Electrical power generation	SHGC was 36% more in the air gap with 20cm air gap thickness and natural ventilation compared to forced ventilation
Salameh *et al.* [41]	BIPV facade	United Arab Emirates (UAE)	Opaque	Reduction in annual energy consumption	Annual energy consumption for air conditioning was lessened by 27.69%
Cekun M. [42]	BIPV-PCM facade	Czech Republic (Brno)	Opaque	PCM cooling capabilities in BIPV	Maximum 3K temperature difference during peak sunshine hours was observed in the cavity air flow velocity using PCM
Goulart *et al.* [43]	BIPV and BAPV	Brazil	Opaque	Electrical power generation	Electrical power production from the PV system with capacity of 111kWp met building energy needs by 148% and Laboratory building energy requirement additionally by 97%
Jois *et al.* [44]	BIPV facade	India	Opaque	Energy requirements	BIPV systems potential based on its geographical location was termed as one of the important influences on systems potential
Shakouri *et al.* [45]	BIPVT-DSF unit	Tehran, Iran	Opaque	Power generation	Configuration with PV module surface only and zero glass surface resulted in payback time period of 1.58years and revenue

Reference	Technology and Building integration	Location	PV module technology	Application	Remarks
					generation of USD5515and additionally lowest greenhouse emission
Liang *et al.* [46]	PVT facade	Dalian, China	Opaque	Power generation	Systems overall efficiency was achieved as 42%
Chen *et al.* [47]	Bi facial BIPV	Guangham, China	Bi facial PV modules	Electrical efficiency enhancement	Use of bifacial PV module resulted in 18% more power production compared to mono-facial PV modules
Sharma *et al.* [48]	BIPVT (PV-TSF)	Jaipur, India	Opaque	Energy	Outer skin transparency significantly influenced the system performance
Rounis *et al.* [49]	BIPVT curtain wall	Montreal, Canada	Opaque	Thermal energy gain	System showed a thermal efficiency of 33%
Jalalizadeh *et al.* [50]	Wall integrated BIPVT	Vancouver, Halifax, Edmonton, Montreal, and Toronto	Opaque	Electrical power production	Annual GHG emission based on 5 cities were reported to have saving in the range of 11-5128 $kgCO_2$
Alrashidi *et al.* [51]	BIPV facade	Penry, United Kingdom	CdTe Semi-transparent PV module	Reduction in cooling energy demand	As compared to clear glazing, CdTe glazing could reduce the cooling energy load by 23%
Bezaatpour *et al.* [52]	Facade based BIPV	Iran	Opaque (c-Si)	Power generation in high rise buildings	Maximum of 55^oC temperature difference in modules of facades were observed.
Ge *et al.* [53]	Wall based BIPVT	Huizhou, China	Opaque	Power generation	Average electrical efficiency was obtained as 12.3%
Zhang *et al.* [54]	Window based BIPV with vacuum glazing	Heifei, China	CdTe	Space heating	Enhancement of heat transfer coefficient was observed from 0.944 to 1.138 W/m^2K
Sohani *et al.* [55]	BIPV facade system	Iran	Opaque	Electricity production	Air gap of 0.15m was found to be optimum for the system that gave payback period of 2.2-3.5 years.

While electrical output and thermal effects are among the most critical measures of BIPVT system performance, several other factors including optical properties, integration design, ventilation strategies, material selection, and local climatic conditions can significantly influence system efficiency and operational stability. These aspects, along with advanced performance evaluation methods such as exergy, exergoeconomic, and life cycle assessments, will be examined in detail in Chapter 2: Literature Review. However, in the present study, the primary focus remains on the thermal energy and electrical performance of the studied system, with particular emphasis on quantified energy generated and corresponding energy savings achievable through the integration of a BIPVT system in the building envelope.

1.6 Alignment with SDGs

The research work undertaken on the BiSPVT facade system finds its alignment with the United Nations set Sustainable Development Goals (SDGs). It supports transition toward inclusive infrastructure that supports low carbon emission and climate resilient in nature particularly in the built environment.

SDG 7 (Affordable and Clean Energy) by promoting the integration of decentralized renewable energy technologies within building structures. The BiSPVT system, through its ability to supply both electricity and thermal energy, enhances energy access in regions with intermittent grid availability, such as cold climatic zones like Srinagar.

In terms of **SDG 9 (Industry, Innovation, and Infrastructure)**, the system demonstrates application of hybrid PV-thermal modules on building facades. It encourages innovation in passive and active solar technologies, contributing to smarter and more sustainable built environments.

Through the lens of **SDG 11 (Sustainable Cities and Communities)**, the research advocates for reduced urban carbon intensity and energy demand by transforming buildings into micro energy hubs. This dual-generation technology helps reduce the reliance on conventional fossil-based energy systems while simultaneously improving indoor thermal comfort.

The research incorporates a thorough Life Cycle Assessment (LCA) of the BiSPVT system, thereby aligning with **SDG 12 (Responsible Consumption and Production)**. It evaluates the embodied energy, emissions, and potential environmental trade-offs associated with system materials and fabrication.

Lastly, by directly contributing to emission reduction strategies, and enhancing renewable energy deployment in building applications, this work aligns strongly with **SDG 13 (Climate Action)**. It also echoes national policy efforts and international climate commitments, serving as a tool for local-level climate mitigation in the building sector.

1.7 Objective of thesis

While previous research on photovoltaic-thermal (PVT) systems has largely focused on standalone collectors, roof-mounted configurations, or conventional PV arrays, limited attention has been given to facade-based semi-transparent BiSPVT systems, particularly under cold climatic conditions. Existing studies seldom address the combined electrical, thermal, exergy, and lifecycle cost implications of such systems, nor do they consider performance variations across diverse weather scenarios within a single location. Moreover, there is a scarcity of comprehensive assessments that integrate exergoeconomic analysis with life cycle and sensitivity evaluations, especially for applications in remote, grid-deficient regions. This gap is significant, as understanding the year-round performance and long-term economic and environmental impacts is essential for informed adoption. The present study addresses these shortcomings by evaluating a forced-ventilated semi-transparent BiSPVT facade system for Srinagar's cold climate, considering multiple weather types, and conducting an integrated energy, exergy, lifecycle, and economic performance analysis.

The primary objective is divided into the following sub-part for the accomplishment of proposed work.

I. To develop a numerical thermal model for a semi-transparent ventilated PV facade that will enable to investigate its potential or advantages in reducing the energy consumption and heating load at cold climatic sites.
II. To study the annual energy performance for a semi-transparent ventilated PV facade for cold climatic zone, Srinagar, India.

III. To conduct exergy, exergoeconomic, and enviroeconomic analyses of the proposed PV facade system.

IV. To perform a life cycle assessment to determine the long-term environmental and economic impacts of the system.

1.8 Organization of Thesis

This thesis comprises seven chapters.

Chapter 1 includes the motivation behind the research work, background of the study done along with the objectives of present work focusing on the field of BiSPVT facades when it comes to enhancing the energy performance in buildings while simultaneously contributing to reduced carbon emissions.

Chapter 2 presents a detailed literature review on Building Integrated Photovoltaic (BIPV) and Building Integrated Photovoltaic Thermal (BIPVT) systems, with emphasis on vertical and semi-transparent facade applications, thermal management, exergy and exergoeconomic assessments, life cycle analysis, and the identification of research gaps.

Chapter 3 describes the modeling and methodology adopted for the study, including the development of a one-dimensional thermal model, calculation of solar radiation and heat transfer coefficients, performance simulations under varied weather types, and the framework for energy, exergy, exergoeconomic, and life cycle analyses.

Chapter 4 discusses the annual energy performance of the BiSPVT facade for cold climatic conditions, presenting results for electrical, thermal, and exergy gains under different seasonal variations.

Chapter 5 elaborates on the exergy, exergoeconomic, and enviroeconomic analyses of the BiSPVT facade, highlighting system efficiency, cost-effectiveness, and long-term economic viability.

Chapter 6 focuses on the life cycle assessment (LCA) of the BiSPVT facade, quantifying greenhouse gas reductions, environmental impacts of component manufacturing, and the global warming potential (GWP) of the system.

Chapter 7 summarizes the major findings of this research work, providing conclusions and outlining the future scope of the work.

2

Literature Review

Chapter Outline:

2.1. Introduction
2.2. Factors affecting the performance of BIPVT system
2.3. Energy performance of a semi-transparent BIPVT system
2.4. Exergy, exergoeconomic and enviroeconomic analysis
2.5. Life cycle analysis: Environmental impacts of BIPVT systems
2.6. Scope of present work
2.7. Summary of Chapter

CHAPTER 2: LITERATURE REVIEW

2.1 Introduction

BIPV/BIPVT systems performance is assessed by its electrical and thermal efficiencies. Solar cell electrical efficiency is measured at Standard Test Conditions (STC) i.e. at 1000W/m^2 solar radiations, 1.5m/s wind speed, AM 1.5 and 25^{o}C ambient temperature [56]. For commercial PV modules used in engineering application electrical efficiency varies in the range of 15-23%. Several factors influence the power generated by PV modules, including incident solar radiation, surface temperature of PV module, angle of incidence, cell packing factor, shading, dust accumulation, and conversion efficiency from DC to AC. PV module surface temperature is one of the major parameters which hampers the PV module efficiency (**Fig. 2.1**). Thus, PV module effective thermal management becomes necessary in order to maintain the temperature at an optimal range. Moreover, the heat extracted can further be utilized for useful purposes like hot water production, space heating, and additional electricity generation. Temperature dependent electrical efficiency is expressed as [56],

$$\eta_{\mathrm{PV}} = \eta_{ref}[1 - \beta_o(T_{PV} - T_o)]$$

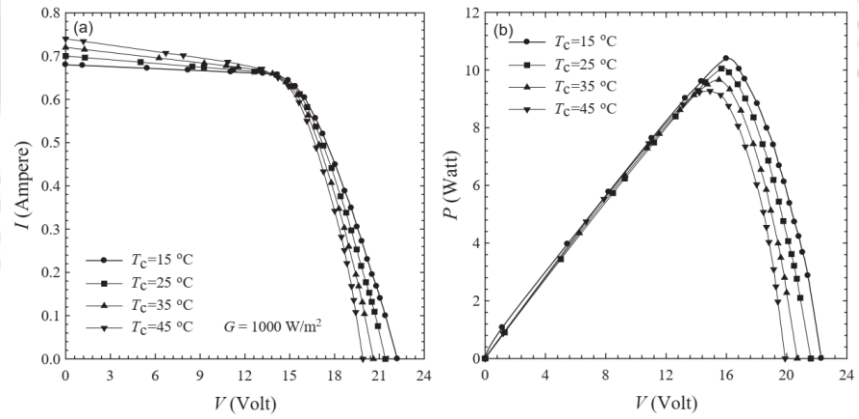

Fig. 2.1 (a) Current (I) – Voltage (V) and (b) Power (P) – Voltage (V) characteristic curves of the PV cell under various temperature conditions [57]

In studies, it has been found that enhancing PV electrical efficiency involves effectively dissipating heat from the module's surface, often achieved by employing forced convection in a fluid medium (water or air) beneath the module's rear layer. These modules, when integrated

into buildings, utilize the space between the module and the building wall as a duct for fluid circulation, removing heat from the PV module.

2.2 Factors affecting the performance of BIPVT system

Temperature difference between PV module and ambient reaches easily up to 60^{o}C in days of receiving solar radiation with high intensity [20]. Air as a medium for cooling PV modules has been found as a cost-effective method to keep PV module temperature in desired range. Installing an air gap between building wall and PV facade utilizes forced or natural air circulation for cooling of PV panels, and the heated air produced can be harnessed to meet heating requirements of the building.

A typical air based BIPV system can be of vented and unvented configuration depending upon the end use of hot air. Solar energy falling on the glazing gets transmitted through and heats cavity air by convection. Heated air rises up in cavity which is then passed into the indoor space. During night, the massive wall delivers the heat energy stored in it to indoor environment by convective heat transfer [56]. The heat that is carried away is further utilized with integration of Trombe wall system. **Fig. 2.2(a)** shows the mechanism of utilization of the hot air in building during summer and winter [58]. During summer, the hot air is discharged to outside while during winter, it is taken to the interiors for space heating. This helps in reducing the energy requirement load for heating during winter in buildings.

An extensive review on BIPV for thermal systems and their applications has been presented by Debbarma *et al.* [59] based on the BIPV systems from 2006 to 2016. The description of BIPV and BIPVT systems based on its functions, aesthetics, applications and its economic analysis was reviewed in this study. Agathokleous & Kalogirou [61] studied the configuration of an air based BIPV assessed the PV wall performance used in residential buildings of Tibet. Effect of width of PV- wall on the indoor temperature was studied along with system performance with respect to electrical and thermal efficiency. Results showed that with increase in Photovoltaic Trombe wall (PVTW) width, indoor air temperature varied linearly while the electrical efficiency was found to be almost constant [62]

Bellazzi *et al.* [63] analysed the performance of an amorphous silicon (a-Si) thin film solar cells integrated as ceramic modules into the ventilated facade of a 2 storied building. Numerical model

developed was validated with the experimental study, upon which a strong relation between the experimental and numerical values characterized with low values of Root Mean Square Error (RSME) was observed.

Gaur *et al.* [26] conducted performance evaluation of a semi-transparent photovoltaic thermal system (BiSPVT) integrated into a building roof, both numerically and experimantally. BIPV system was designed with and without an air duct next to the PV module, aiming to enhance PV efficiency by dissipating heat from the module's back surface and utilizing it to heat indoor spaces. Energy and exergy analyses were performed for Srinagar, India's climate conditions, considering varying air mass flow rates, duct heights, packing factors, and room air change rates. Results indicated that the configuration with the air duct exhibited higher PV efficiency (13.11% vs. 12% without duct).

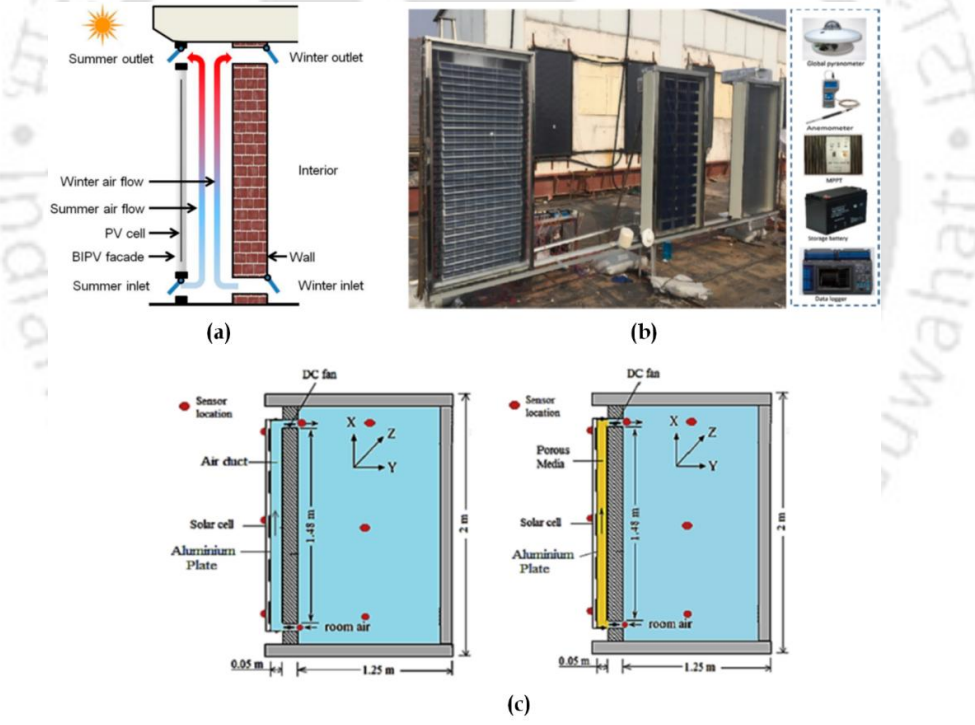

Fig 2.2. (a) Mechanism of PV-TW system (b) Experimental setup of PV-Trombe wall (c) PV-TW configuration with and without using porous medium PV-TW for winter heating with DC fan

Hu *et al.* [65] developed a novel PV facade, integrating photovoltaic modules as blinds (PVBTW) shown in **Fig. 2.2(b)**. Their analysis focused on varying air flow rates and blind angles to assess heat gain and power generation. Comparisons were made among three configurations: PV cells attached as blinds (PVBTW), PV cells integrated with a mass wall (PVMTW), and PV cells mounted on glass (PVGTW), under consistent solar radiation, wind speed, and ambient temperature. PVBTW outperformed PVGTW by 14.5% and PVMTW by 14.1% in total efficiency, combining thermal and electrical efficiency. For an optimal value of 0.45 m/s air flow rate and a 50^{o} blind inclination angle, both PV module electrical efficiency and interior heat gain were deemed favorable.

Ahmed *et al.* [66] studied the effect of DC fan and porous medium for a PVTW system as shown in **Fig. 2.2(c)**. Temperature of the PV cell was found to be lowered and room temperature was increased with the use of DC fan, while the glass cover enhanced the temperature of both cell and room. Addition of the porous medium along with DC fan was found to increase the thermal efficiency by 13% and electrical efficiencies by 4%, respectively.

Using an air gap and the effect of its width on PV module temperature along with its electrical efficiency was studied experimentally by Kaiser *et al.* [67]. Experimental setup consisted of a PVT collector with a single PV module rating of 270Wp. Air gap was varied from 0.1m to 0.16m. It was observed that an aspect ratio of 0.11 proved to be optimal for PV temperature when utilizing ventilation naturally. However, for forced mode ventilation, smaller aspect ratios can be employed. Notably, natural ventilation at an average velocity of 0.5 m/s resulted in a 19% performance improvement compared to forced ventilation at an average velocity of 6 m/s. Some of the existing literatures which studied effect of factors influencing performance of an air based BiPVT system is shown in **Table 2.1.**

Table 2.1 Various operational parameters and its effect on the PV-Wall facade

Reference	Studied Parameter	Experimental/ Numerical	Location	Major Findings
Jie *et al.* [68]	DC fan effect in the air duct	Experimental and Numerical	China	Presence of DC fan increased air circulation in the cavity thereby enhancing PV module

Reference	Studied Parameter	Experimental/ Numerical	Location	Major Findings
				efficiency and improving indoor room temperature.
Koyunbaba *et al.* [69]	DC fan effect in the air duct	Experimental	Turkey	Use of DC fan showed increase of both efficiency (thermal and electrical) of the system
Irshad *et al.* [70]	PV-TW analysed in terms of energy saving and CO_2 emission reduction.	Numerical analysis (TRNSYS)	Malaysia	Double glass with argon found suitable for hot climatic condition. Configuration found favourable for saving energy and lessening CO_2 emission
Irshad *et al.* [71]	PV-TW configuration for different mode of glazing (single, double, glazing filled with Argon)	Numerical analysis	Malaysia	Maximum reduction in temperature was observed using Argon in the double-glazing configuration
Vats *et al.* [72]	Effect of varying packing factor	Numerical	India	PV module electrical efficiency was increased from 0.2 to 0.6% with reduced value of packing factor.
Peng *et al.* [73]	Effect of varying thickness of air gap	Numerical and experimental	China	Recommended an optimum thickness of 0.06m for the air channel in the PV Wall configuration for the given weather condition of China.
Hu *et al.* [74]	Varying mass flow rate	Numerical analysis	China	Recommended an optimal air flow rate of 0.45m/s.
Xu *et al.* [75]	Varying mass flow rate	Numerical analysis	China	Air flow rate flowing through the duct was found to be corelated with factors such as channel size, absorptivity of the coating

Reference	Studied Parameter	Experimental/ Numerical	Location	Major Findings
				used, incident solar radiation and duct height
Jovanovic *et al.* [76]	Effect of Tilt angles of the PV modules	Numerical analysis	Serbia	Tilt angle of the PV module placed is related with the latitude of the location where it is used.
Asefi *et al.* [77]	Varying Channel width	Numerical analysis	China	The optimised value for ratio of width to height of a PV-TW was recommended as 0.2m for this particular configuration.
Taffesse *et al.* [78]	Analysed for optimization of PV wall thickness	Numerical	India	Recommended optimum thickness was 0.4m for the PV-Trombe wall.

Peng *et al.* [79] assessed the performance of a double skin ventilated PV façade (PV-DSF) in terms of its potential of annual energy savings during the summer season in a Mediterranean climate region. The system studied was found to generate 65 kWh of electricity per unit area of the facade. The c-Si PV panels when replaced in the system by semi-transparent cadmium telluride (CdTe) photovoltaic panels resulted in doubling the annual energy production. This is because the amount of solar radiation harnessed through a semi-transparent PV module was higher than the conventional one. Additionally, PV-DSF integrated glazing systems led to an increase in the net current by 50%.

Tiwari *et al.* [80] studied the experimental performance of a PV/T air collector for three modes of air flow: natural flow of air, forced mode flow of air and forced flow of air with double fan. Combined thermal and electrical efficiency up to 43% was reported in the analysis. The experiment was performed for unglazed PVT collector. This experimental work was further extended by Tiwari & Sodha, [81] for glazed PVT collector configuration. The glazed collector with tedlar free PV modules exhibited superior performance attributed to rising the substrate's conductive heat transfer. This implied the significance of thermal conductivity of the material placed between the air duct and PV module.

Bambrook & Sproul [82] performed an experimental analysis on an air-based PVT collector. Principal motive was to increase both electrical efficiency and thermal output simultaneously while taking into consideration that system's generated energy is more than the energy consumed by the fan. Founding of experiment conducted in outdoors of Sydney, Australia revealed that for 0.03-0.05 kg/s/ m^2 range of air flow, the extra energy yield from the cooling of PV has exceeded the power demand of fan. This is because increasing the mass flow rate was able to remove increased amount of heat from the back of PV module resulting in increased electrical efficiency, while heated air contributing to enhancement of Thermal efficiency.

The performance of PV module on long term based surface temperature was studied by Yoon *et al.* [83] Comparative study was done on BIPV windows and clear glass windows. Annual performance of the configuration was analysed for different tilt angles. During winters, the temperature of the window increased for vertical planes and during summers, the temperature of the window was more for horizontal and inclined surfaces. BIPV window surface temperature was lower by 1^{o}C in summer and higher by 2^{o}C in winter, compared to the clear glass window.

Koyunbaba & Yilmaz, [69] compared the performance of three glazing configurations in terms of energy: single, double and semi-transparent PV module mounted on the facade. Using computational fluid dynamics (CFD) for Izmir's climate, it was observed that during night, the double glazing provided the highest insulation, while higher solar radiation gain was observed in the single glazing due to its higher transmittance. Integration of PV modules resulted in lower air temperatures in the channel compared to single- and double-glazing configurations, enhancing PV module efficiency. Irshad *et al*. [84] performed a simulated study on a system comprising of a room with a PV integrated Trombe wall to evaluate room temperature and PV module efficiency. Their analysis considered varying air flow rates for single-glazed, double-glazed, and Argon-enhanced double-glazed systems. Argon filled double glazing decreased air duct temperature and cooling load, boosting PV module electrical efficiency. These studies infer the role of glazing configuration and integration of PV modules for thermal regulation and efficiency improvement.

The use of PV modules in the high-rise towers of Doha, Qatar was studied by Abu-Rub *et al.* [85]. In their work, primary goal was to study the environmental impacts, feasibility condition and

economic aspects of using photovoltaic modules on commercial towers in Qatar. Numerical analysis-based findings showed that for the current configuration of the QFC tower, the PV system would generate an estimated energy production of 62,082 kWh/year resulting in cost savings of 2,360 USD. System was also found beneficial in terms of saving CO_2 emissions annually by a value of 33,334 tonnes.

Aaditya *et al.* [86] conducted the real-time performance assessment of a BIPV system with a capacity of 5.25kWp situated at the Center for Sustainable Technologies within IISc, Bangalore, India. Average overall system efficiency, power ratio, and average inverter efficiency for the period May 2011 to April 2012 were found to be 6%, 0.5, and 91%, respectively.

The air-based PVT systems has certain limitations like lower heat capacity and instant use of hot air for pre-heating, space heating etc. applications. However, water-based PVT systems has storage capacity which allow them to store thermal energy and used it later as per the requirement. Water based BIPV systems consists of glazing, tube in plate type collector with header and riser (thermal absorber), connecting water pipe, and insulation layer. First designed as a single unit, the water based BIPV systems are then incorporated to a wall or mounted on a building roof.

The numerical model developed by Mishra *et al.* [87] consisted of semitransparent PV module in 96 numbers of 75Wp each. The developed thermal model was further validated with a Rooftop semi-transparent Photovoltaic system (RtSPV) installed at a building complex in Varanasi, India shown as shown in **Fig. 2.3 (a)**. Electrical performance of the PV array was enhanced by the flow of water through the top surface of the PV modules in the array at an intermittent rate from 9.45hours to 14.15hours. The time period so chosen was because intensity of solar radiation falling on the system during this time period is higher as compared to the solar radiation in early morning and late afternoon leading to high PV module temperature. Water usage reduces temperature resulting in improved efficiency. The system with water flow produced a net electricity of 10.14 kWh, higher than the BtSPV system without water flow which produced 1.44 kWh. PV cell temperature was found to be reduced with water usage which improved the efficiency as well (shown in **Fig. 2.3(b)**).

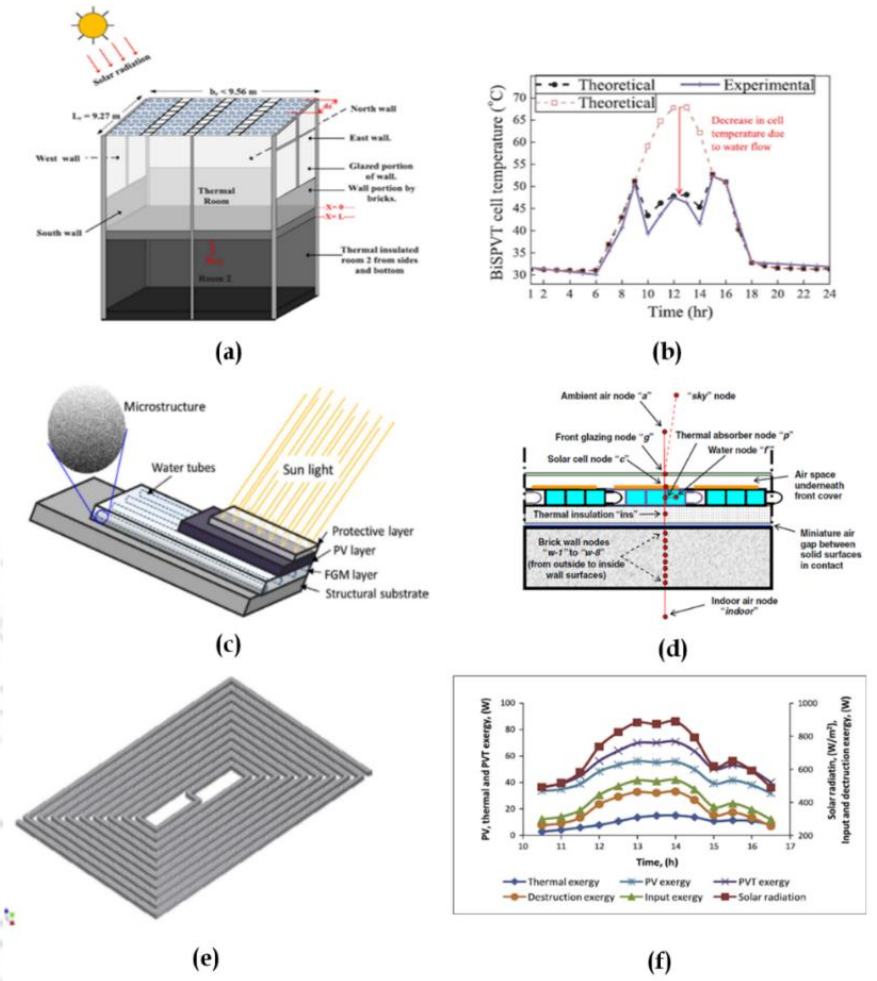

Fig. 2.3. (a) Water based BiSPVT system configuration (b) Hourly PV cell temperature variation (c) Schematic of hybrid solar roofing panel (d) BiPVW collector system (e) Spiral flow absorber (f) Variation of solar radiation and exergy at mass flow rate of 0.027kg/s.

Yin *et al.* [88] developed a BIPVT prototype as shown in **Fig. 2.3(c)** with a protective layer of transparent material and an underlying conductive aluminum layer (K value: 238W/mK). Water-filled pipes within the aluminum layer, coupled with a polyethylene insulating layer underneath, effectively prevented heat conduction to the building. The hybrid solar roofing panel system, tested under artificial lighting at 0.5m x 0.6m dimensions, exhibited a PV module temperature range of 49-51°C at a solar intensity of 850 W/m². Introducing water circulation (20°C) at 33mL/min was able to decrease the temperature of PV module to 32-39°C.

Chow *et al.* [89] analysed a BIPV system on a vertical wall, featuring a flat box-type thermal absorber with polycrystalline PV modules. Collector schematic is shown in **Fig. 2.3(d)**. Insulation on the walls resulted in lower in the surface temperatures, leading to a 50% reduction in space cooling using the PV wall. The study revealed that natural circulation was more efficient than pump-based circulation, with annual thermal efficiency at 37.5% for natural circulation and 35.8% for forced circulation.

Ibrahim *et al.* [91] investigated a water based BIPT system in terms of energy and exergy aspects with a spiral flow absorber attached to it (**Fig. 2.3(e)**). BIPVT collector consisted of a polycrystalline silicon PV module with single glazing. Results from energy analysis of the BIPT system revealed that for solar radiation of 690W/m^2 and 0.027kg/s water flow rate, 48% of thermal efficiency and 10.8% of electrical efficiency was observed. **Fig. 2.3(f)** shows the variation of solar radiation and exergy at mass flow rate of 0.027kg/s of the BIPVT system. Results also showed the exergy efficiency of the PVT as 13.1% while the Improvement potential to be 314W.

In New Zealand, Anderson *et al*. [92] explored BIPVT applications in Danish residential buildings, assessing electricity production and hot water use. The study compared three configurations (BIPV, BIPVT, and solar thermal systems) with varying collector sizes provided they considered same cost at initial stages. Findings revealed that in colder climates, BIPT is applicable under specific conditions, while in warmer climates, it may not be as favorable as traditional BIPV and solar thermal technologies (Gautam & Andresen [93]).

Kim *et al.* [94] constructed a roof integrated BIPVT system utilizing hot water for pre-heating in a 55L boiler. The unglazed collector featured a PV panel integrated to an absorber (sheet and tube, insulated with 50mm-thick layer of glass wool. Water circulation to the boiler activated when the BIPVT system and the tank temperature difference exceeded 4^{o}C, maintaining a flow rate of 10 LPM. The system has 17% electrical and 30% thermal efficiency with a 1.5 kW total power generation.

Martin-Escudero *et al.* [95] conducted a numerical study on a BIPVT collector linked to a 300L water tank, aiding a natural gas boiler. Integration of the BIPVT collector was estimated to save EUR4542 in annual energy consumption, with an additional construction cost of EUR29160 for the BIPV facade. With an electricity cost of EUR 0.09/kWh, the projected total payback time was

approximately 7 years, showcasing reduced primary energy consumption and increased reliance on renewable resources.

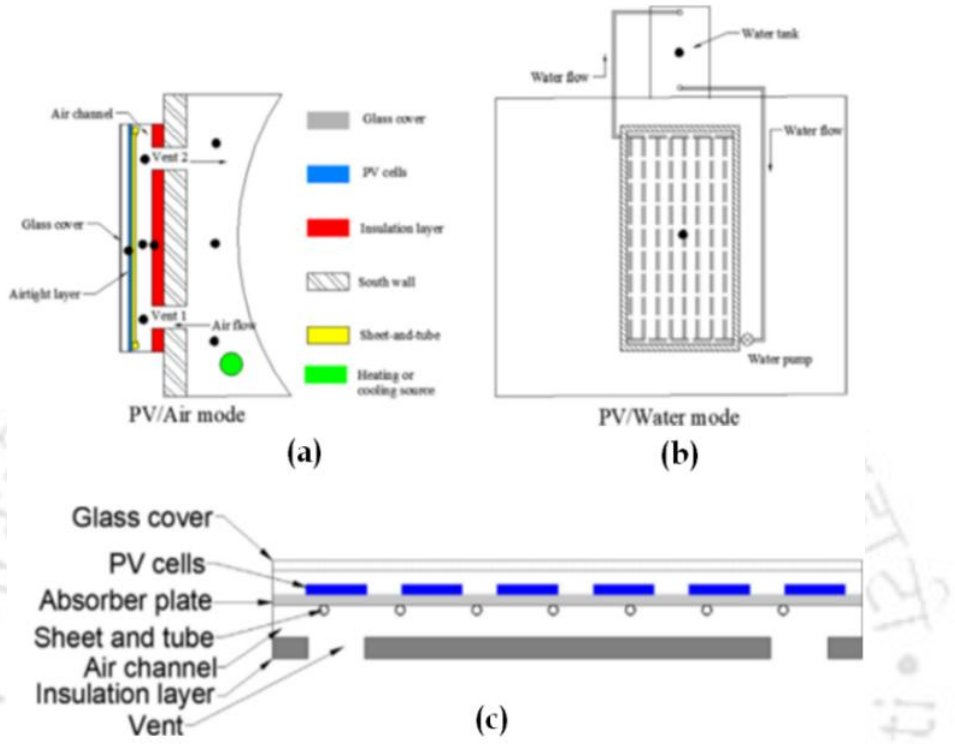

Fig 2.4 PV-Air mode, PV-Water mode, and the components of the BIPVT wall system are depicted in sections (a), (b), and (c), respectively

Taffese *et al.* [78] highlighted the insufficiency of conventional BIPVT systems in China, which typically involved use of air or water space heating or hot water supply, leading to increased overall energy demand. Xu *et al.* [96] studied a multi-functional BIPVT system with both air and water modes to meet year-round energy requirements. This system not only addressed hot water demands during non-heating seasons but also reduced PV cell temperature, thereby enhancing electrical efficiency. System successfully provided indoor space heating during the cold season contributing to decreased building heating loads. The study covered three Chinese cities, reporting significant yearly energy savings and hot water supply percentages. Despite successfully meeting building energy demands, challenges such as fluid denaturation and overheating were noted, which could be mitigated by continuous fluid flow during sunny days. Systems configuration with air mode and water mode is shown in **Fig. 2.4(a)** and **(b)**. **Fig. 2.4(c).**

Hot water demand was also met by 79.1%, 66.8% and 60.4% respectively in these cities. Annual average efficiency of the system was obtained as 12.1%, 10.6% and 11.2%, in Xining, Hefei and Beijing respectively. Meanwhile, Pugsley *et al.* [97] proposed a new BIPT configuration that integrates BIPV, PLVD, and ICSSWH technologies to reduce heat loss during the night.. Theoretical and experimental validations showed promising results, with the system achieving thermal efficiencies of 60% and 50%, respectively, with and without the use of a transparent cover.

Table 2.2 presents the summary of additional studies performed on water based BIPV systems.

Table 2.2 Summary of studies performed on water based BIPV systems

Reference	**Studied technology**	**Location**	**Building integration**	**Technology application**	**BIPV type**	**Fluid type and circulation mode**	**Remarks**
Davidsson *et al.* [98]	Hybrid PVT solar window with reflectors	Sweden	Window	Passive heating	Concentrator	➢ Water ➢ Forced	Comparison showed lesser building energy demand by 1000 kWh using roof solar collector.
Corbin *et al.* [99]	Novel BIPVT collector	Netherland	Roof	Heating space and use of hot water for domestic purpose	Flat plate concentrator	➢ Water ➢ Natural	Thermal efficiency of 19% and combined efficiency of 34.9%
Chow *et al.* [91]	PV module with spiral flow absorber	Malaysia	Facade	Electricity production	Flat plate concentrator	➢ Water ➢ Both	Exergy efficiency 12-14%
Wang *et al.* [100]	HP-BIPVT	Guangzhou, China	Facade	Electricity generation	Flat plate concentrator	➢ Water ➢ Forced	Reported 61.1%, 7.8% and 68.9% of thermal, electrical and total efficiency respectively
Pirathepan *et al.* [101]	BiPVT based solar	Kaitaia, New Zealand	Roof & facade	Indoor space heating	Concentrator	➢ Air and water ➢ Natural	Collector efficiency significantly influenced by heat transfer between

Reference	Studied technology	Location	Building integration	Technology application	BIPV type	Fluid type and circulation mode	Remarks
	concentrator						solar cell and absorber
Wang *et al.* [102]	BiPVT system integrated to wall	Huizhou	Wall	Electricity and thermal gain	Flat plate	➢ Air and water ➢ Forced	Domestic hot water supply for 7 hours with 35°C.

2.3 Energy Performance of a Semi-transparent BIPV system

As aforementioned in chapter 1 (Introduction), semi-transparent BIPV systems offer several advantages, such as generating electricity on-site, lowering thermal loads, and improving daylight availability. Therefore, assessing their overall effectiveness requires examining three key aspects: electrical output, optical behavior, and thermal performance.

Lu and Law [34] introduced a method to analyze the combined energy performance of a single-glazed semi-transparent PV window. Their findings showed that this window design could cut the total heat gain of an office building in Hong Kong by nearly 65%, and depending on the HVAC system installed, it could save 900-1300 kWh of electricity annually when compared with a standard clear-glass window.

Peng *et al*. [103] carried out experimental research on a double-skin, semi-transparent PV façade, evaluating its thermal behavior and power generation under different operating modes. Their measurements showed that the ventilated configuration produced around 3% more electricity than the non-ventilated one due to its lower module temperature. In contrast, the non-ventilated setup reached a solar heat-gain coefficient of 0.12 and a U-value of 4.6, while the ventilated mode achieved lower values of 0.10 and 3.4, respectively. This indicates that ventilation improves power output and reduces solar heat gain, whereas the closed mode offers better insulation performance. In a later numerical study, Peng *et al*. [79], assessed the overall energy performance of the same system. Their simulations showed that installing a south-facing PV double-skin façade in an office in Berkeley could reduce net electricity consumption by nearly 50%. The

integrated façade was capable of producing about 65 kWh/m^2 annually and lowering the. room's net electricity requirement to 54.5 kWh/m^2.

Wang *et al.* [104] introduced a new insulating glass unit incorporating semi-transparent a-Si PV modules and evaluated its overall performance. Their findings showed that this design could save 10.7% more energy than standard single-layer low-E glazing and 25.3% more than typical clear-glass windows. In a subsequent study, Wang *et al.* [105] compared the same PV unit with a PV double-skin façade and found that although the new unit achieved higher energy-saving benefits, it exhibited a lower photovoltaic conversion efficiency. Zhang *et al.* [61] conducted numerical simulations to assess the performance of a semi-transparent PV window. Their results indicated that a south-west orientation delivered the best power-generation output for the proposed design. Additionally, the PV window reduced the net electricity demand of a space by 16% compared with a double-glazed window and by 18% relative to a single clear-glass window. The energy-saving capability of semi-transparent BIPV systems has become an important research focus in recent years.

Bahaj [106] demonstrated that thin-film PV window systems can significantly lower heat gain in regions with high cooling demand, reducing annual cooling loads by up to 31%. Radhi [107] through numerical analysis, showed that installing a vertical PV façade improves the thermal behavior of the building envelope and can lower the building's operational energy use by 1.1-2.2%, largely due to reduced heat transfer. In Singapore, several BIPV configurations achieved 16.7-41.3% energy-saving potential for window-to-wall ratios between 70% and 100% [108].

Wong et al., [109], found that semi-transparent c-Si PV windows can decrease HVAC energy consumption by around 5.3% when compared to standard BIPV roof installations. These PV windows also reduced yearly heat gain by about 65% relative to clear-glass glazing. Didone *et al.* [110] using simulation methods, reported that PV windows delivered the strongest overall energy performance among multiple window types evaluated. Li *et al.* [111] further emphasized that the thermal and optical characteristics of PV components substantially influence their overall energy-saving effectiveness.

Chow *et al*. [112] used the ESP-r simulation platform to analyze the performance of different window configurations. Their study showed that single- and double-glazed PV windows could

lower annual cooling electricity use in Hong Kong by 23% and 28%, respectively. Additional findings indicated that these systems could cut summer cooling loads by 26% and 61% compared with typical absorptive-glazed windows [113]. Semi-transparent PV glazing with about 11.7% transparency was able to reduce yearly energy consumption by up to 12%, while a ventilated PV window with 0.45-0.55 transparency achieved as much as 55% energy savings [112]. Olivieri *et al.* [114] performed numerical evaluations on five semi-transparent PV configurations with different window-to-wall ratios and transparency levels. Their results showed that designs with ratios below 22% achieved less than 5.5% energy savings, whereas systems with ratios above 33% provided reductions ranging from 18% to 59% in net energy use. Liao [115] also studied a-Si semi-transparent PV glazing with various transmittance values and concluded that these systems significantly decreased cooling energy requirements compared with conventional glazing. **Table 2.3** provides a consolidated overview of key research findings related to the overall energy performance assessment of semi-transparent BIPV systems.

Table 2.3 Summary of studies evaluating the comprehensive energy performance of semi-transparent BIPV technologies.

Authors	Study Objective	PV Technology Studied	Location	Major Findings
Lu *et al.* [34]	To assess how a semi-transparent PV window affects a building's energy behavior	a-Si PV window	Hong Kong	Window design lowered heat gains by around 65%, reducing cooling demand
Peng *et al.* [103]	To analyze performance of a double-skin semi-transparent PV façade in different operating modes	a-Si double-skin PV facade	Hong Kong	Ventilated mode improved power output and reduced heat gain; non-ventilated mode offered better insulation
Peng *et al.* [79]	To examine the yearly energy impact of a PV double-skin façade	a-Si PV-DSF	Berkeley	System cut net energy use by ~50% and generated about 65 kWh/m² annually

Authors	Study Objective	PV Technology Studied	Location	Major Findings
Wang et al.[104]	To evaluate a newly developed insulating PV glass unit	a-Si insulating PV glass	Hong Kong	Achieved 25.3% and 10.7% higher energy savings compared to clear and Low-E glazing
Wang *et al.* [105]	To compare performance of a PV-DSF with a new insulating PV glass unit	a-Si PV-DSF & insulating PV unit	Hong Kong	New PV unit saved more energy but had lower PV conversion efficiency
Chow *et al.* [112]	To simulate the performance of various PV window types	a-Si PV windows	Hong Kong	Ventilated PV windows (transmittance 0.45–0.55) reduced annual energy use by up to 55%
Olivieri *et al.* [114]	To assess energy performance of five semi-transparent PV glazing systems	a-Si transparent PV glazing	Madrid, Spain	Designs with >33% WWR saved 18–59% of net energy consumption
Liao *et al.* [115]	To compare PV glazing with conventional glazing types	a-Si PV glazing	China	PV glazing showed significantly better energy performance than clear or double glazing
Zhang *et al.* [115]	To evaluate a semi-transparent PV window against an efficient glazing system	a-Si semi-transparent PV window	Hong Kong	Reduced annual electricity demand by 16–18%
Bahaj *et al.* [106]	To analyze cooling-energy reduction using semi-transparent PV windows	a-Si PV windows	Middle East	Cooling load dropped by up to 31% over a year
Radhi *et al.* [107]	To study energy impact of façade-integrated PV modules	a-Si façade-integrated PV	UAE	Total energy use fell by 1.1–2.2%; payback period shortened by ~10 years

Authors	Study Objective	PV Technology Studied	Location	Major Findings
Didone *et al.* [110]	To evaluate daylighting and energy behavior of multiple window systems	a-Si PV windows	Brazil	PV windows reduced energy use by up to 43%, highest among all systems tested
Miyazaki *et al.* [116]	To identify key factors affecting PV window performance	a-Si PV window	Tokyo	Best performance at 40% transmittance and 50% window-to-wall ratio
Ng *et al.* [108]	To assess energy-saving potential of various BIPV technologies	c-Si & a-Si BIPV	Singapore	Achieved 16.7–41.3% energy-saving depending on configuration
Wong *et al.* [109]	To evaluate energy performance of PV roofing systems	a-Si	Japan	PV roofs produced net energy savings between 3%-8.7%
Li *et al.* [117]	To examine thermal and optical factors influencing PV system efficiency	a-Si	Hong Kong	Thermal-optical characteristics strongly affected overall energy performance
Chow *et al.* [113]	To analyze cooling energy performance of various PV window systems	a-Si	Hong Kong	PV windows reduced annual cooling electricity use by 23-28%

2.4 Exergy, exergoeconomic and enviroeconomic analysis

Energy analysis gives an estimation of total energy that the system produces while exergy by involving second law of thermodynamics gives a measure of useful energy obtained in terms of systems irreversibility. By calculating the magnitude of irreversibility, exergy analysis evaluates how efficiently solar energy is used to enhance system performance. In view of this, analyses have been carried out to demonstrate different BIPV/BIPVT system performance based on its exergy analysis. In addition, exergoeconomic analysis that combines both exergy and economic analysis

is performed on BIPVT system to evaluate the system effectiveness. The main goal of exergoeconomic analysis is to evaluate a thermoeconomic system that considers not only the inefficiencies but also the cost and investment necessary to reduce these inefficiencies.

An in-depth review of various solar thermal system and their exergy analysis was provided in the work of [60]. As concluded in the review, exergy analysis can be a useful parametric quantity for evaluating solar thermal systems potential. Further, a combination of both thermal efficiency and exergy efficiency comparison of solar photovoltaic systems gave appropriate results in determining best configuration. Systems chosen for comparison study were solar photovoltaic systems, solar drying systems, solar heating and solar water desalination systems [118].

Fujisawa and Tani [119] using analysed the exergetic performance of a coverless PVT collector to be more enhanced than a single covered PVT. Tiwari *et al.* [120], in their study found that 0.04 kg/s of air flow rate observed an air mass was optimum for gain of electrical and thermal energy in a five air based PVT collector connected in series.

While BIPV technology offers advantages in energy consumption reduction and environmental impact through power generation, challenges exist, such as economic, institutional, technical, and public acceptance barriers hindering its adoption in the building industry [121]. Researchers have extensively analyzed BIPV systems' technical, economic, and environmental aspects, including factors like societal carbon cost, transmission costs, and raw material expenses [122]. Stakeholder collaboration is identified as essential for fostering BIPV adoption, with governments, manufacturers, and professionals playing crucial roles [123]. Geographical location significantly affects BIPV performance, with colder climates proving optimal for efficiency. Despite the aesthetic appeal of PV integration in building facades, challenges like low electrical efficiency and high investment costs persist, impacting public acceptance.

Afrand *et al.* (2019) proposed two innovative hybrid BIPVT systems integrated with Earth-to-Air Heat Exchangers (EAHE) and evaluated their performance based on both energy and exergy analysis. These systems were capable of pre-heating outdoor air during winters and pre-cooling it during summers, while simultaneously generating electricity. A key feature was the use of building exhaust air to reduce PV panel temperatures in summer, thereby functioning as an

exhaust air heat recovery setup. Later, Shittu *et al.* [124](carried out optimization studies on the same systems and identified the configurations that yielded maximum energy and exergy output.

A brief representation of exergy analysis that has been done on some existential PV systems and their major findings are presented in **Table 2.4** below.

Table 2.4 Exergy analysis on some existential PV systems and their major findings

Reference	Type of study	Type of solar thermal system	Key finding
Chow *et al.* [125]	Energy and exergy analysis of PVT collector with and without glazing *Location: Hong Kong*	Water based Flat hybrid PVT Collector	• Higher exergy efficiency was observed for glazed collector than unglazed collector. • For the PVT system to produce more electrical and overall energy output, it is more appropriated to assess the system performance through second law of thermodynamics. • Exergy output from system enhances with incident solar radiation and ambient temperature.
Rajoria *et al.* [126]	Exergy analysis of hybrid PVT array` *Location: India*	Case1: PVT modules with series configuration are connected in parallel. Case2: PVT modules with parallel configuration are connected in series Each case had different flow patterns	• Case2 reported higher overall exergy gain annually by 10.4%. • Due to its higher heat removal capability, case2 gave greater overall thermal energy gain.
Saadon *et al.* [127]	Exergy and exergoeconomic analysis *Location: Nice, France*	Double Skin PV Facade. Comparison of Opaque and different transparency PV modules	• Exergy efficiency of semitransparent PV systems were found to be higher. • Lower L_{en} (Loss rate) and L_{ex} (Loss ratio) values were observed for configuration semitransparent PV than opaque PV modules as the former exhibits higher values for energy and exergy gain.
Kalogirou *et al.* [128]	Exergy analysis *Location: Limassol, Cyprus*	Naturally ventilated BIPVT system	• Exergy efficiency varied from 13%-16% maximum.

Reference	Type of study	Type of solar thermal system	Key finding
			• Increase in outlet fluid temperature results in increase of exergy
Shahsaver *et al.* [38]	Exergoeconomic analysis *Location: Iran*	Roof based BIPVT With AHU based HVAC unit	• Annually, the system could save 3038.83 kWh of thermal energy. • Useful exergy gained annually was 2968.14 kWh. • Loss ratio variation was proportional with variation of channel depth while decreased as mass flow rate increased.
Jha *et al.* [129]	Energy and Exergy analysis *Location: Silchar, India*	PVT collector	• Highest exergy gain was for March corresponding to 0.007kg/s of mass flow rate of air. • Exergy gain in summer was higher than winters because of higher solar insolation
Zheng *et al.* [23]	Exergy+Exergoeconomic *Location: Beijing, China*	Partially covered parabolic trough photovoltaic thermal collector (PCPTPVT)	• For the considered design conditions, PCPTPVT converted 12.42% of solar energy beam to useful electrical power and 61.38% to thermal energy further utilized for heating the fluid. • Maximum electrical efficiency of 12.42% and thermal efficiency of 64.3% was reported.
Rafae and Mohammed [130]	Exergy analysis *Location: Iraq*	Hybrid PVT (roof based) water heating	• Extracted heat from PVT collected which was further utilized for water heating increased PV electrical efficiency 18%. • Systems exergy efficiency varied in between 12-20%.
Rajoria *et al.* [126]	Exergoeconomic analysis *Location: Srinagar, India*	Glazed hybrid PVT collector	• Glazed hybrid PVT when compared with standalone PV system showed lesser thermodynamic loss rate ratio.

In recent years, the combined application of exergoeconomic and enviroeconomic assessments has emerged as a valuable tool in evaluating the performance and sustainability of energy systems. Exergoeconomic analysis, often referred to as thermoeconomics, offers an integrated approach that links the second law of thermodynamics with economic evaluation. It not only helps identify the locations and magnitude of system inefficiencies but also relates them to their economic implications, including the associated costs of exergy losses and the investment required to mitigate them [131]. This approach is particularly useful in optimizing system design by balancing performance and cost-effectiveness. In parallel, enviroeconomic analysis evaluates the environmental costs tied to system operations by quantifying emissions, primarily carbon dioxide, in monetary terms. It allows for identifying options to reduce the environmental burden of a system while considering the long-term economic impact of those reductions. These methods provide significant insight into how BIPV/T systems can reduce CO_2 emissions and improve energy recovery performance, highlighting their potential for integration in energy-efficient building designs [131]. Together, these methods offer a more holistic understanding of energy systems capturing not just how efficiently they perform, but also how their inefficiencies cost us economically and environmentally over time.

Researchers have explored PV technology utilization potential, evaluating parameters such as energy production rate, EPBT, LCCE, NPV, GPBT, and carbon credit to assess environmental and economic performance [132]. Lifecycle Cost Analysis aids in BIPV option selection based on initial and ongoing expenses, aiming to minimize costs while maximizing profitability [133]. Case studies analyzing BIPV systems' performance in Shanghai [100] [134] shed light on payback periods and CO_2 emissions reduction potential, with considerations for factors like electricity costs and FITs. EPBT analyses for mono-crystalline PV systems show varying results due to different energy estimations [135]. However, Nawaz and Tiwari's [136] analysis showed EPBTs ranging from 8 to 21 years for mono-crystalline PV systems, indicating variation due to different energy estimations.

PV module selection criteria can have significant effect in terms of annual saving of the BIPVT systems under Net metering scheme (NEM). Yatim *et al.* [137] evaluated the optimum performance of a 3.3 kW BIPV system based on comparison of different types of PV modules viz.

Mono-crystalline, Multicrystalline, HIT and Thin film PV module for lowest payback period. HIT module demonstrated higher electrical efficiency compared to other PV module technologies. However, for the climate conditions in Penang, Malaysia, the Multi-crystalline PV module, despite having the lowest panel efficiency, proved to be the most cost-effective choice. The LCOE was found to be 4.94 INR/kWh with a payback period of 10.8 years. Lifecycle Cost (LCC) analysis assesses the expenditure associated with energy production. Agarwal and Tiwari [138] concluded that the cost of generation for a BIPV thermal system amounted to US$ 0.1009. Hou *et al.* [139] highlighting key manufacturing processes and the importance of increasing renewable energy use. An average payback period in China, in their study was revealed to be 1.6-2.3 years with significant changes in the manufacturing process specially energy consumption and emission of greenhouse gases. Yu *et al.* [140] compared environmental impact indexes of solar grade silicon production routes in China, noting advantages in the metallurgical route over purification via the modified Siemens process. In additional studies, study on factors responsible for optimization of PV module utilization in buildings, Addition to that were also have examined. As studied by Li *et al.* [141] use of low concentrated module building applications noted a potential 40.5% reduction in EPBT. Lu and Yang [132] investigated BIPV systems in various orientations and observed a maximum difference of 6.7 years in EPBT. These key factors influencing PV system performance on buildings significantly impact LCA studies. These studies are significant because they offer a thorough understanding of the technical, environmental, and economic aspects of BIPV systems. They emphasize the impact of geographical location, PV module choice, and lifecycle costs on BIPV performance and efficiency. By evaluating environmental and economic factors such as CO_2 emissions reduction and energy payback time, these statistical studies enable one to take up the right decision considering the benefits and challenges of BIPV adoption. Additionally, they raise awareness on how to enhance the sustainability and profitability of BIPV systems within the building industry.

Regarding the potential applications of such BIPVT systems, Saadon *et al.* [127] conducted a performance evaluation of a BiSPVT system integrated into a double skin facade in Nice, France. They evaluated CO_2 emission reductions, enviroeconomic impacts, and conducted an exergy analysis. The findings revealed that higher energy and exergy efficiency was seen for

semitransparent BIPVT system compared to opaque ones. This improved efficiency results in a lower loss rate, leading to more favorable economic and environmental outcomes.

Harajli *et al.* [142] analyzed a roof-mounted 1.8kWp monocrystalline PVT system in Lebanon to assess its effectiveness in achieving carbon reduction targets. The study compared the electrical energy gained by the PVT system to the Lebanese electricity grid and found that, using a functional unit of 1kWh, the PVT system, even with PbA batteries, imposed a lower environmental burden compared to the local electricity mix in terms of the per unit energy generated. The EPBT and CO_2 PBT for the system were approximately 16 and 3 years, respectively. This analysis highlights the benefits of implementing such PVT systems, emphasizing their potential for reducing CO_2 emissions, cost savings, and their overall life cycle assessment. Consequently, these systems present a more advantageous alternative to fossil fuel-based energy sources, enhancing both environmental and financial performance while ensuring occupant satisfaction.

So far, limited studies have examined the performance of PVT systems from the perspectives of exergoeconomic and enviroeconomic analyses, although these assessments are crucial to understand the real value and feasibility of such systems beyond just their technical output. Agrawal and Tiwari [143] conducted one of the early exergoeconomic evaluations on glazed air-based PVT systems. Their findings highlighted that, in addition to generating electricity, such systems show better energy-saving potential when compared to standalone PV modules. Moreover, the dual benefit of electricity generation and space heating makes these systems particularly useful for building applications.

Tiwari *et al.* [144] extended this analysis further by assessing a PVT-integrated active solar distillator in the location of Delhi, India. Their work included both exergoeconomic and enviroeconomic evaluations and demonstrated that the proposed configuration could efficiently meet daily requirements of potable water while also supplying DC electricity. Similarly, Tiwari and Tiwari [145] evaluated a hybrid PVT solar dryer and estimated the payback periods on both thermal and exergy grounds. The findings revealed that the payback period in terms of thermal energy generated was found to be about 1.23 years, and the payback period in terms of useful exergy was extended to 10 years.

Singh and Tiwari [146] also presented a detailed multi-dimensional performance evaluation of solar Stills mounted on PVT CPC collectors. They reported that the double-slope configuration outperformed the single-slope design, with exergoeconomic and enviroeconomic parameters higher by approximately 16.2% and 21.5%, respectively.

Further, Tripathi *et al.* [147] undertook a parametric study evaluation to analyze the exergoeconomic performance and potential carbon credits of three variations of series-connected concentrated PVT (CPVT) systems. These included partially covered, fully covered, and conventional N-CPVT configurations. Among these, the conventional fully covered N-CPVT system showed the best results, with an exergoeconomic cost of 17.85 INR per kWh calculated over a 30-year operational lifespan.

These studies collectively reinforce the importance of combining exergy-based performance metrics with environmental and economic indicators. Such a holistic approach is essential for assessing the long-term viability of PVT and BIPVT technologies in both urban and semi-urban applications.

Enviroeconomic analysis focuses on estimating the environmental cost of a system's Lifecycle. It helps quantify environmental burden in terms of economic considerations. In a study conducted by Agrawal and Tiwari, [148] the enviroeconomic evaluation of a glazed PVT air collector revealed that the annual environmental cost was around 36.97 USD when calculated based on energy, and 8.55 USD when considered in terms of exergy. Their findings also suggested that when manufacturing-related energy inputs were accounted for in exergy terms, the overall efficiency of the system dropped by nearly 25%. In another relevant study by Shahsavar and Rajabi [131] where they analyzed the system (air based BIPVT) behavior for climate conditions of Iran. The system was shown to result in an annual CO_2 emission reduction of 5.94 tons. Additionally, the study reported a yearly electrical output of 2259.64 kWh and a useful exergy yield of 19.97 kWh. These results underline the importance of integrating environmental cost assessments alongside technical evaluations for a more comprehensive understanding of system performance.

Table 2.5 presents a summary of literature studies that have examined environmental aspects related to various PVT system configurations and applications. While many of these systems are

designed for integration into buildings, the reviewed studies also highlight alternative applications of PVT systems. Across these investigations, the primary environmental indicators considered include EPBT, carbon dioxide emissions, and system life cycle cost evaluations. The studies were also conducted under a range of climatic conditions, reflecting the adaptability of PVT systems across different geographic and environmental contexts.

Table 2.5 Literature studies which include exergy, exergoeconomic and energy matrices parameters of PVT systems

Reference	Type of PV Cells	Working Fluid	Type of System / Application	Region	Environmental Issues Studied	Lifespan (Years)	Results
Barnwal and Tiwari [149]	Mono-crystalline silicon	Air	Hybrid PVT dryer	India	EPBT, CO_2 emission reduction, LCCE	30	• EPBT ranges from 3 to 5 years • High potential for reducing post-harvest losses • Effective for drying high-moisture agricultural produce • Minimal maintenance with long-term sustainability
Kalogirou and Tripanagnostopoulos [150]	a-Si	Water	Thermal applications in industry	USA	LCA	20	• Economic viability established for high-temperature industrial use • Amorphous PV cells found cost-effective due to lower capital cost • Supports energy independence in industrial sectors
Kumar [151]	Polycrystalline silicon	Water	PVT-assisted solar distillation unit	India	Embodied energy, LCCE, CO_2 emission reduction	15 and 30	• CO_2 emission savings of 32.5 tons over 30 years • Fabrication energy estimated at 3689 kWh (15 years) and 5990 kWh (30 years) • Supports clean water and energy co-generation

Reference	Type of PV Cells	Working Fluid	Type of System / Application	Region	Environmental Issues Studied	Lifespan (Years)	Results
Kumar and Tiwari [152]	Mono-crystalline silicon	Water	Passive vs. active solar still with PVT	India	System cost analysis, EPBT	15 and 30	• EPBT: Passive system 2.9 years, Active system 4.7 years • Active system produced 3.5 times more potable water • Better long-term utility from active setup despite higher initial energy cost
Nayak *et al.* [153]	Mono, Poly, and Amorphous silicon	Air	PVT greenhouse dryer using different PV cell types	India	Carbon credits, EPBT	-	• Mono-crystalline silicon performed best in all environmental indicators • Demonstrated suitability of system for diversified PV cell technologies • Supports integration of solar drying in agricultural practices
Izquierdo and de Agustín-Camacho [154]	Not specified	Water	PVT-powered heat pump microgrid	Madrid, Spain	CO_2 savings, energy balance	-	• CO_2 savings of 836 kg when compared with gasoil boiler • 574 kg CO_2 savings versus natural gas-based heating • Demonstrated the feasibility of clean microgrid-based heating
Tripathi *et al.* [147]	Various	Water and air (varied)	Multiple PVT applications across sectors	India	CO_2 emission reduction	-	• Highlighted role of PVT systems in building-level decarbonization

Reference	Type of PV Cells	Working Fluid	Type of System / Application	Region	Environmental Issues Studied	Lifespan (Years)	Results
							• Demonstrated emission reduction benefits across residential and industrial use • Reinforced national-scale relevance of solar thermal integration
Renno and Petito [155]	Triple-junction	Water	PVT with high concentration applied	Italy	CO_2 mitigation, energy savings	20	• 3376 kg CO2 emissions reduced per year • High concentration was found to be viable solution in Italy from energy and economy point of view
Chow and Ji [156]	Single-crystalline silicon	Water	BIPVT mounted on wall and standalone BAPVT systems	Hong Kong	Cost analysis, EPBT, embodied energy etc.	15 and 30	• EPBT: 2.8 years (BAPVT) and 3.8 years (BIPVT) • GHG-PBT: 3.2 years (BAPVT) and 4.0 years (BIPVT)
Agrawal and Tiwari [157]	Mono-crystalline silicon	Air	PVT tiles with glazing and non-glazing and conventional hybrid PVT air collectors	India	Energy gain from the system, CO_2 mitigation	30	• Unglazed PVT tiles achieved 62.3% more annual CO, savings, while glazed tiles achieved 27.7% more, compared to the conventional PVT. • The overall annual thermal energy and exergy gain of the unglazed PVT tiles was higher by 27% and 29.3%,

Reference	Type of PV Cells	Working Fluid	Type of System / Application	Region	Environmental Issues Studied	Lifespan (Years)	Results
							respectively, compared to the glazed PVT tiles and by 61% and 59.8%,respectively,compared to the conventional PVT
Rajoria *et al.* [158]		Air	Opaque (case A); solar cell tiles (silicon) (case B); semi-transparent (case C)	New Delhi, India	EPBT, carbon credit, life-cycle cost analysis, etc.	20; 25; 30	• Case C showed the minimum EPBT in terms of energy and exergy (0.70 and 1.84 years, respectively). • Case A showed the maximum EPBT

The preceding section has presented an overview of various PVT system configurations and applications, highlighting how environmental assessments have predominantly focused on system-level indicators such as energy payback time, carbon dioxide emission reduction, and exergy and exergoeconomic parameters. While these metrics are valuable for evaluating the overall environmental performance of PVT systems, they often overlook the environmental implications of the individual components that constitute these systems, particularly in the context of building integration. In Building Integrated Photovoltaic Thermal (BIPVT) systems, the choice of materials, fabrication processes, and structural integration with the building envelope introduces additional layers of environmental impact that extend beyond operational energy savings.

The design of BIPVT systems typically involves materials such as glass, aluminum, polymers, insulating foams, and photovoltaic cells, each of which carries its own embodied energy and emissions footprint from extraction through processing and manufacturing. For instance, the production of PV modules involves energy-intensive steps like silicon purification and wafer fabrication, while the use of framing and mounting materials contributes to resource depletion and additional greenhouse gas emissions. Furthermore, the integration of these systems into building facades or roofs can affect thermal insulation, daylight availability, and indoor comfort, all of which have indirect environmental consequences related to building energy consumption.

Therefore, it becomes necessary to shift the focus of environmental assessment toward the component-level evaluation of BIPVT systems, particularly through the lens of Life Cycle Assessment (LCA). This approach allows for a more granular understanding of which materials and design decisions contribute most to environmental impact, and helps identify opportunities for optimization through material substitution, recycling strategies, or design improvements. The following section critically reviews literature that specifically addresses the environmental impacts of BIPVT components, with attention to material selection, embodied carbon, toxicity, and end-of-life management practices. This component-level analysis is essential for guiding future BIPVT designs that are not only energy-efficient but also environmentally responsible across their entire life cycle.

2.5 Life Cycle Analysis: Environmental Impacts of PVT Systems

BIPV technology although offers advantages in energy consumption reduction and environmental impact through power generation, challenges exist, such as economic, institutional, technical, and public acceptance barriers hindering its adoption in the building industry [121]. Researchers have extensively analyzed BIPV systems technical, economic, and environmental aspects, including factors like societal carbon cost, transmission costs, and raw material expenses [122]. Stakeholder collaboration is identified as essential for fostering BIPV adoption, with governments, manufacturers, and professionals playing crucial roles [14]. Geographical location significantly affects BIPV performance, with colder climates proving optimal for efficiency. Despite the aesthetic appeal of PV integration in building facades, challenges like low electrical efficiency and high investment costs persist, impacting public acceptance.

Researchers have explored PV technology utilization potential, evaluating parameters such as energy production rate, EPBT, LCCE, NPV, GPBT, and carbon credit to assess environmental and economic performance [132]. Lifecycle Cost Analysis aids in BIPV option selection based on initial and ongoing expenses, aiming to minimize costs while maximizing profitability [133]. Case studies analyzing BIPV systems performance in Shanghai [159] and Bahrain [134] shed light on payback periods and CO_2 emissions reduction potential, with considerations for factors like electricity costs and Feed in Tariffs (FITs). EPBT analyses for mono-crystalline PV systems show varying results due to different energy estimations [135]. However, Nawaz and Tiwari's [136] analysis showed EPBTs ranging from 8 to 21 years for mono-crystalline PV systems, indicating variation due to different energy estimations.

The environmental performance of Building Integrated Photovoltaic Thermal (BIPVT) systems is shaped by a range of design and material-related choices. Several studies have explored these in depth, highlighting that materials used in different parts of the system, such as PV modules, facades, walls, and even storage components can significantly influence the system's overall environmental impact. The type, lifespan, and end-of-life handling of these materials (such as the extent of recyclability or use of secondary materials) all matter [160].

The type of PV cell used is also a crucial factor. Some technologies involve hazardous materials in the manufacturing process. This not only raises environmental concerns during production but also influences end-of-life management [160]. Proper recycling protocols and the use of secondary materials are recommended to minimize such impacts.

The working fluid used in the thermal recovery section affects overall system efficiency. Studies comparing air-based and water-based systems show that air-based systems generally have higher energy and CO_2 payback times due to lower heat transfer efficiency [161]. This choice directly links to the carbon footprint of the system across its operational phase.

Another determinant is how the BIPVT unit is integrated into the building. Systems installed on rooftops, facades, or as shading devices show different solar exposure levels depending on tilt angle, orientation, and geographic latitude. Improper integration or suboptimal design leads to shadow effects and loss in energy output, thereby worsening the environmental balance of the system [162].

The use of natural ventilation, where feasible, can reduce the energy load needed for forced air movement. This design simplification not only lowers operational energy consumption but also reduces system complexity [128]. Systems with passive airflow show better environmental performance, particularly in designs that do not require continuous fan operation.

Studies also underline that BIPVT systems contribute positively to energy-efficient buildings by reducing external electricity needs and supporting net-zero energy goals. Reduced grid dependency and CO_2 emissions are among the commonly cited benefits [163] In cases of semi-transparent PV modules, daylight savings contribute to reduced lighting loads, indirectly enhancing the environmental profile of the building as a whole [164] [165].

The design of thermal storage, especially when including materials with high embodied energy or large metal content, needs careful consideration. Systems designed with low-impact materials and efficient insulation tend to perform better across life cycle impact indicators [166].

Country-specific electricity generation mix also plays a major role in determining the impact. In nations with fossil-dominated grids, the embedded emissions of manufacturing and operation increase significantly. Conversely, in cleaner grids, the relative life cycle impacts are lower [160].

Furthermore, for applications in agriculture such as greenhouses, integration of BIPVT systems brings both thermal and electrical benefits, supporting low-carbon agriculture. This adds a new dimension to their use beyond residential and commercial buildings. If the BIPVT system is integrated with energy storage, particularly with battery units, the impact of battery type and chemistry becomes important. Batteries with materials like lead or nickel can raise toxicity indicators, while lithium-based batteries have a different profile, often dependent on supply chain and recycling infrastructure [167].

Finally, because BIPVT systems are integrated directly into the building envelope, they influence the building's total environmental performance, both directly (from material impact) and indirectly (for example, through enhanced daylighting that reduces indoor lighting loads) [168] [165]. This makes it essential to assess the BIPVT not in isolation, but as an integrated component of the building. **Table 2.6** presents a summary of recent studies on Building-Integrated Photovoltaic Thermal (BIPVT) systems, highlighting system configurations and their environmental implications.

Table 2.6 Key parameters related to BIPVT environmental profile.

Author (Year)	Type of BIPVT System and Description	Relation to Environmental Performance
Saadon *et al.* [163]	BIPVT in a net-zero energy office building	Decrease in building cooling needs
Lin *et al.* [169]	PCM-enhanced building in combination with a roof-integrated PVT and ventilation	Combination of a roof-integrated PVT system with other building components
Gholampour and Ameri [170]	Wall-integrated PVT modules with transpired collectors	Transpired plate and air-channel casing material: steel
Chen and Yin [140]	BIPVT panel as a multi-functional roofing system	Replacement of the materials of a roof
Khaki *et al.* [171]	Glazed and un-glazed BIPVT configurations	Use of a glass cover over the PV modules means: 1) use of an additional component/material, 2) increase in PVT thermal performance, 3) decrease in PVT electrical performance
Gautam and Andresen [93]	BIPVT vs. solar thermal and Building-Integrated Photovoltaic (BIPV) technologies: investment	In cold climates, BIPVT technology can be competitive (in comparison to traditional technologies) but only in certain cases

Author (Year)	Type of BIPVT System and Description	Relation to Environmental Performance
	price ratios; utility rates; weather conditions	(e.g. favourable electricity to heat price ratio)
Tiwari and Tiwari [147]	BIPVT for heating of slurry for a biogas plant: greenhouse-integrated configuration	BIPVT: energy-savings in the frame of agricultural applications
Deo *et al.* [164]	Semi-transparent BIPVT for roof-integrated applications	Influence of BIPVT on the room temperature affects the energy consumption of the building e.g. in terms of air-conditioning
Buonomano *et al.* [172]	Combination of adsorption chiller with BIPVT	Primary-energy savings and reduction in CO_2 emissions
Asaee *et al.* [173]	BIPVT with heat pump	Reduction in greenhouse-gas emissions and energy savings
Bigaila and Athienitis [174]	Combination of BIPVT with heat pump and PCM	Reduction in power demand
Assoa *et al.* [175]	BIPVT for a drying system (drying of fodder)	Energy savings in agriculture
Piratheepan and Anderson [176]	Building-Integrated Concentrating Photovoltaic/Thermal (BICPVT) for facade-integrated applications	BICPVT systems offer benefits in the frame of net zero energy buildings
Wang *et al.* [177]	The effect of frame shadow on BIPVT performance	Frame shadow reduces PV efficiency
Debbarma *et al.* [178]	Weatherproofing; insulation	BIPVT replaces the materials e.g. of a facade but, at the same time, new materials (in order to achieve weatherproofing and insulation) are used
Moreno *et al.* [179]	BICPVT based on concentrators of cylindrical shape	Modelled system: partial covering of thermal/electrical needs by using a radiant floor and a heat pump for space heating/cooling; an electrical circuit that offers both direct consumption and battery storage was considered
Gupta and Tiwari [180]	Heat capacity and water flow (evaporative cooling) over semi-transparent BIPVT modules	The water that flows over the PV modules offers an increase in PV cell efficiency; this means higher power output over system lifespan and improvement of certain environmental indicators

Author (Year)	Type of BIPVT System and Description	Relation to Environmental Performance
Agathokleous *et al.* [181]	BIPVT with natural ventilation	By adopting natural ventilation there is no need for energy inputs in order to power mechanically driven fans
Shahsavar and Rajabi [182]	Energy and enviro-economic analysis of BIPVT configurations	Reduction in CO_2 emissions and energy savings

Table 2.7 summarizes key studies on the life cycle assessment (LCA) of photovoltaic systems, highlighting panel types, installation methods, locations, tools used, methodologies, and main findings. It provides a quick comparison of environmental performance across different PV technologies and regions.

Table 2.7 Key studies on the life cycle assessment (LCA) of photovoltaic systems

Author (Year)	PV Panel Type	Type of Installation	Location	Software & Database	Methodology	Results
Zhiqiang Yu *et al.* [140]	Multi-crystalline silicon (metallurgical route)	Ground-mounted, Grid-connected	Ningxia, China	Balance v4.7, CLCD v0.8	LCA based on ISO 14040 & 14044; ECER-125 & ISCP 2009	EPBT = 3.06 years; Environmental impact 56–66% lower than other nations' PV; Retirement stage yields 99.5% benefit
Lu & Yang [132]	Single-crystalline silicon	Roof-mounted, Building-integrated	Hong Kong	Not specified	EPBT and GHG Payback Time	EPBT = 7.3 years; GHG Payback = 5.2 years
Hou *et al.* [139]	Mono & Multi-crystalline silicon	Large-scale, Grid-connected	China	Not specified	LCA including EPBT & GHG emissions	EPBT = 1.6-2.3 years; GHG = 60.1-87.3 g CO_2 eq/kWh
Fu *et al.* [183]	Multi-crystalline silicon	Ground-mounted	China	GaBi4, Ecoinvent	PED, EPBT	PED = 12.61 MJ/Wp; EPBT = 2.2-6.1 years
Zhang *et al.* [184]	mc, sc, a-Si (modified Siemens)	Roof-mounted	Southern Europe	SimaPro 7.3.3, Ecoinvent 2.2	CED, GWP, EPBT	EPBT = 0.68-1.96 years; GWP = 15.8-38.1 g CO_2 eq/kWh
Alsema [185]	Multi & Amorphous	Roof-mounted	US	SimaPro 6.0	EPBT, NER, CO_2	EPBT = 3.2-7.5 years; CO_2 = 34.3-72.4 g/kWh
Richards & Watt [186]	Single-crystalline	Distributed, Roof-mounted	Singapore	Not specified	EPBT, CO_2	EPBT = 1.8-5.87 years; GWP = 68–217g CO_2 eq/kWh
Stoppato [187]	Multi-crystalline (UCC)	Grid-connected, Roof-mounted	EU, Austria, US	Boustead Model V5.0	EPBT, CO_2	EPBT = 3.3-6.6 years; CO_2 = 4–840 g/kWh

Author (Year)	PV Panel Type	Type of Installation	Location	Software & Database	Methodology	Results
Pehnt [188]	Mono, Multi, CdTe	Large-scale, Grid-connected	China	Not specified	EPBT, CO_2	EPBT = 1.8-2.5 years; CO_2 = 43–54 g/kWh
Fthenakis & Kim [189]	mc, sc, CdTe	Roof-mounted	Southern Europe	RMP, ENSAD	EPBT, CO_2	EPBT = 1.0-2.7 years; GWP = 20-45 g CO_2eq/kWh
Zhao *et al.* [159]	Multi-crystalline (UCC)	Large-scale, Ground-mounted	Greece	GaBi, Ecoinvent	EI99	CO_{2eq} = 2.38-6.34 g/kWh
Saygin *et al.* [190]	mc, sc, a-Si	Ground-mounted	Spain	SimaPro 6.0	EPBT	EPBT = 3.67-4.94 years (mc), 7.08-9.57 years (sc), 3.43-4.45 years (a-Si)

The performance of Photovoltaic Thermal (PVT) systems from an environmental standpoint is influenced by a range of interconnected factors including PV cell material, choice of heat transfer fluid, sunlight concentration techniques, and the use of alternative construction materials like polymers. Innovations such as building integration type, application context, incorporation of reflectors, recycling practices, and material durability also significantly shape the environmental profile of PVT systems.

While many existing studies emphasize metrics like energy payback time (EPBT) and CO_2 emissions, these offer only a partial understanding of the systems lifecycle impacts. A clear gap remains in the adoption of more holistic Life Cycle Impact Assessment (LCIA) methods such as ReCiPe midpoint and endpoint approaches, which can capture broader environmental trade-offs across multiple impact categories. Furthermore, current literature often underrepresents comprehensive LCA studies on advanced configurations such as BIPVT and their industrial or commercial applications.

Thus, future research should expand beyond conventional indicators to incorporate diverse environmental impact metrics, especially for integrated and application-specific PVT systems. This approach will not only deepen our understanding of their sustainability potential but also inform more effective design, policy, and deployment strategies aligned with low-carbon development goals.

In line with these insights, our investigation will involve a detailed analysis of BIPVT components using comprehensive life cycle assessment (LCA) methodologies, aiming to evaluate their broader environmental impacts beyond conventional indicators like EPBT and CO_2 emissions.

2.6 Scope of Present Work

While several studies have been conducted on photovoltaic thermal (PVT) and building-integrated photovoltaic (BIPV) systems, there are still some important gaps that need to be addressed, especially for cold climatic regions. Most research available till now focuses on standalone or roof-mounted systems using monocrystalline or polycrystalline modules and analyses their performance mainly from energy and exergy perspectives. However, there is very limited work that looks into a facade-based, semi-transparent building-integrated photovoltaic thermal (BiSPVT) system, particularly one that includes a forced ventilation mechanism for enhanced thermal output. The following key research gaps have been outlined:

- **Inadequate evaluation under varied weather conditions:** Most previous studies use average or ideal weather data. This work addresses the gap by considering four different types of weather conditions—Type a (clear), Type b (hazy), Type c (hazy and cloudy), and Type d (cloudy), across each month of the year. Such detailed categorization has not been adopted widely in earlier research and helps in understanding realistic system behavior.
- **Lack of comprehensive lifecycle cost and environmental analysis:** Although BIPV economic viability have been widely studied, detailed lifecycle assessments (LCA) assessing the long-term feasibility and environmental impact of adopting BiSPVT systems are missing, which is an important aspect of sustainable building design.
- **Limited sensitivity analysis for BiSPVT frameworks:** Work on how variations in system design or operating conditions affect BiSPVT performance is limited. Sensitivity analysis is crucial for optimization, yet this aspect remains underrepresented in current literature.

Based on the current challenges and research gaps, the following objectives have been addressed in the present investigation:

I. To develop a numerical thermal model for a semi-transparent ventilated PV facade that will enable to investigate its potential or advantages in reducing the energy consumption and heating load at cold climatic sites.
II. To study the annual energy performance for a semi-transparent ventilated PV facade for cold climatic zone, Srinagar, India.
III. To conduct exergy, exergoeconomic, and enviroeconomic analyses of the proposed PV facade system.
IV. To perform a life cycle assessment to determine the long-term environmental and economic impacts of the system.

2.7 Summary of the Chapter

This chapter has presented a detailed review of the existing research carried out in the area of photovoltaic thermal systems, particularly focusing on their integration in building structures. Special attention has been given to building-integrated photovoltaic thermal (BIPVT) systems, with an emphasis on their energy performance, exergy behavior, economic viability, and environmental impact. The review covered different types of PVT configurations, working fluids, system layouts, and their respective applications including those beyond buildings such as crop drying and water distillation. The studies considered have highlighted the role of such systems in reducing dependency on conventional energy and enhancing thermal and

electrical energy utilization. Similarly, enviroeconomic investigations provided useful insights into environmental cost analysis, linking carbon emissions and system sustainability with long-term operational impact. In addition to the performance-based literature, component-level environmental impacts of BIPVT systems were also explored. These include embodied energy, environmental cost of materials, recyclability, and end-of-life handling.

Based on the critical review, specific research gaps have been identified, particularly the lack of detailed and location specific environmental assessments of semi-transparent BIPVT facades under cold climate conditions. These gaps form the foundation for the present research. The objectives of the study have been developed considering these gaps and a structured methodology has been framed to address them effectively. The next chapter (Chapter 3) outlines this methodology in detail, including the modeling framework, numerical analysis, and the approach adopted for evaluating exergy, exergoeconomic, and environmental performance of the proposed BIPVT system.

3

Methodology and Modeling

Chapter Outline:

CHAPTER 3: METHODOLOGY AND MODELING

3.1 Introduction

This chapter consist of the detailed methodology involving a comprehensive simulation and analysis framework for evaluating the performance of the BiSPVT facade system. Starting with development of 1-D thermal model with the input of geometric design parameters, ambient temperature, wind speed, and solar radiation (beam and diffuse), followed by the estimation of total solar radiation incident on the facade using the Liu and Jordan model for a vertical surface ($\beta = 90°$). Heat transfer coefficients are then calculated for various system components, enabling the determination of room temperature (T_r), outlet fluid temperature (T_{fo}), and average fluid temperature (T_f). Using these results, the PV module temperature and corresponding electrical and thermal efficiencies under different weather types (a, b, c, d) are computed to estimate energy output over hourly, daily, and monthly periods. The analysis is extended to determine overall thermal efficiency and heat gain.

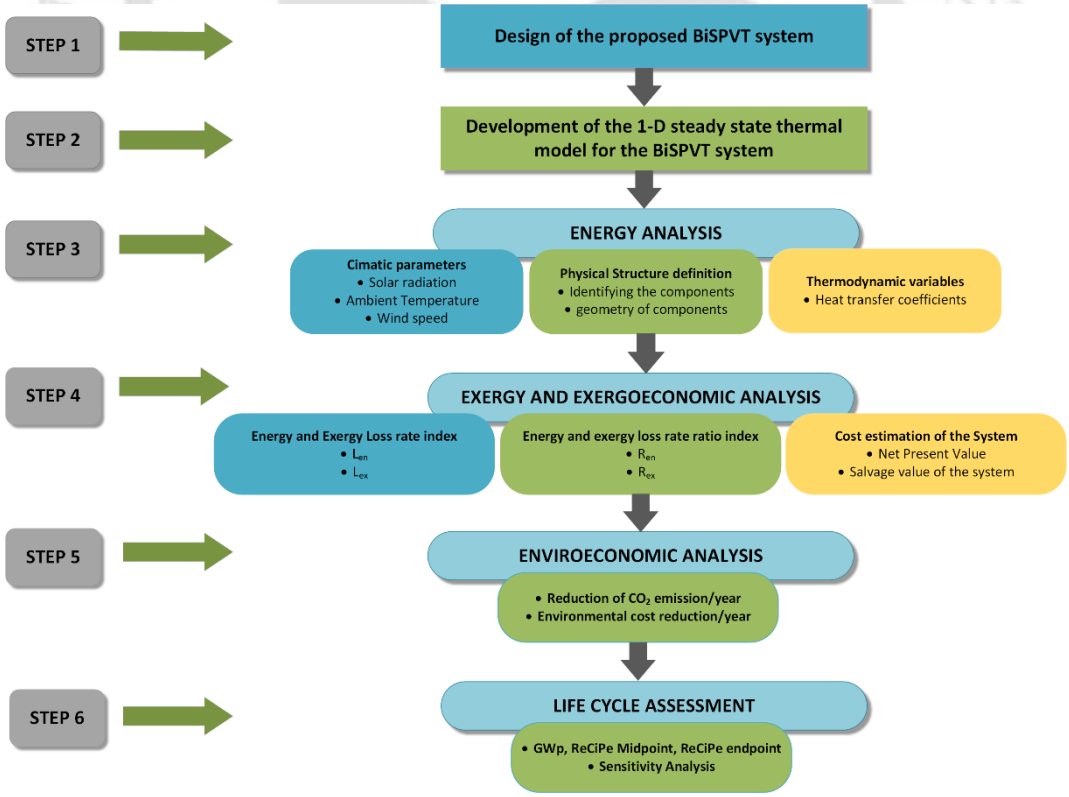

Fig. 3.1 Overall Research Framework

Subsequently, energy, exergy, and exergoeconomic analyses are conducted, supported by thermal loss evaluations. A life cycle assessment (LCA) is performed using SimaPro, integrating inputs from exergy and cost estimation parameters (NPV, L_{en}, L_{ex}, R_{en}, R_{ex}). Finally,

a sensitivity analysis is conducted to evaluate the impact of variable parameters on system performance, concluding the simulation workflow. The overall research framework is given in **Fig. 3.1.**

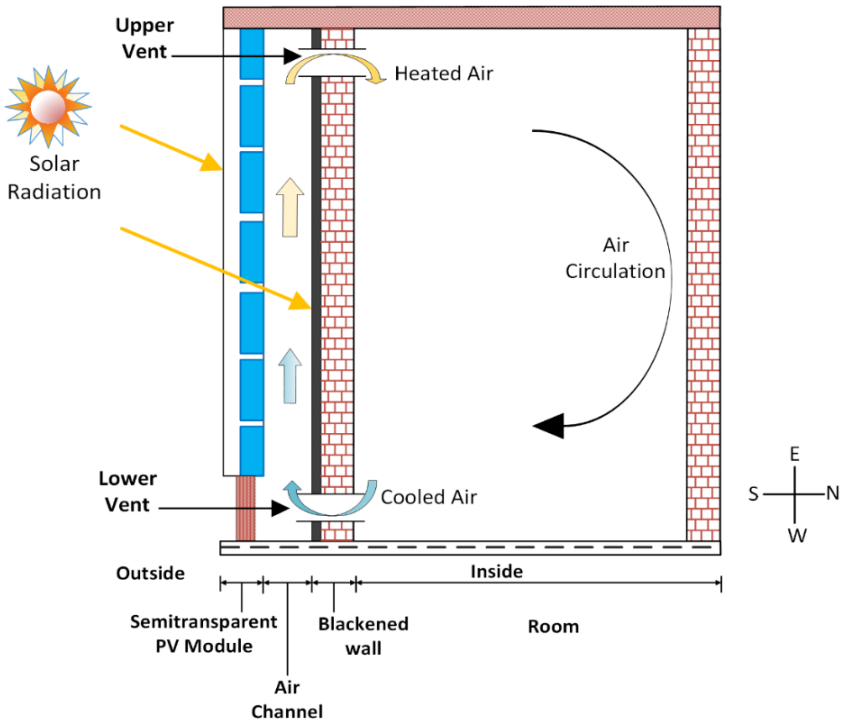

Fig. 3.2 Configuration of the BiSPV Facade system

3.2 System Description

The system comprises of three layers: PV glass panel, an air channel in between, followed by a black painted wall to enhance the absorption of solar radiation intensity. Principal motive behind the considered configuration of BiSPV facade is to improve PV panel electrical efficiency by cooling the surface of PV module in addition to space heating of indoor space. Proposed system configuration is shown in **Fig. 3.2**.

Solar radiation incident on the packing area of the PV module gets absorbed by the solar cell and the solar radiation incident on non-packing area of PV module gets transmitted directly through the glass and absorbed by the blackened wall. The air within the cavity gets heated through convection from the blackened wall and from the rear side of the PV module. Heated air within the cavity rises up throughout its length and is directed to the indoor space. During night-time, the heat stored in the wall is released to the indoor environment by the process of convection and radiation, thereby contributing to space heating. This cycle of air movement continuous circulating the air between cavity and room. Configuration of the BiSPV Facade

system is shown in **Fig. 3.2**. **Fig. 3.3** shows the various heat transfer mechanisms taking place in the PV facade system.

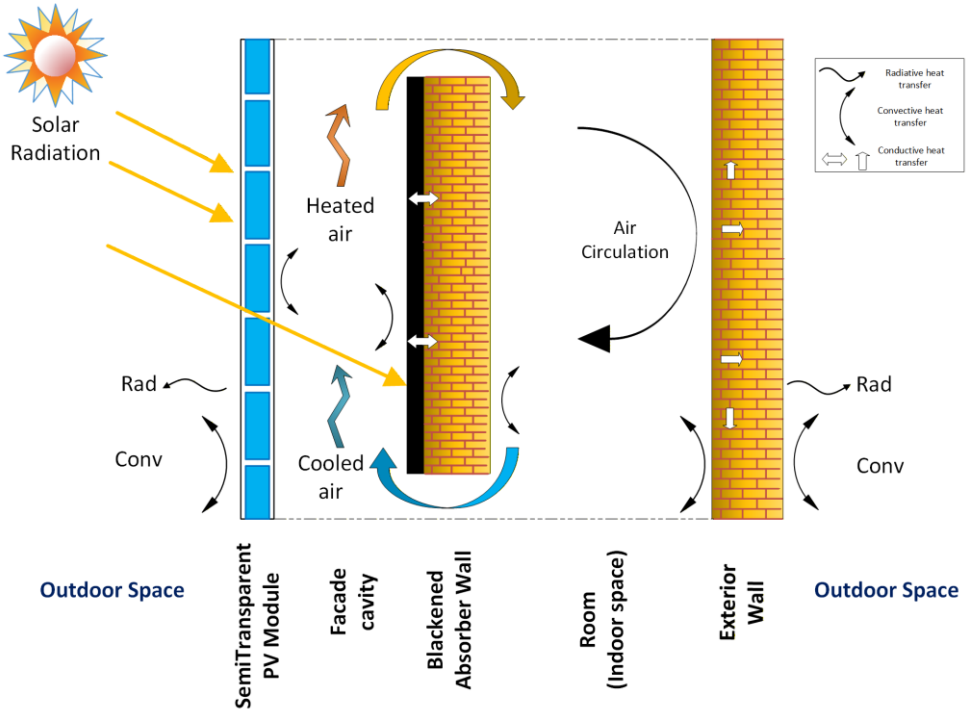

Fig. 3.3 Heat transfer mechanisms in the BiSPV Facade system

Specification of PV module used in the BiSPVT facade system is given in **Table 3.1.** The room considered for modelling has been assumed a dimension of 3.6m(L) x 3m(B) x 3.2m(H). The construction materials for the wall of a room consist of brick, cement and insulation. Properties of different layers of the wall is given in **Table 3.2.**

Table 3.1 Specification of PV module used in the PV facade system

Design parameters		
Component	**Dimension**	**Specification**
PV Module	Dimension of each module = 0.605m x 1m. No of c-Si solar cell per module=36 (circular in shape) Number of PV module used: 14	<u>Rating of the PV module (at STC):</u> P_{max} = 115W (each PV module) V_{mp} = 17V I_{mp} = 6.5A V_{oc} = 21V I_{sc} = 7.4A FF = 0.7 η_o = 19% β_o= 0.045%/°C

Table 3.2 Properties of wall considered for the room

Material	Thermal conductivity (W/mK)	Thickness (m)
Brick	0.6	0.12
Cement	0.6	0.04
Insulation	0.049	0.04

3.3 Thermal Modeling of the BISPVT Facade

The 1-D steady state thermal model follows an established methodology by Gaur *et al.* [26] where they have studied the roof integrated system. In present study we have numerically assesses the south facing PVT facade. The numerical modeling framework in a flowchart has been represented in **Fig. 3.4**. Schematic of thermal resistance network of the BiSPVT system is shown in **Fig. 3.5**.

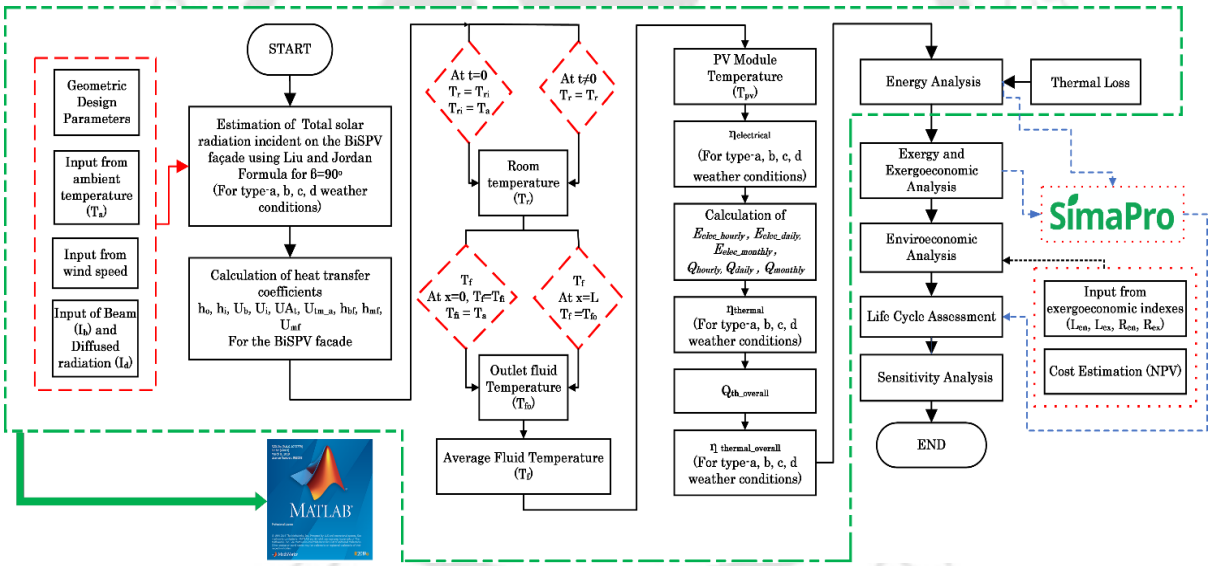

Fig. 3.4 Numerical Modeling framework

In addition to numerical modeling, the systems performance has been evaluated in terms of Life Cycle Assessment (LCA). The Life Cycle Assessment (LCA) of the BiSPVT facade system has been conducted using SimaPro in accordance with ISO 14040:2006 and ISO 14044:2006, covering life cycle inventory, impact assessment, and interpretation. LCA provides a systematic framework to evaluate the environmental performance of PV and PVT technologies by accounting for impacts associated with material extraction, manufacturing, installation, operation, and end-of-life stages. This assessment is particularly relevant for

building-integrated PVT systems, as they replace conventional building envelope materials and directly influence the overall environmental footprint of the building.

In the present study, the numerical outputs obtained from the detailed energy and exergy evaluation of the BiSPVT façade, as developed through the simulation framework, are incorporated as input parameters in SimaPro. These include quantified thermal energy gains, electrical energy generation, and exergy performance indicators over the system's operational lifespan. Integrating these performance-based outputs into the LCA model ensures consistency between the thermo-energetic analysis and the environmental assessment, thereby enabling a holistic evaluation of the BiSPVT system's sustainability performance.

Certain assumptions have been considered while formulating the energy balance equations for each component of the BiSPV facade:

1. 1-D heat conduction in quasi steady-state is considered.
2. Ohmic losses throughout the metallic contacts of PV module and through solar cells are considered negligible.
3. Uniform distribution of temperature throughout the surface of each component of BiSPV facade.
4. Average value of fluid temperature is considered throughout the length of the air cavity.
5. Physical air properties remain constant throughout the operating temperatures
6. The room is considered to be thermally insulated.

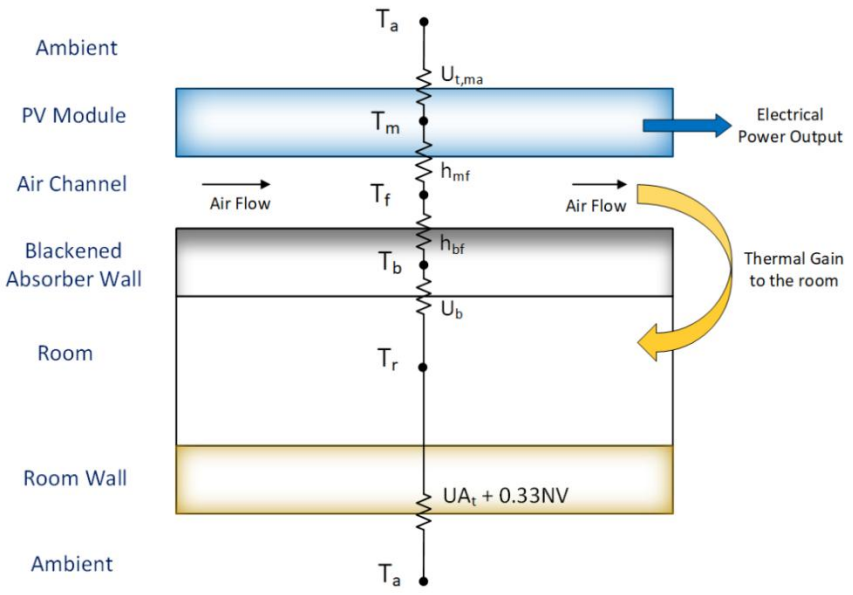

Fig. 3.5 Schematic of thermal resistance network of the BiSPVT system

Thermal resistance network for the BiSPVT system is shown in **Fig. 3.5** considering different heat transfer coefficient associated with each layer. Energy balance of each components are given as:

1. **PV Module**

$$\alpha_c \tau_g \beta_c I(t) A_m = [U_{t,ma}(T_m - T_a) + h_{mf}(T_m - T_f)]A_m + [\eta_m I(t) A_m] \quad (3.1)$$

Term on left indicates the total solar radiation available in the PV module which equals to summation of useful energy output and losses. Losses here are in the form of heat transfer from PV module to ambient and from PV module back surface to air cavity. The term $\eta_m I(t) A_m$ represents the useful electrical output from the PV module.

Equation (3.1) represents the expression for module temperature as,

$$T_m = \frac{[\alpha_c \tau_g \beta_c I(t)] + (U_{t,ma} T_a) + (h_{mf} T_r) - (\eta_m \mathrm{I(t)})}{U_{t,ma} + \mathrm{h}_{mf}} \quad (3.2)$$

Where,

$$U_{t,ma} = [\frac{L_g}{K_g} + \frac{1}{h_o}]^{-1} \quad (3.3)$$

$$h_{mf} = [\frac{L_g}{K_g} + \frac{1}{h_{bf}}]^{-1} \quad (3.4)$$

1. **Blackened absorber plate**

$$\tau_g{}^2 \alpha_b (1-\beta) I(t) A_m = [h_{bf}(T_b - T_f) + U_b(T_b - T_r)]A_m \quad (3.5)$$

Absorber plate placed in between air cavity and room gets heated directly through the non-packing area of semi-transparent PV module and interaction of heat occurs between Absorber wall to room and absorber wall to air cavity. Term on left indicated the heat gain by the blackened absorber wall from the solar radiation directly incident on it and terms on left represents the heat transfers taking from the absorber wall.

T_b Can also be written as:

$$T_b = \frac{\{\tau_g^2 \alpha_b (1-\beta) I(t)\} + (h_{bf} T_f) + (U_b T_r)}{h_{bf} + U_b} \quad (3.6)$$

where,

$$h_{bf} = \frac{K}{L} 0.332\, Re_L^{0.5} P_r^{0.33} \tag{3.7}$$

Re_L and P_r represents dimensionless Reynolds Number and Prandtl Number respectively.

2. Air in the air channel

$$\left[h_{mf}(T_m - T_f) + h_{bf}(T_b - T_f)\right] b dx = \dot{m}_f C_f \frac{dT_f}{dx} dx \tag{3.8}$$

The useful energy gain in consideration with this layer is the thermal energy gain directed upper vent to the room (term on right) and exchange of heat occurs between PV module -fluid and absorber wall-fluid.

From equations (3.1) and (3.6) substituting the values of T_m and T_b into (3.8), we obtain the value of T_{fo} (outlet fluid temperature) and T_f (average fluid temperature):

Solution of T_f is given in the form differential equation as:

$$T_f = \frac{A}{B}[1 - (exp(-Bx)] + T_{fi}(exp(-Bx) \tag{3.9}$$

Applying boundary condition to the above,

When, x = 0, $T_f = T_{fi}$, T_{fi} is the initial fluid temperature

x = L, $T_f = T_{fo}$, T_{fo} is the outlet fluid temperature and L is the air duct length considered in the configuration.

Thus,

$$T_{fo} = \frac{[(AT)I(t)b] + (U_{fa}T_a b)}{(U_{fa} + U_{fr})b}[1 - exp(-BL)] + T_{fi}\exp(-BL) \tag{3.10}$$

Where,

$$U_{fa} = \frac{U_{t,ma} h_{mf}}{U_{t,ma} + h_{mf}}$$

$$U_{fr} = \frac{U_b h_{bf}}{U_b + h_{bf}}$$

Average fluid temperature obtained as,

$$T_f = \frac{1}{L}\int_{x=0}^{L} T_f\, dx \tag{3.11}$$

$$T_f = \frac{[(AT)I(t)b) + (U_{fa}T_a b)]}{(U_{fa} + U_{fr})b}\left\{1 + \frac{exp(-BL)}{BL}\right\} - T_{fi}\frac{(\exp(-BL)-1)}{BL} \quad (3.12)$$

3. Room air

$$\dot{m}_f C_f(T_{fo} - T_{fi}) + U_b(T_b - T_r) = M_a C_a \frac{dT_r}{dt} + UA_r(T_r - T_a) + 0.33NV(T_r - T_a) \quad (3.13)$$

Input while formulating room air energy balance equation is thermal gain through the duct to room and convective heat transfer from absorber wall to room. Losses are by means of heat loss due to air changes and through the openings from doors and windows.

Upon substituting from equation (3.10) and (3.12) the values of T_{fo} and T_f respectively in the energy balance equation for room air (3.13), we have expression for T_r as:

$$\frac{dT_r}{dt} + aT_r = f(t) \quad (3.14)$$

The solution of the above expression is given by,

$$T_r = \frac{f(t)}{a}\{1 - (e^{-at})\} + T_{ri}(e^{-at}) \quad (3.15)$$

where,

$$a = \frac{(F_r U_{fa} b) + UA_t + 0.33NV}{M_a C_a}$$

$$f(t) = \frac{[F_r(AT)I(t)] + [(F_r U_{fa} b) + UA_t + 0.33NV]T_a}{M_a C_a}$$

$$F_r = \frac{\dot{m}_f C_f\{1 - exp(-BL)\}}{(U_{fa} + U_{fr})b}$$

PV module electrical efficiency which is dependent on solar cell operating temperature is given as:

$$\eta_m = \eta_o[1 - \beta_o(T_m - T_o)] \quad (3.16)$$

Substituting the values of $(T_m - T_o)$, we have,

$$\eta_m = \frac{(1 - \beta_o[B + C - T_o])}{1 - D - (E \times F)} \quad (3.17)$$

where,

$$B = \frac{\alpha_c \tau_g \beta I(t) + T_a U_{tm,a}}{h_{mf} + U_{tm,a}}$$

$$C = \frac{h_{mcf}}{h_{mf} + U_{tm,a}} \left\{ \frac{(\alpha\tau)_{eff} I(t) + U_{fa} b T_a}{b(U_{fa} + U_{fr})} (1 + \theta) + A \left\{ \frac{U_{fr}(1 + \theta)}{U_{fa} + U_{fr}} - \theta \right\} \right\}$$

$$D = \left[\frac{\eta_0 \beta_0 I(t)}{U_{tm,a} + h_{mf}} \left(1 + \frac{H_{f1} h_{mf}}{b(U_{fa} + U_{fr})} (1 + \theta) \right) \right]$$

$$E = \frac{\eta_0 \beta_0 I(t) H_{f1} h_{mf} F_R}{U_{tm,a} + h_{mf}} \left(\frac{U_{fr}(1 + \theta)}{U_{fa} + U_{fr}} - \theta \right)$$

$$F = \frac{(1 - \exp(-at))}{F_R b U_{fa} + (UA)_t + 0.33NV}$$

$$\theta = \frac{(\exp(-BL) - 1)}{BL}$$

$$A = \left(\frac{F_R (\alpha\tau)_{eff} I(t)}{F_R b U_{fa} + (UA)_t + 0.33NV} + T_a \right) (1 - \exp(-at)) + T_{r0} \exp(-at)$$

The various heat transfer coefficients associated with energy balance equations are calculated using following relations:

Free convection taking place between PV module and ambient:

$h_o = 5.7 + 3.8v$; v = wind speed on PV module top surface.

Free convection taking place between room wall and ambient:

$h_i = 2.8 + 3v$; v = wind speed on PV module back surface

Heat transfer coefficient for air circulation of fluid in the air channel:

$$h_{bf} = \frac{K}{L} 0.332 Re_L^{0.5} P_r^{0.33}$$

Analytical expressions considered for performance evaluation of BiSPVT facade system:

Hourly electrical energy in Watt (W) developed by the PV module is given by,

$$E_{elec,hourly} = \eta_m \times A_{PV} \times I(t) \tag{3.18}$$

Hourly electrical energy production from the PV module in Watt (W) is given by,

$$E_{elec,daily} = \sum_{i=1}^{N_i} \frac{E_{elec,hourly,i}}{1000} \tag{3.19}$$

Where, N_i denotes number of iterations for sunshine hours in a day.

Thermal energy gain from the system with air cavity is stated as,

$$\dot{Q}_{hourly,i} = \dot{m}_f C_f (T_{fo} - T_r) \tag{3.20}$$

Daily thermal energy (kWh) after summing it for considered sunshine hours per day is given by,

$$Q_{daily} = \sum_{i=1}^{N_i} \frac{\dot{Q}_{hourly,i}}{1000} \tag{3.21}$$

The electrical energy equivalent of its thermal energy can be converted by considering a factor of 0.38, termed as the electrical power generation efficiency of a conventional power plant Daily equivalent of thermal energy can be obtained from,

$$E_{th,daily} = \frac{E_{elec,daily}}{0.38} \tag{3.22}$$

Overall thermal energy obtained can be stated as,

$$Q_{th,overall} = E_{th,daily} + Q_{daily} \tag{3.23}$$

The thermal efficiency is given as,

$$\eta_{\text{thermal}} = \frac{Q_{daily}}{I(t)A_{PV}} \tag{3.24}$$

The overall thermal efficiency is given

$$\eta_{\text{thermal,overall}} = \eta_{\text{thermal}} + \frac{\eta_{\text{elec}}}{0.38} \tag{3.25}$$

3.4 Exergy analysis

Systems daily exergy with air duct is expressed as follows,

$$Ex_{th,daily} = Q_{th,daily}\left(1 - \frac{T_a + 273}{T_{fo} + 273}\right) \tag{3.26}$$

Overall daily exergy is given by,

$$Ex_{daily,overall} = Ex_{th,daily} + E_{elec,daily} \tag{3.27}$$

Systems overall exergy efficiency with air duct can be obtained from,

$$\eta_{\text{exergy,overall}} = \eta_{\text{PV,electrical}} + \eta_{\text{thermal}}\left(1 - \frac{T_a + 273}{T_{fo} + 273}\right) \tag{3.28}$$

3.5 Exergy Loss Rate Analysis

Exergy energy balance equation for the BiSPVT system can be written as,

$$Ex_{solar,daily} = Ex_{th,daily} + L_{ex} \tag{3.29}$$

Where, $Ex_{solar,daily}$ represents the total solar exergy incident on the BiSPVT facade, $Ex_{th,daily}$ is the daily useful exergy obtained from the system and L_{ex} denotes exergy loss or exergy loss rate from the system.

$Ex_{th,daily}$ can be calculated from equation (3.25) and representation of $Ex_{solar,daily}$ has been taken as given in Petela [191].

$$\dot{E}x_{\text{solar}} = G(t)WL\left[1 - \left(\frac{4T_a}{3T_s}\right) + \frac{1}{3}\left(\frac{T_a}{T_s}\right)^4\right] \tag{3.30}$$

(3.31)

The representations of equation (30) is same as equation (10). The common form for equation (3.29) can also be given as:

$$L_{ex} = Ex_{solar,daily} - Ex_{th,daily}$$

Similarly, for loss rate of energy, the expression can be written in the form of

$$L_{en} = Ex_{solar,daily} - Q_{th,overall} \tag{3.32}$$

3.6 Exergoeconomic analysis

The exergy and exergoeconomic parameters when balanced for the system, an optimal design in sense of reducing energy loss and capital costs can be obtained. The analyses performed by including a correlation between exergy loss, system lifetime and capital cost can design a system optimized in energy and exergy perspectives. Parameters associated with exergoeconomic calculations are R_{en}andR_{ex}, also termed as energy and exergy loss rate respectively. The exergoeconomic parameter in this system has been calculated by the following equations[192].

$$R_{en} = \frac{L_{en}}{P_n} \tag{3.33}$$

$$R_{ex} = \frac{L_{ex}}{P_n} \tag{3.34}$$

Following Saadon *et al.* [127], by considering lifetime of n years and capital cost p, the net present value (P_n) can be calculated as,

$$P_n = Total\ initial\ cost\ (P) + operational\ and\ maintanence\ sost\ (OM) \times Unacost\ present\ value\ factor\ (F_{rpi,,n}) - Salvage\ value\ x\ Present\ value\ factor\ (F_{sp,i,n}) \quad (3.35)$$

Where, $F_{rp,i,n} = \frac{(1+i)^n - 1}{i(1+i)^n}$ and $F_{sp,i,n} = (1+i)^{-n}$

3.7 Energy Matrices Evaluation

Table. 3.3 presents the expressions used for analysis of the energy matrices

Table 3.3 Expressions for energy matrices

Equation	Equation No.
$EPBT = \frac{E_{input}\ (kWh)}{E_{output}\ (\frac{kWh}{year})}\ years$	(3.36)
$EPF = \frac{E_{output} * T}{E_{input}}$	(3.37)
$LCCE = \frac{E_{output} * T - E_{input}}{E_{rad,annual} * T}$	(3.38)
$UAC = NPV * CRF$	(3.39)
$NPV = P + R_1\left[\frac{(i+1)^n - 1}{i(i+1)^n}\right]_{i,n} + R_{3,1}\left[\frac{1}{(i+1)^n}\right]_{i,3} + R_{6,2}\left[\frac{1}{(i+1)^n}\right]_{i,6} + R_{9,3}\left[\frac{1}{(i+1)^n}\right]_{i,9} + \cdots - S\left[\frac{1}{(i+1)^n}\right]_{i,n}$	(3.40)
$CRF = \frac{i(i+1)^n}{(i+1)^n - 1}$	(3.41)

E_{input} refers to the embodied energy of the ; E_{output} denotes annual energy output from the BiSPVT system; T denotes systems lifetime in years; $E_{rad,annual}$ denotes annual solar radiation received by the PV facade system; NPV refers to Net Present Value of the system and CRF represents Capital recovery factor. A capital recovery factor is a factor used to transform a current value into a series of uniform annual payments spread over a set period, considering a predetermined discount rate or interest. CRF is given by expression in equation 3.41. where n refers to systems lifespan. R_1, R_1, . . .; R_n represents operational, maintenance and replacement costs of PVT air collector. $R_{3,1}$; $R6_{,2}$; . . .; $R_{n,n}$ represents painting, cleaning and glass replacement costs of PVT air collector, i and n denotes rate of interest and systems lifespan respectively. S denotes salvage value of the system. Operational and Maintenance

cost are taken as 2% of the PV modules while fabrication cost is taken as 10% of the cost of PV modules.

3.8 Environmental Performance Indicators

The environmental performance of the BiSPVT system is assessed through three main indicators: i) CO_2 emission reduction, ii) carbon credits, and iii) GPBT emission. These indicators are grounded in the fact that, while PV technologies generate electricity from solar energy and are considered sustainable during operation, their manufacturing, production, balance of systems, transportation, and installation involve significant energy consumption. Therefore, evaluating the sustainability of BIPVT systems in terms of environmental performance is crucial. This evaluation particularly focuses on CO_2 emission reduction and GPBT. CO_2 emission is also dependent on CO_2 emission factor which in turn is based on local electrical mix. As per a study by Junedi *et al.* [193], revealed that BIPV systems emission rate varied with varying location of being installed. A significant portion of the environmental impact comes from the PV manufacturing process within the BIPV system. Consequently, the electricity mix in the country or region where the manufacturing takes place is crucial in determining the overall environmental impact throughout the BIPV system's life cycle. The GHG emission rate varies based on geographic location because producing PV systems in countries with low carbon intensity results in lower GHG emissions, and vice versa. Additionally, the solar irradiance of a specific location plays a crucial role in assessing the environmental performance of BIPV systems. Higher solar irradiance leads to greater electrical energy production, thereby reducing the GHG emission rate [194]. The evaluation of the considered BiSPVT system for the climate of Srinagar, India has thus been based on CO_2 emission rate based on India is 0.96 kg $CO_{2eq.}$

i. CO_2 emission reduction

Carbon dioxide (CO_2) emission to the environment comes as a major threat not only to environment but also to humankind. Thus, assessment of the proposed system in terms of environment is needed. The reference value for CO_2 emissions per kilowatt-hour (kWh) generated by coal-powered electricity throughout its lifetime is estimated to be around 0.96 kilograms. However, when factoring in transmission and distribution losses, which account for 40% and 20% respectively, this figure increases to approximately 2 kilograms of CO_2 per kWh. Expression for amount of CO_2 emitted from the proposed BIPV facade system is calculated as

$$\text{Reduction of } CO_2 \text{ emission/year} = (\text{Annual overall energy gain} \times 2 \text{ kg } CO_2)/1000 \quad (3.42)$$

i. Carbon Credit

Carbon credit is also referred as environmental cost reduction of the PV facade system per year. For BiSPVT system it was obtained using,

$$\text{Environmental cost reduction/year } (Z_{C02}) = CO_2 \text{ emission reduction/year} \times 14.5\$ \quad (3.43)$$

Where, Global cost of CO_2 (z_{CO2}) comes between (13 -16) \$/t CO_2. An average of this value as 14.5 \$/t CO_2 was taken for the study of BiSPVT system [195].

ii. Greenhouse gas payback time period (GPBT) estimation

GPBT is a critical metric in assessing the environmental impact of Building Integrated Photovoltaic (BIPV) technologies. While EPBT calculates the duration for a photovoltaic system to produce the equivalent amount of energy used in its manufacturing and operation, GPBT goes further by considering the emissions associated with that energy production. GPBT accounts for the reduction in greenhouse gas emissions achieved by generating renewable energy compared to using conventional energy sources. PV modules when in operation does not contribute to the process of CO_2 generation. But it generates CO_2 along with other gases during its lifecycle which includes process of manufacturing and disposal. Understanding and analysing GPBT of BIPVT systems is thus vital to evaluate PV systems sustainability and to get a predictability of how 'greenness' the PV systems are. GPBT is given by:

$$GPBT = \frac{GHG_{system} + GHG_{BOS}}{GHG_{s,output}} \quad (3.44)$$

where, GHG_{system} is the embodied GHG of the BISPVT system (PV modules) in kg CO_{2eq}; GHG_{BOS} is the embodied GHG of the Balance of systems (BOS) in kg CO_{2eq}; $GHG_{s,output}$ is the greenhouse gases emitted by a local power plant for the electricity generated by the PV system in kg CO_{2eq}.

3.9 Selection of Location

Srinagar was chosen for this study mainly because of its cold climate, where heating is needed for a large part of the year. This makes it a suitable place to test how a PVT system can be used not just for electricity, but also for heating purposes. The idea was to use the heat collected from the back of the PV module to warm indoor spaces, which can help reduce the use of conventional sources like electric heaters or gas-based systems. This not only saves energy but also lowers electricity bills and emissions. Since Srinagar also gets a decent amount of sunlight

during winter, it helped to properly analyze the performance of the system in real cold-weather conditions. Additionally, the growing energy demand and limited grid reliability in hilly and remote areas like Srinagar highlight the need for decentralized renewable energy solutions. Studying the PVT system in such a context enables the evaluation of its dual benefits of electrical and thermal application, thereby supporting its applicability for cold climate sustainable energy planning.

Climatological Information of Srinagar, India

The climate of Srinagar consists of cold winters and hot summers. Located in the northwest region of India, Srinagar is situated at 5250ft above sea level. The regions hold a latitude and longitude of 34.0837°N and 74.7973°E respectively.

Srinagar experiences maximum cold during January where the average temperature is 2.7^{o}C, with a maximum of 7.7^{o}C and a minimum temperature of -2.3^{o}C. During winter nights, the temperature drops to -5.5^{o}C. The recorded maximum and minimum temperatures during July are 30.5^{o}C and 18.3^{o}C respectively. The average sunshine hours in Srinagar for summers and winters are around 8 hours and 11 hours respectively. The variation of solar radiation in this region varies with weather conditions. The different weather conditions for Srinagar is mentioned in Table 1. Among the months in a year, Srinagar experiences the greater number of clear sunshine days (type-a) for the months of September and October. The results here are discussed for the month of October for a-type and b-type weather condition followed by annual energy and exergy evaluation from the PV facade system.

Classification of days for each weather condition in Srinagar

Table 3.4 presents the distribution of days under various weather classifications observed throughout the year in Srinagar. By organizing data month-wise across distinct weather types, it offers insights into seasonal patterns and the changing nature of weather conditions.

Table 3.4 No of days for each weather classification

Month-> Weather Type	**Jan**	**Feb**	**Mar**	**Apr**	**May**	**June**	**July**	**Aug**	**Sept**	**Oct**	**Nov**	**Dec**
a	5	7	8	10	13	11	7	6	14	12	5	3
b	17	14	17	17	15	12	17	18	12	12	14	8

Month-> Weather Type	**Jan**	**Feb**	**Mar**	**Apr**	**May**	**June**	**July**	**Aug**	**Sept**	**Oct**	**Nov**	**Dec**
c	7	4	3	2	2	4	4	3	3	5	8	19
d	2	3	3	1	1	3	3	4	2	2	3	1

3.10 Summary of the chapter

This chapter presents a comprehensive overview of the methodology adopted for the investigation of the Building-integrated Semi-Transparent Photovoltaic Thermal (BiSPVT) facade system. It outlines the overall research framework, beginning with the conceptual modeling of the BiSPVT configuration and progressing towards its numerical implementation in MATLAB. The detailed methodology includes thermal and electrical performance modeling, supported by a systematic approach to data input, boundary condition definition, and simulation workflow. Additionally, the chapter covers the selection of the study location, with Srinagar, India chosen for its distinct climatic characteristics and relevance to building energy applications. Furthermore, this chapter incorporates exergy, exergoeconomic, and enviroeconomic analyses to provide a holistic evaluation of system performance beyond conventional energy metrics. These integrated modeling approaches form the basis for the performance assessment carried out in the following chapters. The next chapter (Chapter 4) focuses on the annual energy performance evaluation of the BiSPVT facade system, providing insights into its long-term feasibility and effectiveness in real-world conditions.

भारतीय प्रौद्योगिकी संस्थान गुवाहाटी
Indian Institute of Technology Guwahati

4

Annual Energy Analysis of Building Integrated Semi-Transparent Photovoltaic Thermal Facade

Chapter Outline:

CHAPTER 4: ANNUAL ENERGY ANALYSIS OF BUILDING INTEGRATED SEMI-TRANSPARENT PHOTOVOLTAIC THERMAL FACADE

4.1 Introduction

This chapter consists analysis of results attained from the thermal modeling of Building Integrated Semi-transparent Photovoltaic Thermal Facade (BiSPVT) system. The thermal modelling of the present BiSPV configuration has been performed in MATLAB(R2019b). The developed model is used to analyze annual energy output in the form of electrical and thermal energy along with efficiency indexes that includes - electrical, thermal, overall thermal, exergy and overall exergy efficiency. Furthermore, system evaluation in terms of thermal losses is also presented in this chapter.

The analysis is done for four different weather conditions of Srinagar-namely (i) clear day, (ii) hazy day, (iii) hazy and cloudy day, and (iv) cloudy day. Estimation of solar radiation has been done for these four weather conditions. The incident solar radiation, wind speed, ambient temperature, system design parameters and PV module specification has been taken as the input parameter for the MATLAB programme, various temperatures and efficiencies have been estimated as the output of the MATLAB programme. The systems annual performance has been evaluated by estimating the electrical and thermal energy for all weather conditions of each month of whole year.

4.2 Variation of solar radiation with ambient temperature

Hourly evaluation of solar radiation and ambient temperature for a-type and b-type climatic condition for the month of October at Srinagar

Variation of solar intensity (I(t)) and ambient temperature T_a on an hourly basis on the semi-transparent building integrated PV facade (BiSPV) for October month has been shown in **Fig. 4.1**. Calculation of total incident solar radiation on the PV facade has been carried out using formulation of Liu and Jordan. Hourly solar radiation variation was studied from 08:00 hours to 16:00 hours in a day. The incident solar intensity variation was found to be gradually increasing from 08:00 hours, becoming maximum at 12:00-13:00 hours, and then gradually decreasing to become minimum at 16:00 hours. The trend of total solar radiation of PV facade system for the b-type weather condition can be explained as same.

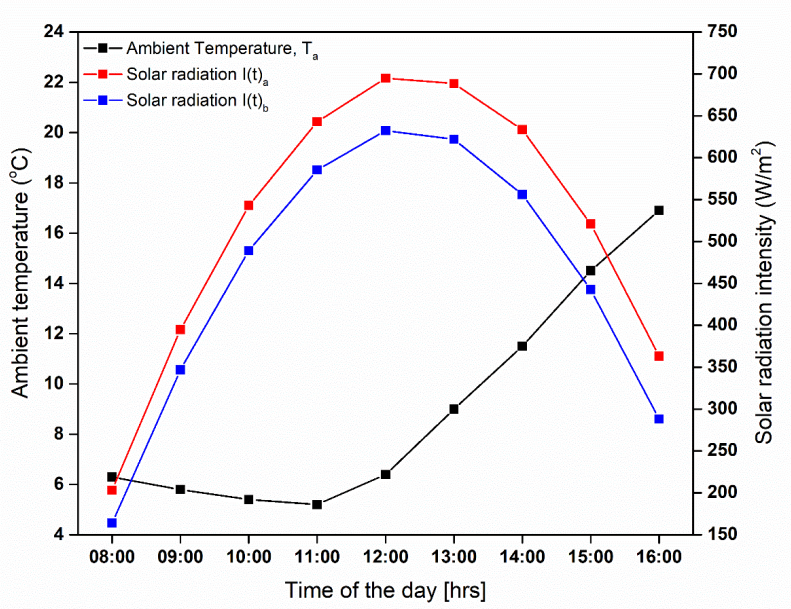

Fig. 4.1 Hourly variation of solar radiation and ambient temperature for a-type and b-type climatic condition in the month of October at Srinagar

4.3 Analysis of BiPVT facade system temperature profiles

Variation of PV module temperatures and its effect of PV module efficiencies

Variation of various temperatures and module efficiency (electrical and thermal) for PV facade system at Srinagar in October month for a-type weather condition is shown in **Fig. 4.2**. Temperature variation is shown for PV module (T_m), Average fluid temperature (T_f), Outlet fluid temperature (T_{fo}), Blackened wall temperature (T_b) and room temperature (T_r). For BiSPVT system with air channel, maximum temperature of PV module was observed for clear days (type-a) climate since it received the maximum amount of total solar radiation intensity. Highest temperature attained for PV module was 33.6°C against a PV module efficiency of 18.26%. At 10:00 hours, with solar cell temperature being 27°C, the module achieved its highest electrical efficiency of 18.8%. Now, with increased temperature of module, its electrical efficiency decreases. This rise in temperature is attributed to the infrared radiation from the spectrum incident on the PV module that goes unutilized and generates heat in the PV modules causing a rise of the solar cell temperature. Thus, at 16:00 hours when the T_m drops to a value of 29.2°C from highest T_m of 33.6°C; its electrical efficiency increases from 18.26% to 18.64%.

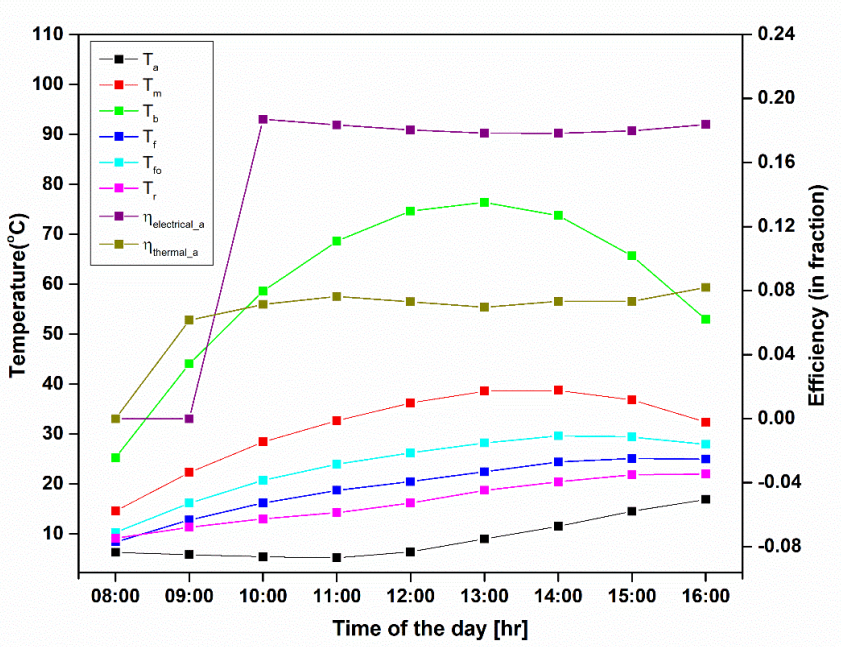

Fig. 4.2 Hourly variation of different temperatures in the PV facade system vs PV module efficiency and thermal efficiency- a type (October)

Cavity air experiences heating due to extracted heat from PV module back surface and through solar radiation that is incident on the absorber wall via non-packing area of the semi-transparent PV module. Maximum module temperature (T_m) thus leads to a maximum T_{fo} value of 29.63 °C at 14:00 hours. Outlet fluid temperature is crucial as it involves the amount of thermal energy input to the room carried out in motive of space heating. Maximum T_r attained in the indoor space was 21.98°C at 15:00 hours. This T_r was obtained when outside ambient temperature (T_a) was 16.9°C. A difference of 5.08°C between T_a and T_r was obtained during 15:00 hours by the use of PV facade. A maximum temperature difference between T_r and T_a was observed during 12:00 hours i.e. 9.76 °C when T_r was 16.16°C and T_a was 6.4°C. In the Fig. 4.2, as can be seen, the values of T_b, T_m, T_{fo}, T_f gradually increased at first and then decreased.

BiSPVT system thermal efficiency is a function of useful thermal energy supplied to the room as well as heat loss from walls and openings of room to ambient. Average fluid temperature (T_f) gets heated gradually as I(t) and T_m increase gradually. Increased T_{fo} further increases T_r as seen in Fig. 4.2. The drop in thermal efficiency although with an increase of T_m can be explained from the fact that the temperature difference from module to ambient and room to ambient is also increasing with time, reaching maximum losses at peak sunshine hours. This signifies that increased heat loss from the systems envelope is related with systems decreased

thermal efficiency. Maximum thermal efficiency achieved was 8.19°C at 16:00hours. Similar explanation can be given for variation of different temperatures with electrical and thermal efficiencies for type-b weather condition in the month of October, shown in **Fig. 4.3**.

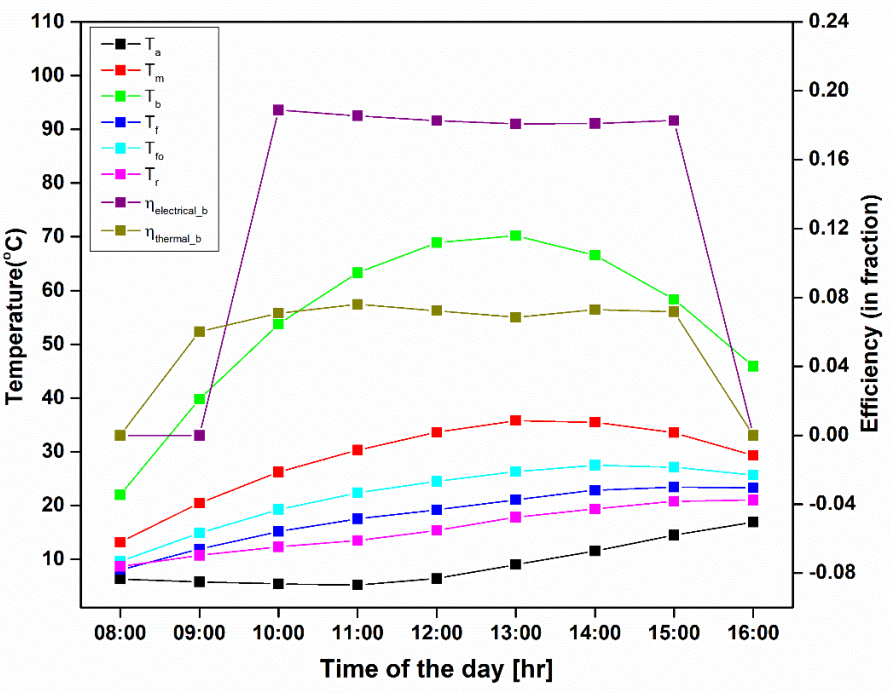

Fig. 4.3 Hourly variation of different temperatures in the PV facade system vs PV module efficiency and thermal efficiency- b type (October)

4.4 Monthly energy evaluation of the BiSPVT system

Energy analysis of the PV facade system for the month of October

The energy analysis comprises of daily electrical, thermal and overall thermal energy obtained from the PV facade system. For a-type weather condition, maximum daily electrical gain obtained from the PV facade system is 0.12 kWh/m^2 and the maximum daily thermal energy gain obtained from the system was 0.58 kWh/m^2 shown in **Fig. 4.4**.

PV systems overall thermal energy gain is a combination of both thermal and electrical energy. Since electrical energy is considered higher grade energy and thermal energy as lower grade, direct addition is not possible. To make the combination pertinent, a factor of 0.38 considered as electrical power generation efficiency for Indian quality coal is used as an equivalent factor, to convert electrical energy to its thermal energy equivalent.

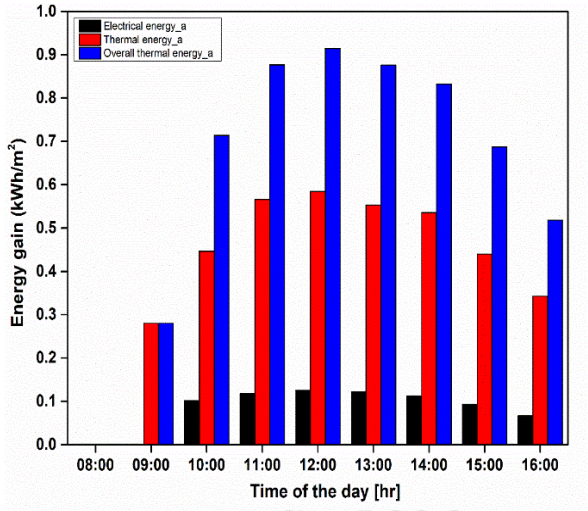

Fig. 4.4 Daily energy gain (electrical, thermal, overall thermal) from the system (Type-a) for the month of October at Srinagar

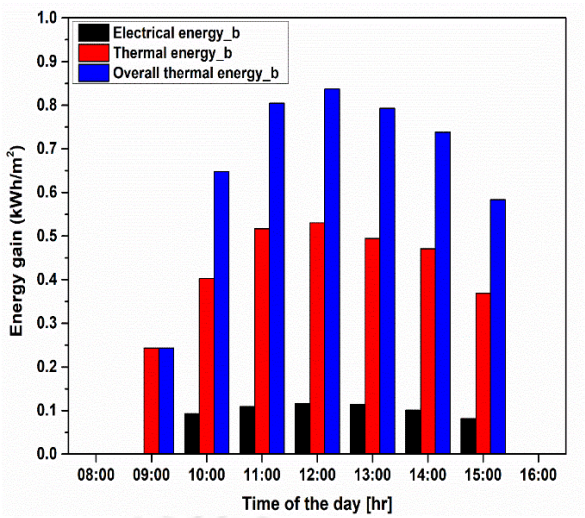

Fig. 4.5 Daily energy gain (electrical, thermal, overall thermal) from the system (Type-b) for the month of October at Srinagar

The maximum overall daily thermal gain is obtained as 0.91 kWh/m². In type-a weather condition, T_f and T_{fo} of air is higher than that of b-type weather condition PV facade. Thus, air temperature was higher in type-a weather condition. This high temperature air was supplied to the room through the duct resulting in higher thermal energy gain. For type-b weather condition in October as shown in **Fig. 4.5**, the maximum electrical, thermal and overall thermal energy gain from the BiSPV system was found to be 0.61 kWh/m², 3.02 kWh/m², and 4.64 kWh/m² respectively.

4.5 Monthly exergy evaluation of the BiSPVT system

To assess PV facade systems attainable quality of useful energy exergy analysis is performed. Based on second law of thermodynamics, this analysis gives an estimation of quality of energy obtained as well as the irreversibilities associated with the energy conversion system. **Fig. 4.6** represents daily overall exergy variation obtained for type-a and type-b weather condition. Maximum overall exergy was for type-a weather condition with a value of 0.16kWh/m² and 0.14 kWh/m² for type-b weather condition. In Fig. 4.6, the absence of exergy output at 16:00 is attributed to the assumptions adopted in the numerical modelling. When the module temperature falls below 25 °C, corresponding to the standard test condition (STC) of the considered PV modules, the electrical efficiency is assumed to be zero in the model. Consequently, this assumption results in no electrical energy generation, which in turn leads to zero calculated energy and exergy outputs at that time step.

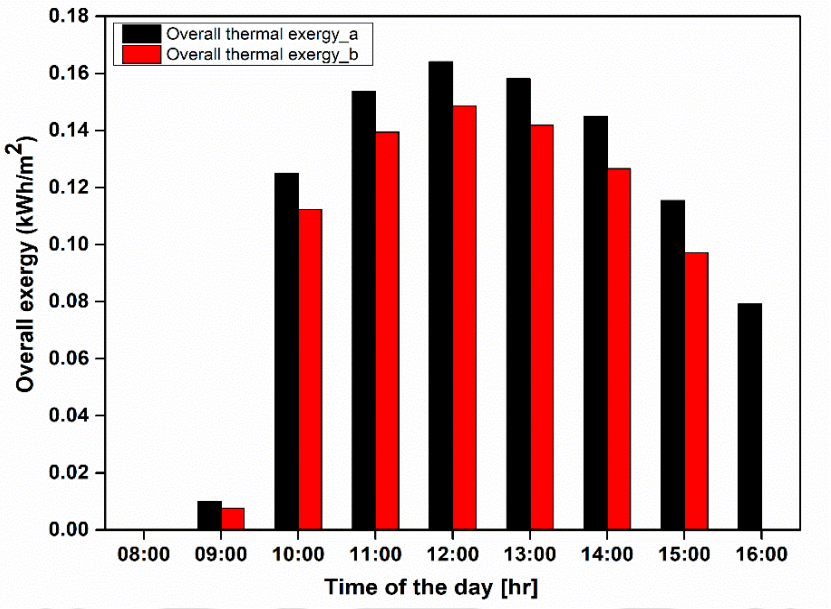

Fig. 4.6 Daily overall exergy of the system (Type a and type b) October

4.6 Significance of outlet fluid temperature

Variation of Outlet fluid temperature (T_{fo}) with Efficiency (overall thermal efficiency and overall exergy efficiency)

Variation of overall thermal and exergy efficiency as a function of T_{fo} is shown in **Fig. 4.7**. Observations indicate that the daily overall thermal energy and exergy efficiencies are higher for type-a conditions owing to higher incident solar radiation. Daily maximum overall thermal efficiency has been obtained as 56.53% and exergy efficiency has been found as 18.67% respectively for type a climatic condition and 56.41% and 18.99% respectively for type b climatic condition. Thermal efficiency indicates the effectiveness of the BiSPVT system in converting incident solar energy into useful thermal output. Exergy efficiency evaluates the quality of energy conversion by accounting for thermodynamic irreversibilities and the usable work potential of the system. The numerically lower exergy efficiency value is primarily due to the low-grade nature of the recovered thermal energy and the relatively small temperature difference between the working fluid and the ambient environment, which significantly limits the available work potential despite a high thermal energy yield.

Decrease in thermal efficiency from 09:00 and 10:00 hours may be due to increase in temperature difference between T_r and T_a as seen in Fig. 4.2 and Fig. 4.3 for type- and type-b respectively. It can be seen that as the fluid temperature T_{fo} is rising, both overall thermal energy and exergy efficiency is rising. Sharp peak rise from 09:00 hours to 10:00 hours can be because of sudden rise in incident solar radiation on the PV faced along with rise of module

temperature, T_m which eventually causes increase of T_f and T_{fo}. The same explanation can be given for b-type weather condition for the sharp rise and fall in efficiency in between 09:00 - 10:00 hours and 13:00 -14:00 hours respectively.

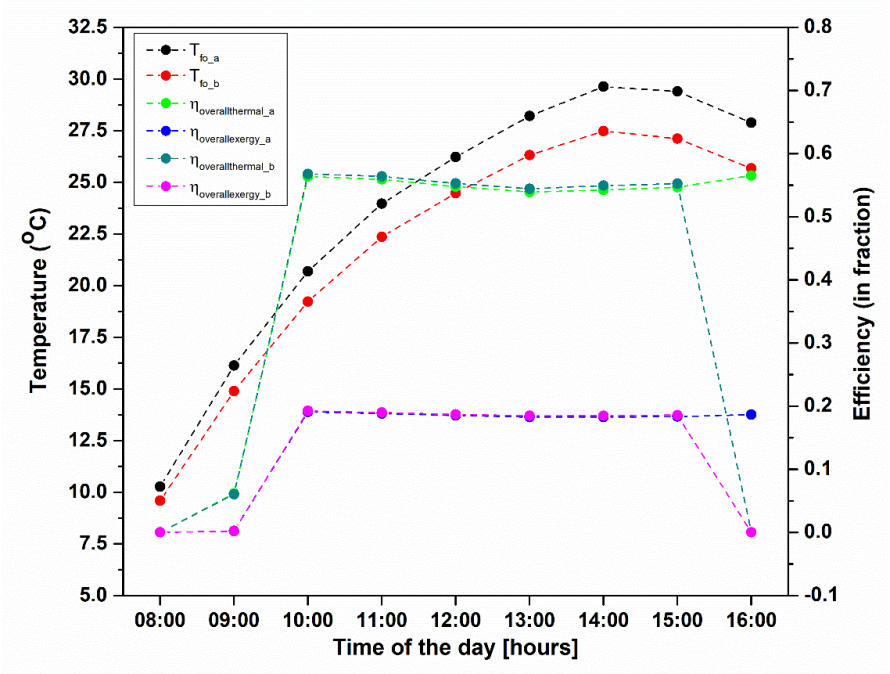

Fig. 4.7 Outlet fluid temperature (T_{fo}) vs efficiency (overall thermal efficiency and overall exergy efficiency) (a, b-type)

4.7 Instantaneous efficiency

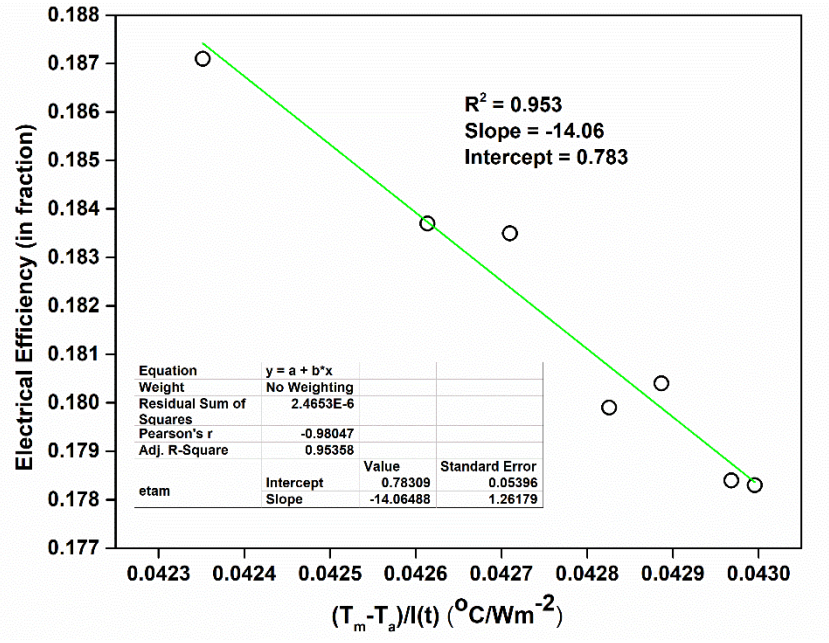

Fig. 4.8 Plot of electrical efficiency vs $(T_m-T_a)/I(t)$ for the BIPV system

Fig. 4.8 shows the electrical efficiency variation as a function of $(T_m-T_a)/I(t)$, known as the flat plate collector characteristic curve. This curve represents how thermal and electrical efficiency varies with heat loss between PV module - ambient and room – ambient environment. Rate of heat loss depends on (T_m-T_a) and (T_r-T_a). Greater the difference, more will be the thermal loss to the surrounding and lesser will be useful energy output. The efficiency here is termed as instantaneous electrical efficiency and instantaneous thermal efficiency.

Effective optical efficiency along with heat loss coefficient from the BiSPVT system has been determined by a linear fitted graph. Instantaneous electrical efficiency variation with reduced temperature $(T_m-T_a)/I(t)$ is presented in Fig. 4.8. Slope here represents heat loss coefficient and intercept indicates the optical efficiency obtained as 14.06 W m^{-2} K^{-1} and 78.3 % respectively, shown in **Fig. 4.8**. Similarly, **Fig. 4.9** presents instantaneous thermal efficiency obtained. Slope in this plot gave a value of 55.17 W m^{-2} K^{-1} and intercept 84.9% indicating heat loss coefficient and optical efficiency respectively.

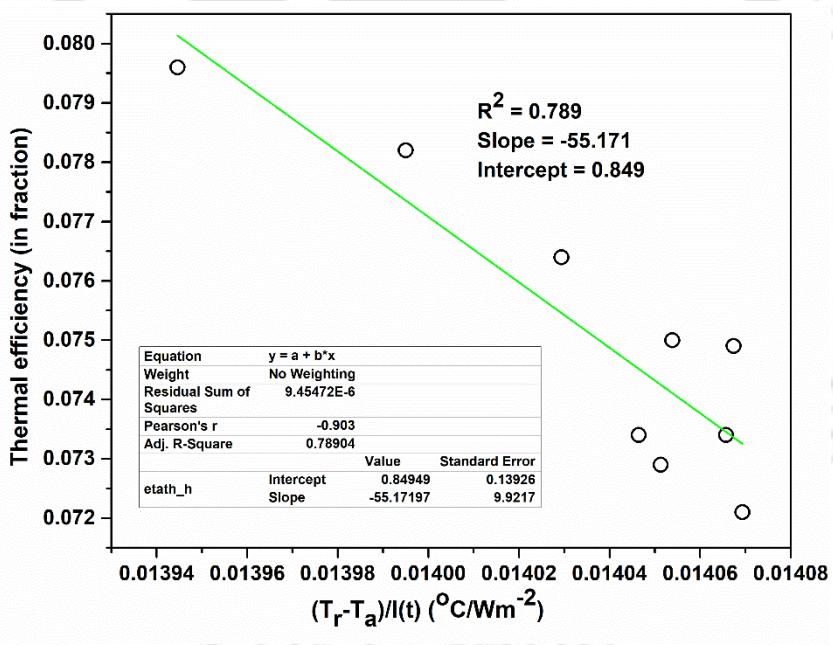

Fig. 4.9 Plot of efficiency vs $(T_r-T_a)/I(t)$ for the BIPV system

4.8 Thermal load levelling (TLL)

Room air temperature variation is influenced by solar intensity as well as ambient air temperature. Hence, air temperature in room experiences fluctuation. Higher fluctuation signifies thermal discomfort of the occupants. The index used for fluctuation of T_r is Thermal Load Levelling (TLL). Values of TLL closer to zero is preferred for non-AC rooms, as lower values imply less indoor air variability. **Table 4.1** presents the TLL values for both a and b-

type weather condition. For a-type in October month, TLL is obtained as 0.413 and for b-type as 0.417. Minimum fluctuation of air inside the room was observed for type -a condition indicating a greater space heating of the room. The expression used for thermal load leveling (TLL) is as follows:

$$\text{TLL} = \frac{(T_{r,max} - T_{r.min})}{(T_{r,max} + T_{r,min})} \tag{4.1}$$

Table 4.1 Thermal load levelling for BISPVT system

	$T_{r,max}$	$T_{r.min}$	TLL
a	21.989	9.120	**0.413**
b	20.995	8.635	**0.417**

4.9 Annual Energy and Exergy Gain from the PV facade

Annual electrical energy gain from the BiSPVT system is shown in **Fig. 4.10**. Highest electrical energy gain has been obtained as 8.72 kWh/m².for the month of January. However, among the months maximum electrical energy gain from the system has been obtained for October as 17.27 kWh/m². This is because intensity of solar radiation on PV facade is higher for October compared to January. PV panels generate more electricity during clearer days as observed for type-a condition. For Srinagar, maximum clearer days are observed for the month of September and October. Increase in cell temperature reduces the electrical efficiency of PV modules which further cause a reduction in electrical energy generated from the PV facade system. The annual electrical energy gain from the BiSPVT facade has been found to be 121.22 kWh/m². For weather conditions of C- and D-type, the energy gain has been observed to be lower compared to A- and B-type climates due to lesser solar intensity in the former. Specifically, C-type conditions exhibit an overall annual thermal energy gain of about 8-14 kWh/m² and an overall annual exergy gain of about 2- 4 kWh/m².

Annual thermal energy gain by the system is shown in **Fig. 4.11**. Total Thermal energy gain for January has been observed as 7.24 kWh/m². The outlet temperature of air primarily decides the thermal gain obtained from the PV facade system. Higher intensity during January and October led to higher values of thermal energy output. For October, total thermal energy gain was obtained as 7.5 kWh/m². Higher heat extraction from the system is also accompanied by a greater number of clearer days in a month. Since maximum clear days was observed for type a condition followed by b-type, c-type and d type, a-type condition attributed the

maximum to the monthly thermal energy gain. Annually, thermal gain was obtained as 61.06 kWh/m^2. The maximum thermal gain for October found as maximum considering larger number of clearer sunshine days or maximum solar radiation and minimum during June due to a smaller number of clear sunshine days.

Monthly overall thermal energy gain has been shown in **Fig. 4.12**. Overall thermal energy gain has been observed to be maximum for October whereas minimum for the month of June. It is also observed that 366.23 kWh/m^2/year of overall thermal energy gain has been witnessed from the PV facade system. **Fig. 4.13** presents the overall useful exergy obtained from the system. As observed, maximum value for gained exergy is for October (17.67 kWh/m^2) and minimum for June (4.32 kWh/m^2). The system also generated yearly useful overall exergy gained of 122.36 kWh/m^2.

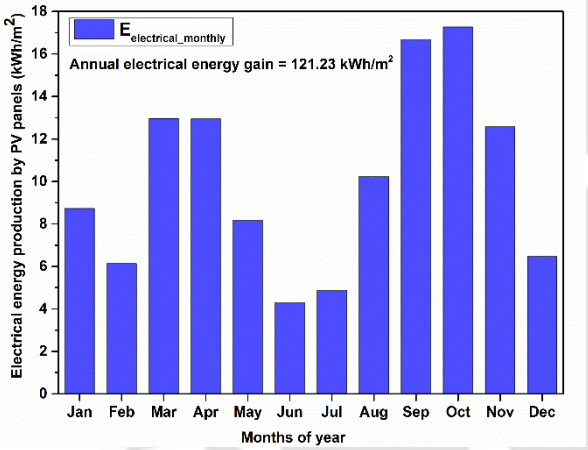

Fig. 4.10 Monthly electrical energy production by the BiSPVT system

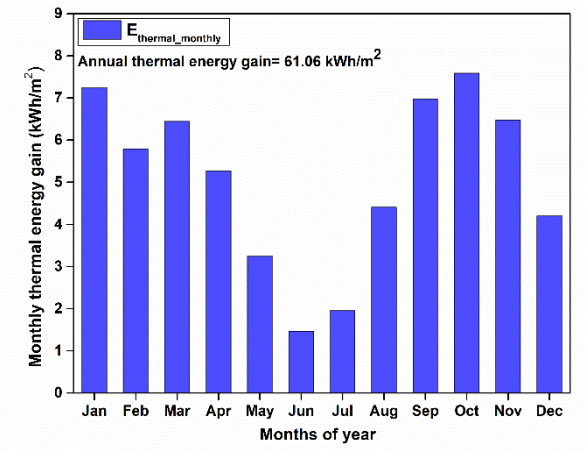

Fig. 4.11 Monthly thermal energy production by the BiSPVT system

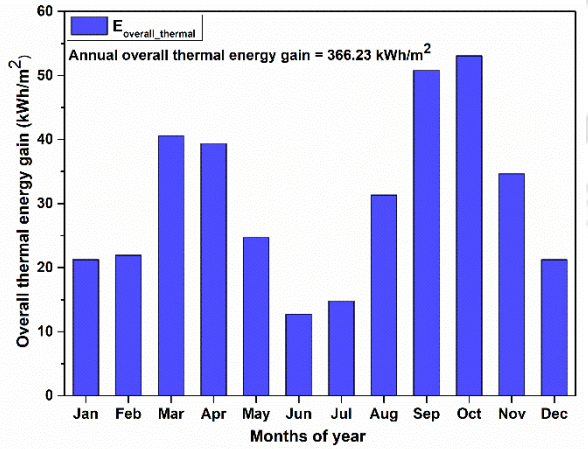

Fig. 4.12 Monthly overall thermal energy production by the BiSPVT system

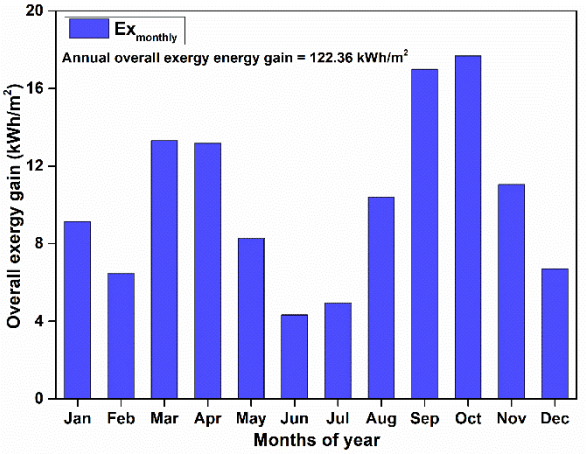

Fig. 4.13 Monthly useful exergy production by the BiSPVT system

4.10 Evaluation of thermal loss

Thermal Losses in a-type condition for the months of January, February, September, October

For BiSPVT system performance assessment concerning electrical energy production and losses, analysis has been carried out for the daily thermal losses in relation to electrical energy production form the PV. Thermal losses are associated with the solar cell operating temperature. With increase in Solar radiation incident on PV panel, the cell temperature rises causing accumulation of heat in the modules. The heat accrued over time, decreases the electrical efficiency and thus its electrical energy production. For better predictability of systems performance, it is thus necessary to investigate the systems thermal losses. Estimation of system thermal losses are possible after the determination of module temperature, T_m. To calculate the thermal losses, $L_{thermal}$, following procedure and parameters are introduced.

Expression for PV module electrical efficiency which is dependent on temperature is given by,

$$\eta_m = \eta_0[1 - \beta_o(T_m - T_o)] \quad (4.2)$$

Where, η_0 denotes PV module standard efficiency; β_o represents temperature coefficient of PV module; T_m is the calculated PV module temperature; T_o denotes standard temperature of solar cell at STC (temperature T_a = 25 °C and irradiance I(t) = 1000 W/m², AM = 1.5)

$E_{reference}$ is referred as PV module energy yield defined by the ratio of solar radiation incident on the PV module to reference power equal to 1 kW/m². To calculate systems energy yield (E_{system}) relating to the effect of T_m and reference energy yield ($E_{reference}$), following expression has been used,

$$E_{system} = E_{reference}[1 - \Upsilon(T_m - T_o)] \quad (4.3)$$

Thermal Loss from the system is obtained from,

$$L_{thermal} = E_{reference} - E_{system} \quad (4.4)$$

E_{system} , $E_{reference}$, and $L_{thermal}$ here are shown for months under consideration i.e. January, February, September, October for clear conditions only (type-a). Number of clear days for September and October implies higher solar radiation incident on PV facade. Increase in temperature reduces the electrical efficiency which further reduces systems electrical output i.e. the amount of thermal losses increases. **Fig. 4.14** shows the daily variation electrical energy yield and thermal losses for a clear day in January. The peak $L_{thermal}$ was observed as

0.028kWh/kWp/day at 13:00hours considering highest solar radiation and T_m at 13:00hours. Peak $L_{thermal}$ for February (**Fig. 4.15**), September (**Fig. 4.16**) and October (**Fig. 4.17**) was witnessed as 0.050 kWh/kWp/day, 0.035 kWh/kWp/day and 0.042 kWh/kWp/day respectively.

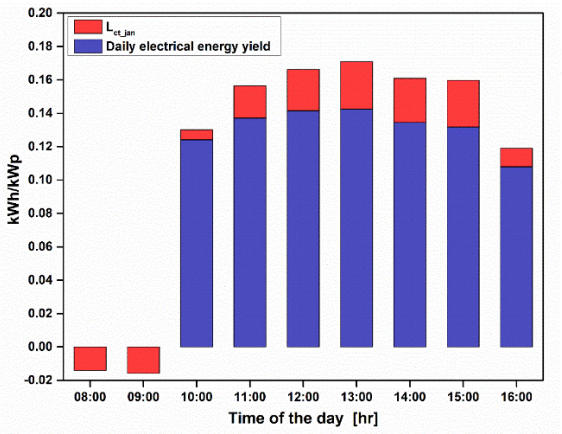

Fig. 4.14 Variation of daily electrical energy yield and thermal losses for Jan (clear day)

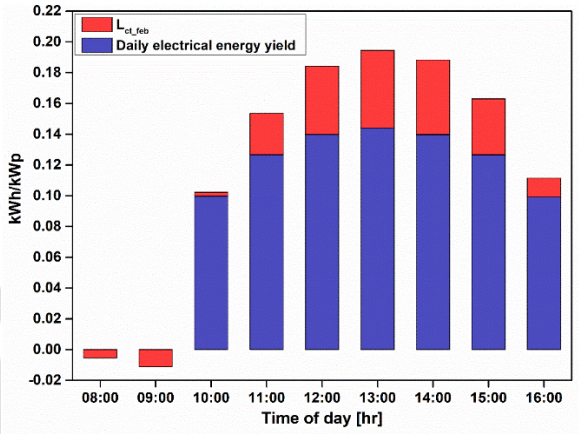

Fig. 4.15 Variation of daily electrical energy yield and thermal losses for February (clear day)

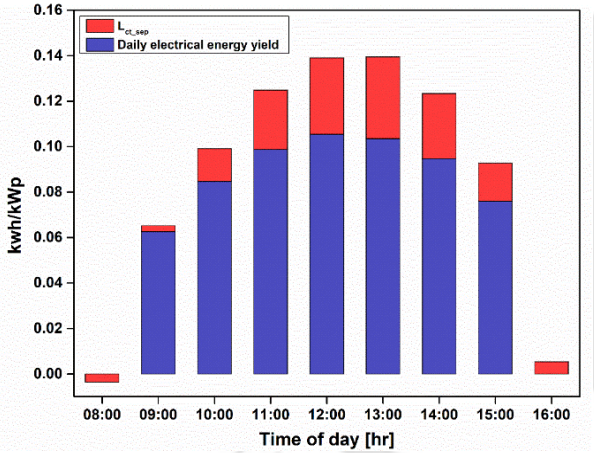

Fig. 4.16 Variation of daily electrical energy yield and thermal losses for September (clear day)

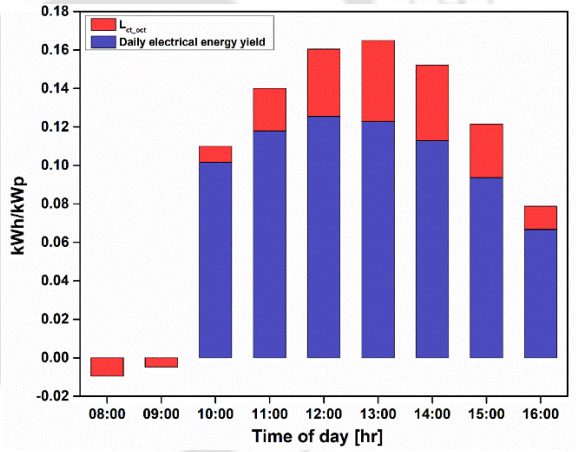

Fig. 4.17 Variation of daily electrical energy yield and thermal losses for October (clear day)

4.11 Summary of the chapter

This chapter analyses the performance of a BiSPVT system from the perspective of energy gain and temperature dependent efficiency for four distinct climatic conditions in the location of Srinagar, India. Based on detailed analysis performed for the present work, it can be seen that the BiSPVT system has been able to generate annual electrical and overall thermal energy gain of 121.22 kWh/m² and 366.23 kWh/m² respectively. The system has been also justified in terms of useful overall exergy supplied with an annual value of 122.36 kWh/m². This paper

also analyses several parameters of temperatures associated with the BiSPVT system and its effect on electrical and thermal of the system. Thorough numerical analysis shows that semi-transparent PV module application as building facade with air channel placed next to it, has the bilateral advantage of enhanced module efficiency and increased thermal energy gain to the indoor space. This application is thus proven to be more beneficial for its use in the cold climatic region where indoor space temperature can be heated sustainably without its dependent on conventional energy source. The maximum temperature difference that the present system has been able to deliver had a difference of 12.83^{o}C between room temperature and ambient temperature. From the standpoint of useful heating energy supplied to the indoor space, it has been observed that indoor air temperature is primarily dependent on temperature of air outlet from air channel to room. Further effective optical efficiency and effective heat loss coefficient was obtained as 78.3 % and 1.422 W m^{-2} K^{-1} respectively. The BiSPVT system thus considered finds its application by providing both electrical and thermal energy gain to buildings by replacing the conventional energy sources and also befitting in locations with limited accessibility to grid electricity.

After establishing the energy performance of the system, the focus shifts to exergy and exergoeconomic parameters, which provide deeper insight into the quality of energy conversion, thermodynamic irreversibilities, and the economic feasibility of the system components in relation to their exergy performance. These advanced evaluations allow for a more rigorous understanding of the system's sustainability and cost-effectiveness. Chapter 5 elaborates on these analyses in detail, extending the scope of the present study toward a more comprehensive performance and viability assessment of the BiSPVT facade system.

5

Exergy, Exergoeconomic And Enviroeconomic Analysis of the BiSPVT Facade

Chapter Outline:

CHAPTER 5: EXERGY, EXERGOECONOMIC AND ENVIROECONOMIC ANALYSIS OF THE BISPVT FACADE

5.1 Introduction

Exergy and exergoeconomic analysis offer a deeper thermodynamic and economic perspective in evaluating photovoltaic thermal (PVT) and building integrated photovoltaic thermal (BIPVT) systems. While conventional energy analysis focuses on the quantity of energy, exergy analysis emphasizes the quality and usability of that energy by accounting for system irreversibilities and ambient conditions. This makes exergy a more appropriate metric for assessing the true performance of PVT systems under varying operational and climatic conditions. Several studies across diverse configurations, from glazed collectors and sinusoidal finned channels to semi-transparent facades, have shown that exergy efficiency is strongly influenced by factors such as solar irradiance, temperature gradients, flow arrangements, and working fluids [196][197]. Moreover, exergoeconomic analysis integrates cost considerations by evaluating the economic performance in terms of cost per unit of useful exergy delivered. This combined perspective helps in identifying not only the thermodynamic bottlenecks but also the cost intensive components of the system. The exergoeconomic approach thus aids in optimizing system design by balancing performance enhancement with economic feasibility, making it a vital tool for sustainable energy system evaluation, particularly in applications where both thermal and electrical outputs are critical.

In this chapter we present the exergy, exergoeconomic, and enviroeconomic analysis of the BiSPVT facade system, evaluating its performance in alignment with the second law of thermodynamics. The study focuses on useful energy output, system irreversibilities, and the economic value of energy quality, specifically for the climate of Srinagar, India. Key exergoeconomic parameters such as energy (L_{en}) and exergy loss rates (L_{ex}), and their corresponding cost ratios (R_{en} and R_{ex}), were computed, revealing low loss rate ratios, indicating high system efficiency and economic viability.

5.2 Annual energy and exergy gain analysis of the BiSPVT facade system

In the previous chapter, the BiSPVT system was evaluated for its monthly and annual performance in terms of electrical output, thermal gain, overall thermal energy, and useful exergy under varying climatic conditions in Srinagar, India. The analysis as indicated in **Fig. 5.1** showed that October recorded the highest monthly electrical energy gain of approximately

17.27 kWh/m², while the overall useful exergy gain peaked at 17.67 kWh/m² in the same month. Conversely, the lowest values for both electrical and exergy outputs were observed during June, corresponding to reduced solar radiation levels. The system achieved an annual electrical energy gain of 121.22 kWh/m², thermal gain of 61.06 kWh/m², overall thermal energy gain of 366.23 kWh/m², and useful exergy output of 122.36 kWh/m². These results, summarized in the graph below, establish a strong baseline for assessing the system's energy conversion capabilities. Building upon these insights, the current chapter advances into the exergy, exergoeconomic, and enviroeconomic analysis, offering a more holistic evaluation of the system's thermodynamic quality, cost performance, and environmental impact.

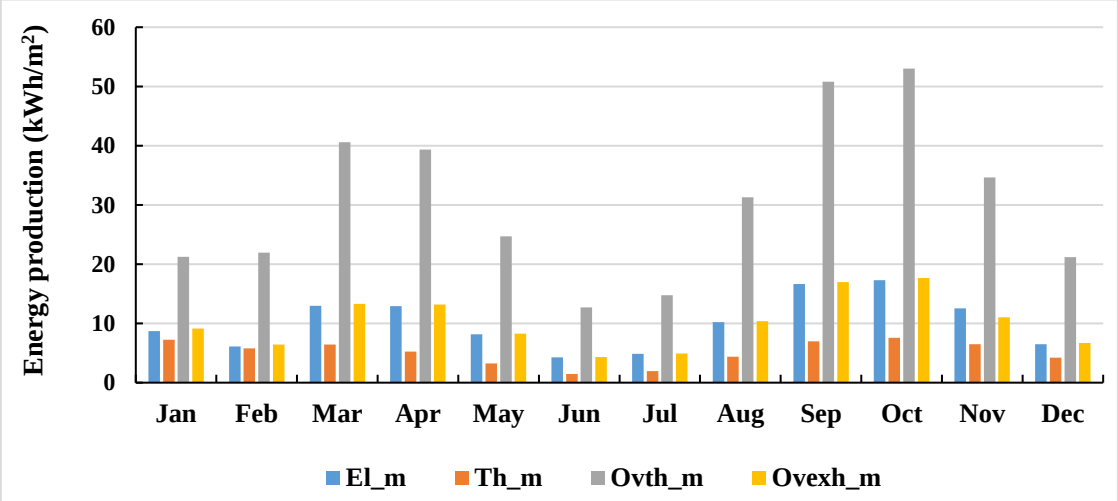

Fig. 5.1 Monthly variation of electrical, thermal, overall thermal and exergy gain from the system (all weather conditions)

5.3 Energy and exergy loss rate analysis

Energy loss rate for the BiSPVT system with all weather conditions are shown in **Fig. 5.2**. Energy loss rate has been observed as highest for b-type weather conditions considering the highest number of hazy day conditions. Losses for c and d type weather conditions were less cause of lesser incident total solar radiation on the BiSPVT system. The system has an annual energy loss rate of 425.6 kWh/m², shown in **Fig. 5.3**.

For annual energy loss rate, Maximum loss of energy was obtained for the month of January with 59.8 kWh/m² and minimum for September with 25.3 kWh/m². For annual exergy loss rate Lex, maximum was observed in the month of January with a value of 66.48 kWh/m² and minimum for June with 36.08 kWh/m² (**Fig. 5.4**). Annually, exergy loss rate (Lex) from the

system was obtained as 617.74 kWh/m² shown in **Fig. 5.5**. Exergy loss rates were found to be minimum during the months of June and July, as solar radiation incident on the PV facades was less for those months compared to January and December. With higher radiation intensity, electrical performance of the module dropped resulting in increase of optical losses and reduced electrical efficiency. PV module electrical performance is adversely affected by a considerable increase of its cell temperature by upon absorbing solar radiation incident on it. Thus, the BIPV facade system produce higher energy and exergy gain rate during January, February, September and October compared to June and July, resulting in decrease of L_{en} and L_{ex} value. Similar, explanation can be drawn for annual L_{en} and L_{ex} values as shown in **Fig. 5.4** and **Fig. 5.5**.

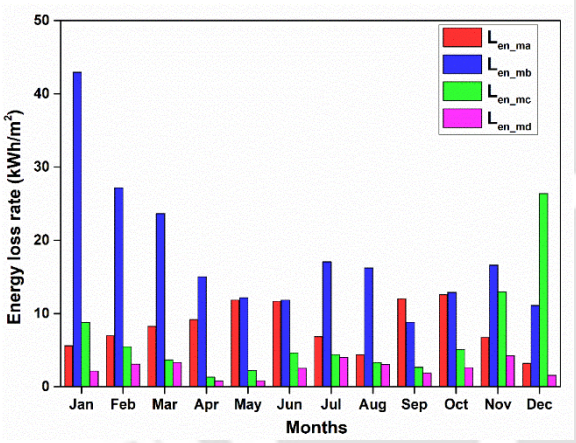

Fig. 5.2 Monthly variation of energy (L_{en}) loss rate (a, b, c, d condition)

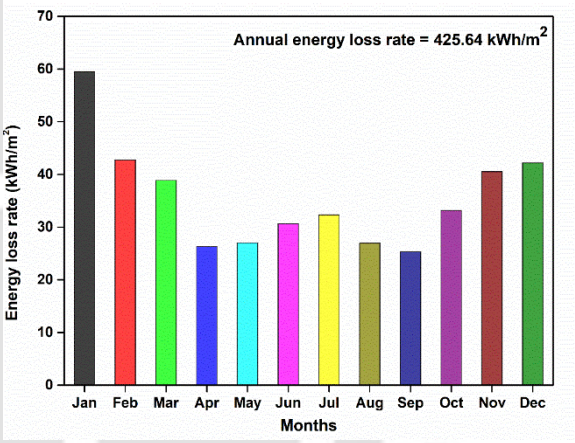

Fig. 5.3 Monthly variation of energy loss rate (L_{en})

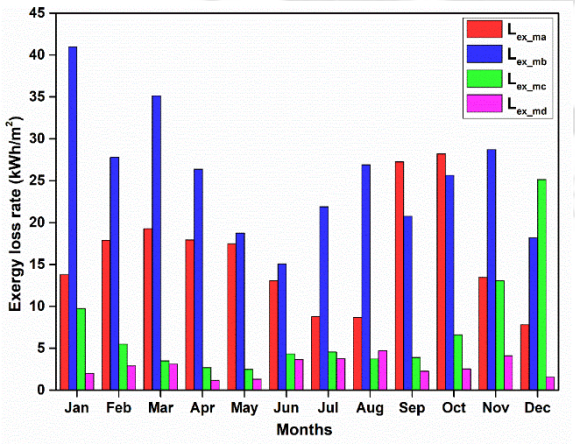

Fig. 5.4 Monthly variation of exergy (L_{ex}) loss rate (a, b, c, d condition)

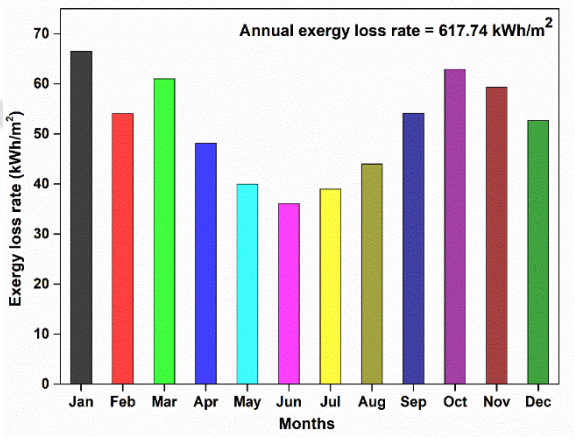

Fig. 5.5 Monthly variation of exergy loss rate (L_{ex})

A comparison of the annual L_{ex} and L_{en} by considering all four specific climatic conditions (a-d type) for the BiSPVT has been shown in **Fig. 5.6**, which further illustrated the previous explanation. Energy and exergy loss rates were dominant during the winter seasons whereas it was minimum during the summer seasons. Electrical power gain from the BiSPVT system was higher for cooler months viz, January, February, September and October. Consequently, loss rate was observed less for these months in comparison to June and July. Thus, from above, it can also be accomplished that BiSPVT system offers higher energy and environmental cost benefits in winters as compared to the summers.

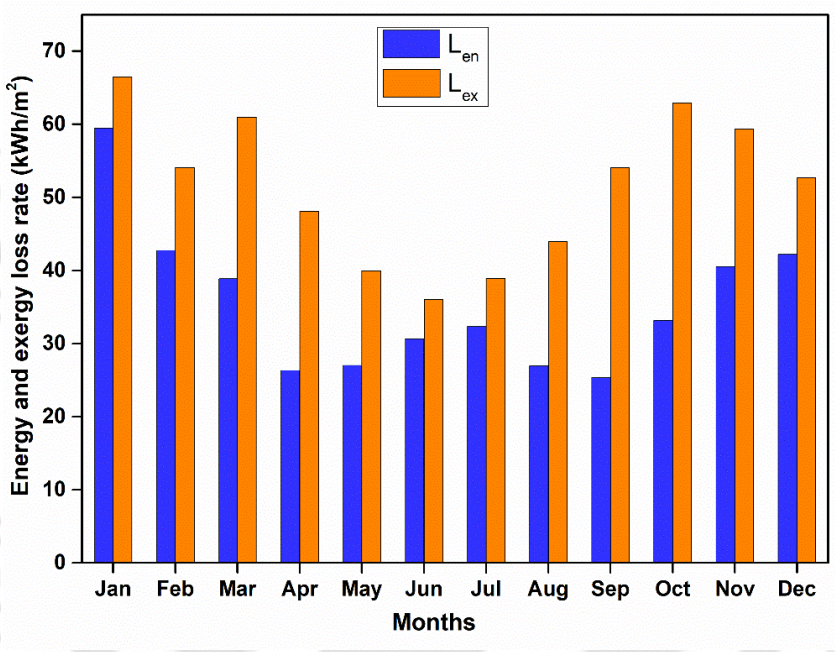

Fig. 5.6 Comparison of monthly L_{en} and L_{ex} of the BiSPVT system

5.4 Energy matrices evaluation

Energy Matrices evaluated for systems lifespan of 30 years. **Table 5.1** shows the calculated embodied energy assembling all the components of the BiSPVT system obtained to be 13917 kWh. The reference values used while calculating the embodied energy value has been sourced from established literature sources [122], Using equation 8, the values for EPBT in terms of overall thermal energy and overall exergy was obtained as 3.2 years and 9.8 years respectively. As shown in Table 5.2, the thermal energy payback time of 3.30 years indicates rapid recovery of the embodied energy through useful heat generation, demonstrating the suitability of the BiSPVT system for low-temperature thermal applications. In contrast, the exergy payback time of 9.87 years is considerably higher due to the lower work potential

associated with low-grade thermal energy and thermodynamic irreversibilities, highlighting the importance of exergy-based assessment for a realistic evaluation of system sustainability.

Table 5.2 displays the estimated EPBT for the overall gain in thermal energy and exergy. **Table 5.3** presents the calculated EPF and LCCE for the BiSPVT system over each 10-year period within its 30-year lifespan. A value of EPF greater than 1 for both thermal energy and exergy indicates that the system has generated surplus energy beyond what was required for its manufacturing. LCCE which is dependent on embodied energy, total energy output generated by the system, solar radiation received and systems lifetime of 30 years were obtained closer to 1, indicating the system to be energy efficient. NPV evaluation for the system is based on its capital cost (P), salvage value, operational and maintenance cost assumed to be 2% of PV modules cost [198], and expected revenue streams over the system's lifetime, discounted to present value.

Table 5.1 Embodied energy estimation of semi-transparent PV facade components

Particulars	**Quantity**	**Size**	**Individual Embodied energy**	**Total embodied energy (kWh)**
PV Module	14(11.52 m^2)	11.52 m^2	998 kWh/m^2	11496
AI Frame	0.0013482 m^2	3.653	55.28 kWh/kg	201.93
Glass Wool	1.728 m^2	2.9088	24.8MJ/kg	6.89
Nuts/Bolts/Screws	40	1.5	55.28 kWh/kg	82.92
Union	10	1.8	50 MJ	13.88
Galvanized iron with Mild steel support	2	200	9.67 kWh/kg	1934
Paint	5L	5	25.11 kWh/kg	125.55
Rubber gasket	91.56 m	21.36	11.83 MJ/kg	3.29
PVC Pipes	0.3 m	14.89	92.6 MJ/kg	25.73
DC FAN's components embodied energy				
	Total weight (kg)		**Embodied energy (kWh/kg)**	
Aluminum	0.39		55.28	21.5592
Iron	0.22		8.89	1.9558
Plastic	0.12		19.44	2.3328
Copper Wire	0.05		19.61	0.9805
TOTAL				**13917**

Table 5.2 Annual overall thermal energy and exergy savings, EPBT from BiSPVT system

Energy	Annual Energy Savings(kWh)	Embodied Energy (E_{in})	Energy Payback Time (EPBT) (year)
Overall thermal energy	4218.99	13917.01	3.30
Exergy	1409.59	13917.01	9.87

Table 5.3 EPF and LCCE on energy and exergy savings across various lifespan of the BiSPVT system

Life span (years)	EPF		LCCE	
	Overall thermal energy	Exergy	Overall thermal energy	Exergy
10	3.032	1.013	0.240	0.002
20	6.063	2.026	0.299	0.060
30	9.095	3.039	0.318	0.080

Table 5.4 represents systems NPV with salvage values being obtained for systems lifetime of 10, 20, and 30 years respectively. Further using obtained NPV, the Unified Levelized Cost of Electricity (Unacost) calculation for the BiSPVT system was obtained. Unacost accounts for all costs associated with the BIPVT system over its lifetime, including initial installation, operation, maintenance, and decommissioning, as well as the energy generated over the system's lifespan.

Table 5.4 Net present value (NPV) of semi-transparent PV facade

SI No	Particulars	Quantity (in no's, m², Litre, meters)	Amount (kg)	Cost (Rs)	Total cost (Rs)	Salvage value of different components (SS) at the inflation rate of 4% (Present values of scrap for, iron @ Rs 30/kg, aluminum @ Rs 105/kg and copper @ Rs 425/kg)			
						Components	**After 10 year (Rs/kg)**	**After 20 year (Rs/kg)**	**After 30 year (Rs/kg)**
						Iron scrap	44.24	65.25	96.23
						Aluminum	154.86	228.4	336.89
						Copper	626.84	924.5	1363.6
1	PV Module	14	11.52m²	Rs 5500/m	63360		9911.28	14618	21561
2	AI Frame	0.013482 m²	3.65	Rs 350/kg	1278.6		565.7036	834.4	1230.7
3	Glass Wool	1.728 m²	2.91	Rs 125/ m²	216		-	-	-
4	Nuts/Bolts/Screws	40	1.5	Rs 55/kg	82.5		66.36	97.88	144.35
5	Union	10	1.8	Rs 55/kg	99		79.632	117.5	173.21
6	Mild steel support	2	100	Rs 45/kg	4500		4424	6525	9623
7	Paint	5L	5	Rs 471/L	2355		-	-	-
8	Rubber gasket	44.94m	21.4	Rs 75/m	3370.5		-	-	-
9	PVC Pipes	0.3 m	14.9	Rs 85/kg	1265.7		658.7336	971.6	1432.9
10	DC FAN	1	-	Rs 2320.6	2320.6		825.94	1218	1796.8
11	Battery cost	3	3.5 kWh	0.11$/Wh	31570		-	-	-
12	Fabrication charges		10% of PV modules cost		18900		-	-	-
13	O&M cost		2% of PV modules cost		3780		-	-	-
14	**Capital Cost (in Rupees)**				**133097**		**16531.65**	**24383**	**35962**
15	**Capital Cost (in USD)**	***1$ = Rs 83.35(1.12.2023)***			**$1596.83**		**$200.84**	**$303.51**	**$436.90**

Figure 5.7 illustrates the calculated UAC for the overall gain in thermal energy, while **Fig. 5.8** displays the UAC for the overall gain in exergy. The minimum UAC obtained is 0.031 $/kWh on overall thermal energy basis for interest rates of 4%, however the maximum value of UAC is 0.20 $/kWh for interest rates of 10% on overall exergy basis. UAC for thermal exergy gain at 4% IRR varied from 0.09-0.16 $/kWh which is 7.5-13.3 INR/kWh with respect to the per unit electricity paid in India using fossil powered sources which is around INR7/kWh. The discount rate (r) has been observed as a crucial economic factor affecting the present value of investments. It reflects the rate at which future cash flows or benefits are adjusted to their current value, considering factors like time and risk (such as inflation). As depicted in Fig. 5.7 and Fig. 5.8, when the discount rate (r) is altered within the range of 4 to 10%, by retaining all other factors constant, the UAC for BiSPVT system increases. The same can be observed for EPF and LCCE values obtained (Table 5.3). Furthermore, the values obtained for per unit electricity signifies to the potential of using the BiSPVT facade that has the ability to produce per unit electricity at less or equivalent values to coal powered electricity output.

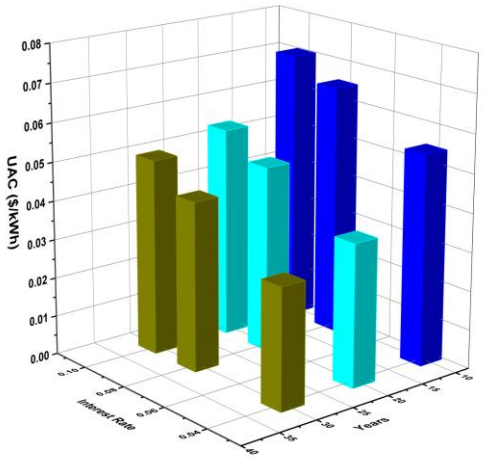

Fig. 5.7 Uniform annualized cost in terms of overall thermal energy of the BiSPVT system

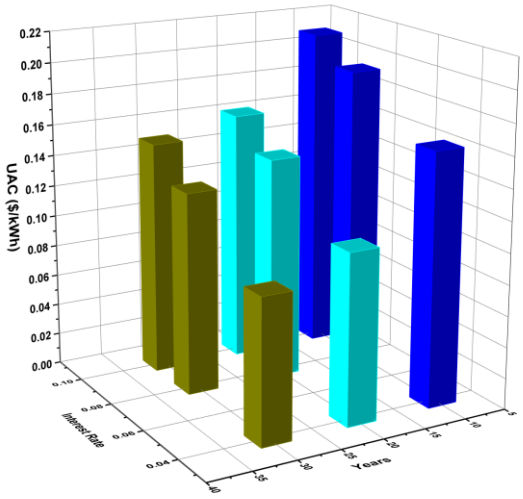

Fig. 5.8 Uniform annualized cost in terms of overall exergy of the BiSPVT system

5.5 Environmental performance evaluation

5.5.1 CO_2 emission reduction and carbon credit

The annual CO_2 emission and carbon credit earned in a year is tabulated in **Table 5.5**. The CO_2 reduction values presented in Table 5.5 represent the operational-phase emission savings

achieved through energy generation from the BiSPVT system, primarily by offsetting conventional grid electricity and thermal energy sources. These estimates do not account for emissions associated with material extraction, manufacturing, transportation, installation, maintenance, and end-of-life stages of the system. Consequently, the reported CO_2 reduction figures may be overestimated when interpreted as full life cycle savings. Inclusion of a comprehensive cradle-to-grave LCA would provide a more conservative and realistic assessment of net CO_2 mitigation potential; however, the current values remain useful for comparing operational performance and short-term emission benefits.

Table 5.5 Annual gain in overall exergy, CO_2 emission reduction and environmental cost reduction in BIPV facade system.

Parameter	Annual Energy saving (kWh)	CO_2 reduction (tones/ CO_2)	Environmental cost reduction ($/month)
Overall thermal energy gain	4218.99	8.43	122.23
Overall exergy gain	1409.59	2.81	40.87

5.5.2 Greenhouse gas payback time period (GPBT) estimation

For the BiSPVT system in consideration, annual overall thermal energy output from the system was estimated to be 4218.99 kWh corresponding to this, the equivalent CO_2 emissions saved is 4050.23 kg CO_{2eq}. In the process of fabricating cells for photovoltaic (PV) modules, 463 kg CO_{2eq} /m^2 was determined to be the amount of embodied greenhouse gases emitted per square meter [199]. Additionally, for the balance of system (BOS) in BIPV installations, the greenhouse gas emissions were estimated at 6.1 kg CO_2eq/m^2 for supporting the array and the cable cost associated [136], and for batteries considered as 125 kg CO_{2eq} /m^2 [185]. It's important to note that emissions from transportation and disposal were not considered. Altogether, the total greenhouse gas emissions from manufacturing and installing the PV system were calculated to be 6844.03 kg CO_{2eq}. the calculated GPBT from equation 16. was obtained as 2.5 years. Furthermore, GPBT calculation also varies with location which indicates the influence of local power supply mix. For example, while calculating GHG emission factor for Chengdu province, China, the CO_2 emission factor for coal powered electricity is 0.36 kg

CO_{2eq} which for India is 0.96 kg CO_{2eq} [132] . Therefore, considering the benchmark value of coal-powered electricity as a reference point will facilitate an accurate computation.

5.6 Summary of the chapter

The study here investigates the exergy and exergoeconomic performance of a facade based semi-transparent building integrated photovoltaic system with rated power of 1.6kWp integrated to a buildings southern wall in Srinagar, India. Yearly reduction of CO_2 emission by the studied system accounts to 2.81 tonnes leading to 40.87 $/annum environmental cost reduction. For the system, with 30 years of considered lifetime at a 4% interest rate, the energy (R_{en}) and exergy loss rate ratio (R_{ex}) values were found to minimum.

The present study carried out on the BiSPVT system in concord with the second law of thermodynamics thus proves its essentiality in building energy systems by focusing on useful energy gain from the proposed system which further can reduce usage of conventional energy sources in the building sector. Present investigation also supports how total conversion of thermal energy into useful work is subjected to certain limitations or losses, which are indicated as irreversibilities. Moreover, the analysis based on economic value of the system in accordance with useful energy generated encourages in finding better credentials with respect to quality of energy produced and issues pertaining to costs.

In continuation of the thermodynamic and economic evaluation, the next chapter (Chapter 6) presents a detailed life cycle analysis (LCA) of the BiSPVT system, assessing its environmental impact across all stages of its operational lifespan. This enables a comprehensive understanding of the system's long-term sustainability and resource efficiency.

6

Life Cycle Assessment of the BiSPVT Facade

Chapter Outline:

CHAPTER 6: LIFE CYCLE ASSESSMENT OF THE SEMI-TRANSPARENT BUILDING INTEGRATED PHOTOVOLTAIC FACADE

6.1 Introduction

Life Cycle Assessment (LCA) is increasingly being used as a tool to evaluate the environmental performance of renewable energy systems, including photovoltaic and photovoltaic thermal (PVT) technologies. While PVT systems contribute positively by generating both electricity and thermal energy from the same surface area, it is also important to consider the environmental impact associated with the materials, manufacturing processes, and system lifespan. This becomes even more relevant in the context of building-integrated applications, where systems like BIPVT are directly replacing conventional construction materials.

The aim of this chapter is to evaluate the environmental footprint of the semi-transparent BIPVT facade system analysed in the present work, considering its full life cycle, from raw material extraction and manufacturing to operation and end-of-life. Although the use phase of such systems helps offset conventional energy demand and reduces greenhouse gas emissions, the embodied impacts from production cannot be ignored. For this reason, studies such as those by Lamnatou and Chemisana [160] have highlighted the need for detailed LCA on BIPVT systems, especially given the limited research available that goes beyond just energy payback time or carbon savings.

Literature shows that certain configurations, such as double-pass air-based systems [144] or glazed BIPVT systems [158], have reported promising environmental benefits. However, most studies still focus on specific indicators like CO_2 mitigation or EPBT, without evaluating broader categories such as human toxicity, resource depletion, or ecosystem impacts. Chow and Ji [156], for instance, pointed out that building-integrated configurations may have slightly higher EPBT than building-added ones, but offer more benefits when material displacement and multifunctionality are considered.

In this chapter, a life cycle-based environmental analysis is carried out for the proposed BIPVT system using standard impact assessment methods. The objective is not just to quantify emissions or payback periods, but to provide a more holistic understanding of where the major impacts lie, whether in the PV module itself, the supporting materials, or other components of the system. The results are intended to inform future system design decisions

and contribute to ongoing discussions on the sustainability of integrated solar technologies in the building sector.

6.2 Material and methods used for LCA analysis of BiSPVT system using SimaPro

6.2.1 Type of inventory modelling

The life cycle inventory, impact assessment methods and their interpretation has been adopted according to ISO 14040:2006 and ISO 14044:2006 [200]. Inventory modeling of LCA consist of two type- attributional modeling and consequential modeling. Attributional modeling is used for assessing a systems probable environmental effect throughout its lifecycle. This approach utilizes factual measurable data linked to uncertainty known or knowable to model the system as it currently exists, has existed in the past, or is projected to be in the future. On the other hand, consequential modeling approach is based on a hypothetical supply chain which is more predictive in nature based on potential consequences of the discussion [201]. Based on type of life cycle inventory modelling, attributional modeling has been chosen for the present study.

6.2.2 Functional unit and system boundaries considered

The life cycle assessment (LCA) of the 1.6kWp building-integrated semi-transparent photovoltaic thermal (BiSPVT) system is focused on the climate of Srinagar, India. Annually, the system produces annual overall thermal energy gain of 366.23 kWh/m^2. The total area of the BiSPVT system, including the PV modules, is 11.52 m^2, with each individual PV module covering an area of 0.605 m^2.

The LCA considers the material manufacturing processes for all the components of the BiSPVT system. The environmental impacts are allocated based on the mass (kg) and area (m^2) of the facade system. The study only includes the stages of material manufacturing and disposal, and excludes the transportation of the system components from the factory to the building and from the building to the disposal site, as the impact of this transportation is expected to be minimal for a single-room installation (3.6m x 3m x 3.2m). Additionally, the recycling scenario for the system components has not been considered in this LCA. In **Table 6.1**, details about the components/materials of one PVT module are presented.

Table 6.1 Life-cycle inventory of the BiSPVT system

Particulars	Quantity	Size
PV Module	14(11.52 m^2)	11.52 m^2
AI Frame	0.0963 m^2	3.653 kg
Glass Wool	1.728 m^2	2.9088 kg
Nuts/Bolts/Screws	40 in no's	1.5 kg
Union	10 in no's	1.8 kg
Galvanized iron with Mild steel support	2 in no's	200 kg
Paint	5L	5 kg
Rubber gasket	91.56 m	21.36 kg
PVC Pipes	0.3 m	14.89 kg
DC FAN	**1**	**Total weight (kg)**
Aluminum		0.39
Iron		0.22
Plastic		0.12
Copper Wire		0.05

6.2.3 Sources of data and boundaries adopted

The present study examines the life cycle assessment of the BiSPVT system using SimaPro. Using this software tool, users can assess the environmental consequences of products or processes throughout their entire life cycle, spanning from the extraction of raw materials to their disposal or recycling. With Simapro, users can input data regarding resource use, energy consumption, emissions, and waste generation at each stage of the life span, enabling comprehensive evaluation and comparison of environmental footprints [202]. Ecoinvent 3 is a detailed database within Simapro containing numerous life-cycle inventory datasets [203]. Using SimaPro 8 and the Ecoinvent 3 database the overall scores and impacts of the components were assessed. Impacts were measured per kg of material (or per m^2 for PV module) for the calculations.

Regarding the geographic origins of materials, the GLO (Global) option which includes activities applicable worldwide was applied to PV modules; Aluminum Frame; Glass wool (insulation); Nuts, Bolts and Union; Gasket; DC fan materials included of Aluminum, Iron and Copper Wire. For Paint and Plastic, the ROW (Rest of the World) option was used. For the details of the BiSPVT system components and their amount/sizes used, Table 3 is used for reference. Data collection for the BiSPVT system for Ecoinvent Database has been shown in **Table 6.2.**

Table 6.2 Data collection for the BiSPVT system from Ecoinvent 3 database

Component selection from database (Ecoinvent 3)	BiSPVT Components
Photovoltaic panel {RoW}| market for | APOS, U	PV module
Aluminum alloy, AlLi {GLO}| market for | APOS, U	PV module frame (Aluminum)
Steel engineering steel/GLO	Steel Support
Glass wool mat {GLO}| market for | APOS, U	Glass wool
Acrylic varnish, without water, in 87.5% solution state {ROW}| market for | APOS, U	Paint (Black)
Synthetic rubber {GLO}| market for | APOS, U	Gasket (Rubber)
PVC pipe E	PVC pipes
Steel, low-alloyed {GLO}| market for | APOS, U	Nuts and Bolts
Steel, chromium steel {GLO}| market for | APOS, U	Union
Aluminium alloy, AlMg3 {GLO}| market for | APOS, U	DC Fan (Aluminium)
Cast iron {GLO}| market for | APOS, U	DC Fan (Iron)
Polypropylene, granulate {ROW}| production | APOS, U	DC Fan (Plastic)
Copper-rich materials {GLO}| market for copper-rich materials | APOS, U	DC Fan (Copper wire)

6.2.4 Life cycle impact assessment methods and environmental indicators

Environmental assessment indicators has been based on the following methods [201]:

i. IPCC 2021 GWP20 V1.01; IPCC 2021 GWP 100 V1.01

ii. ReCiPe Endpoint 2016 (H) V1.1 (single-score)

iii. ReCiPe Endpoint 2016 (H) V1.1 (with characterization)

iv. ReCiPe Midpoint 2016 (H) V1.1 (with characterization)

Three scenarios were evaluated considering various Global Warming Potential (GWP) timeframes: GWP 20 (20 years) and GWP 100 (100 years), of which GWP 100 is the commonly used scenario. These variations were considered to offer a comprehensive view of GWP, recognizing that certain substances exhibit gradual decomposition over time. The considered scenarios pertain to the material manufacturing stage and are aligned with the climate change factors outlined by the Intergovernmental Panel on Climate Change (IPCC) for 20, 100, and 500-year timeframes. The ReCiPe methodology incorporates both midpoint (problem-oriented) and endpoint (damage-oriented) impact categories, utilizing a 'hierarchist' (H) perspective for assessment purposes. **Table 6.3** shows in details about the impact assessment categories in detail.

Table 6.3 LCA indexes and methods described in detail

Impact category indexes	Impact category name	Unit	Description
IPCC 2021	Global Warming Potential- GWP- 20,100	Kg CO_2 eq	• IPCC's GWP factors for climate change account for 20, 100-year periods. • GWP of greenhouse gases is expressed in kg CO_2eq, referencing the effect of each gas to that of 1 kg of CO_2
ReCiPe Midpoint	Stratospheric ozone depletion	kg CFC-11 eq	• Stratospheric ozone layer protects us from harmful UV-B radiation, and its depletion raises the risk of skin cancer and plant damage. • Impact of ozone-depleting substances is measured in kgCFC-11eq, with all substances converted to their trichlorofluoromethane (Freon-11 or R-11) equivalents.

Impact category indexes	Impact category name	Unit	Description
	Human carcinogenic toxicity	kg 1,4-DCB	• Measures potential human health impacts from absorbing substances through air, water, and soil. • It does not currently account for the direct effects of products on human health.
	Human non-carcinogenic toxicity	kg 1,4-DCB	
	Marine ecotoxicity	kg 1,4-DCB	Refers to damage of marine ecosystem due to absorption of toxic substances
	Freshwater ecotoxicity	kg 1,4-DCB	Refers to damage of air, water and soil due to expose of toxic substances
ReCiPe Endpoint (single-score)	Resources, Ecosystem, Human Health	Pts (Points)	Midpoint categories are coupled together to give endpoint damage assessment in terms of Resources, Ecosystem and Human Health.
ReCiPe Endpoint (characterization)	Human Health	Disability adjusted Life years (DALY)	• The metric combines years of life lost (YLL) due to premature death with years of life lost to disability (YLD) from living with a disease or its consequences: DALY = YLL + YLD. • Quantifies the burden of human disease caused by environmental pollution, attributing it to the life cycle of products.
ReCiPe Endpoint (characterization)	Ecosystem	Species per year	Loss of species from an ecosystem per year when exposed to harmful pollutants in environment

Based on the explanations presented above, in **Fig. 6.1**, a schematic of the present LCA study is illustrated. Further, **Fig. 6.2** represents system boundary of the LCA study for the BiSPVT system considered.

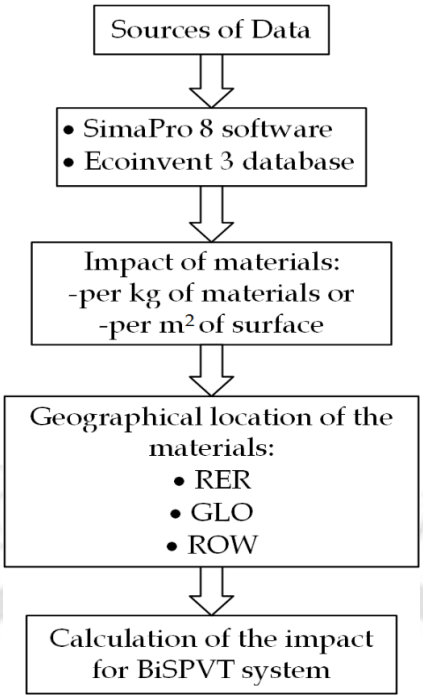

Fig. 6.1 A schematic about the present LCA study

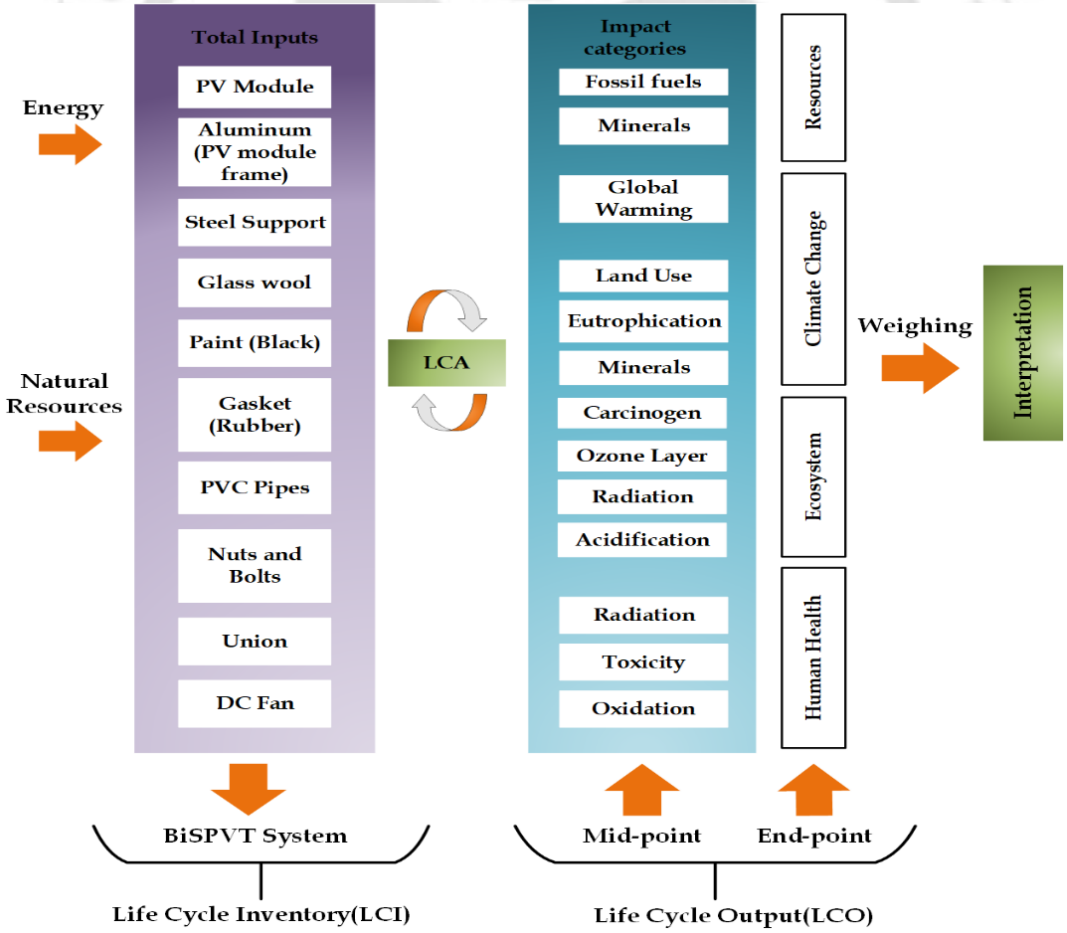

Fig. 6.2 System boundary of the life-cycle assessment of the BiSPVT system

6.3 Interpretation of the findings from SimaPro LCA study

Life Cycle Assessment (LCA) studies using SimaPro software are highly effective for evaluating BIPV systems. These assessments provide a thorough analysis of environmental impacts, including resource depletion, human health (measured in Disability-Adjusted Life Years or DALYs), species loss in ecosystems, and global warming potential from the components associated with assembling a BIPVT system. Such detailed insights are instrumental in promoting novel built-environment optimization strategies, particularly in ecologically-disturbed locales [204]. This can be explained by the ReCiPe midpoint (cradle-to-gate) and endpoint (cradle-to-grave) assessments that offers a comprehensive breakdown of environmental impacts at various stages, helping stakeholders to identify critical areas for improvement. Furthermore, IPCC approach is employed to assess the greenhouse gas emission rate based on hazardous gas emissions like CO_2, CH_4, nitrous oxide, etc. This enables the selection of BIPV system components that maximize sustainability and minimize ecological disruption. By focusing on these insights, BIPV systems can be encouraged that are not only energy-efficient but also aligned with broader environmental conservation and UN sustainability development goals (SDG 7: Affordable and clean Energy; SDG 11:Sustainable cities and communities; SDG 13: Climate actions). The findings based on LCA assessment of the BiSPVT from SimaPro is inclusive of BIPV systems components accepted globally (GLO) making the interpretations of results in terms of environment assessment robust.

6.3.1 Results based on Global Warming Potential (GWP)

Each component of the BiSPVT system and its contribution to the total global warming potential across three timeframes- 20 years and 100 years (the default) has been illustrated in **Fig. 6.3**. Notably, PV modules and steel support exhibit the maximum GWP values, in the range of 142 to 580 kg CO_2 equivalent (based on GWP 20). As expected, shorter time horizons correlate with higher GWP values, highlighting the significance of considering varying temporal perspectives in assessing environmental impact. The impact of the proposed BiSPVT system per square meter of the facade, based on primary materials, resulted in 0.98 t $CO_{2,eq}/m^2$ according to the GWP 100 scenario. This finding aligns well with existing literature on the subject. The available literature includes work of [199] who reported a value of 0.46 t $CO_{2,eq}$ for 1m^2 of the PV module in its application on PV and PVT systems integrated on roof. Another work reported GWP 100a value of a glazed PVT system as 0.43 t $CO_{2,eq}$ finding its application to roofs of building [205].

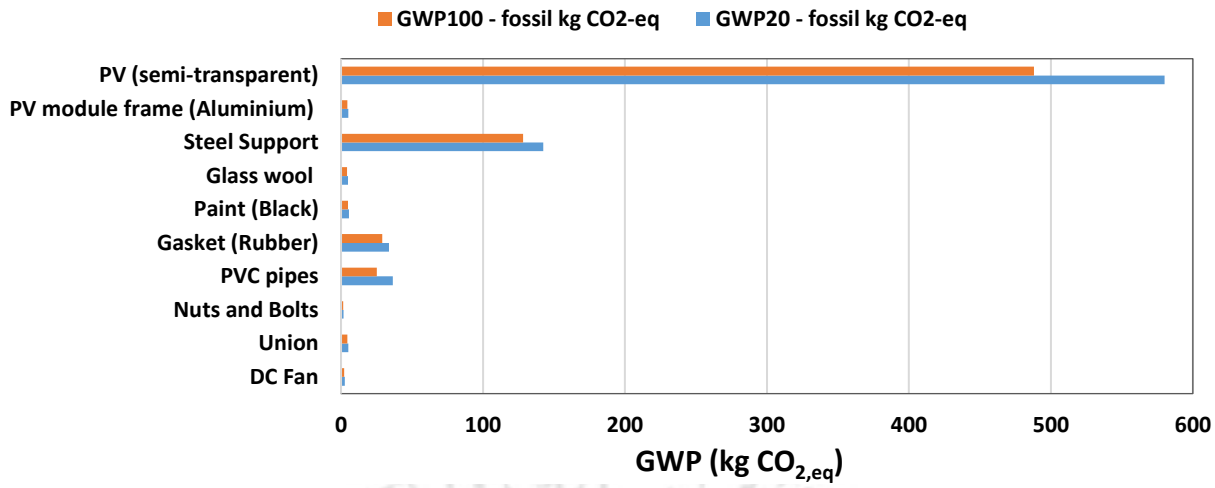

Fig. 6.3 Results for Global Warming Potential (GWP) corresponding to timeframes of 20 and 100 years

6.3.2 Results based upon ReCiPe endpoint (single-score)

In **Fig. 6.4**, the ReCiPe endpoint single-score reveals that PV modules and steel supports exhibit the maximum values, in the range from 5 to 28 Points across all endpoint classes (Ecosystems, Human Health and Resources), while other components score below 1 Point. Notably, Human health categories consistently show significantly higher scores compared to Resources and Ecosystems. Particularly for PV module and steel support, the disparities between Ecosystems and Human health, Human health categories are evident. Additionally, the impact on Human health to PV was found to be three times higher than that of steel.

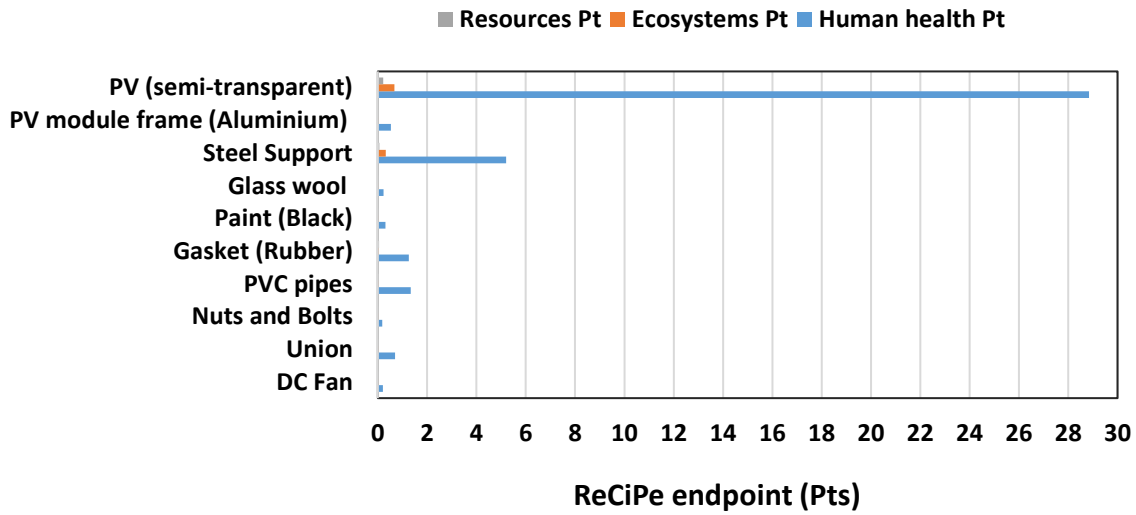

Fig. 6.4 ReCiPe endpoint, single score: BiSPVT system effect on Resources, Ecosystem and Human Resources

6.3.3 Results based upon ReCiPe endpoint (with characterization)

In **Fig. 6.5** and **Fig. 6.6** depicts the outcomes utilizing ReCiPe endpoint with characterization are illustrated. Fig. 6.5 presents data using Disability-Adjusted Life Years (DALY)as a metric: Total impact includes categories of Global warming/Human health; stratospheric ozone depletion; ionizing radiation; Ozone formation in regards to human health and terrestrial ecosystem, fine particulate matter formation and human carcinogenic and non-carcinogenic toxicity. Fig. 6.6 is based on species.yr: Overall impact includes categories of global warming based on terrestrial and freshwater ecosystem; freshwater eutrophication; terrestrial acidification; marine eutrophication; land use and toxicity in terms of terrestrial, freshwater and marine. Both the metrices: DALY and species.yr, confirms that the PV module and the two vessels exhibit the highest impacts, ranging from 0.0003115 to 0.0017288 DALY and from 1.198E-06 to 2.467E-06 species.yr.

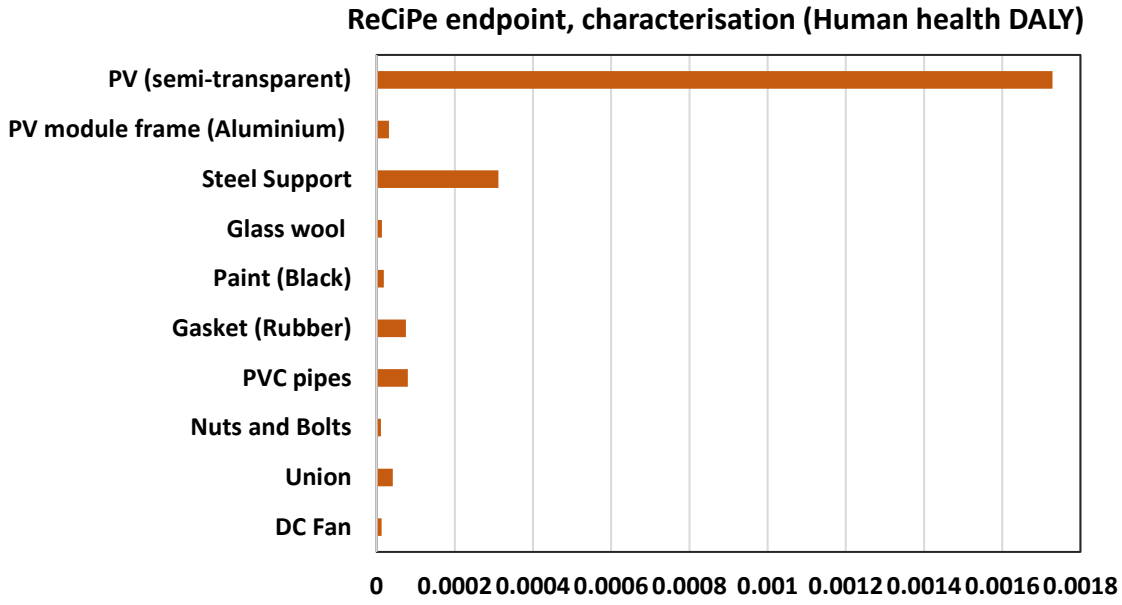

Fig. 6.5 ReCiPe endpoint, characterization (DALY)

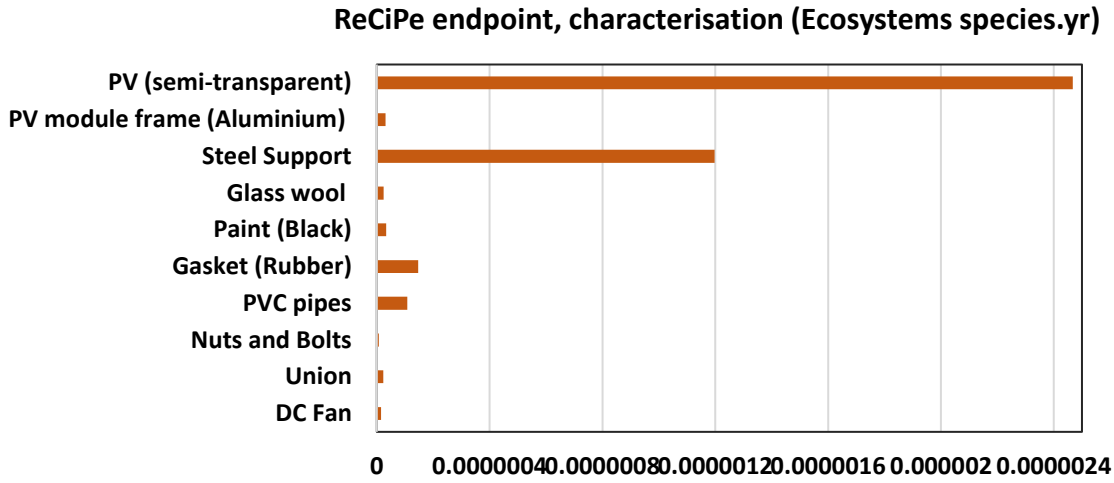

Fig. 6.6 ReCiPe endpoint, characterization (species.yr)

6.3.4 Results based on ReCiPe midpoint (with characterization)

Results using climate change and ozone depletion as included part of ReCiPe midpoint characterization is depicted in **Fig. 6.7** and **Fig. 6.8**. Both figures highlight that PV module and steel support bear the greatest impacts in both categories. Additionally, there's a significant contrast between the impact of PV module and that of steel support and rubber gasket, especially evident in the ozone depletion category. While steel support and PV module exhibit values ranging from 130 to 500 kg CO_2 eq for climate change, the effect of PV module is ~4 times greater to that of the steel support and approximately 14 times higher compared to the rubber gasket in the ozone depletion category.

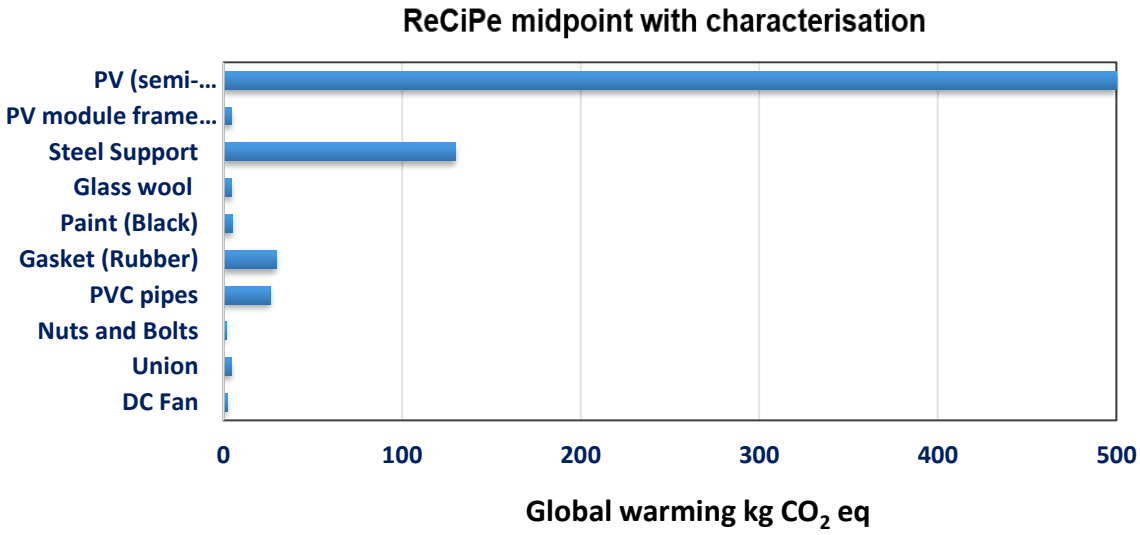

Fig. 6.7 ReCiPe midpoint with characterization according to global warming

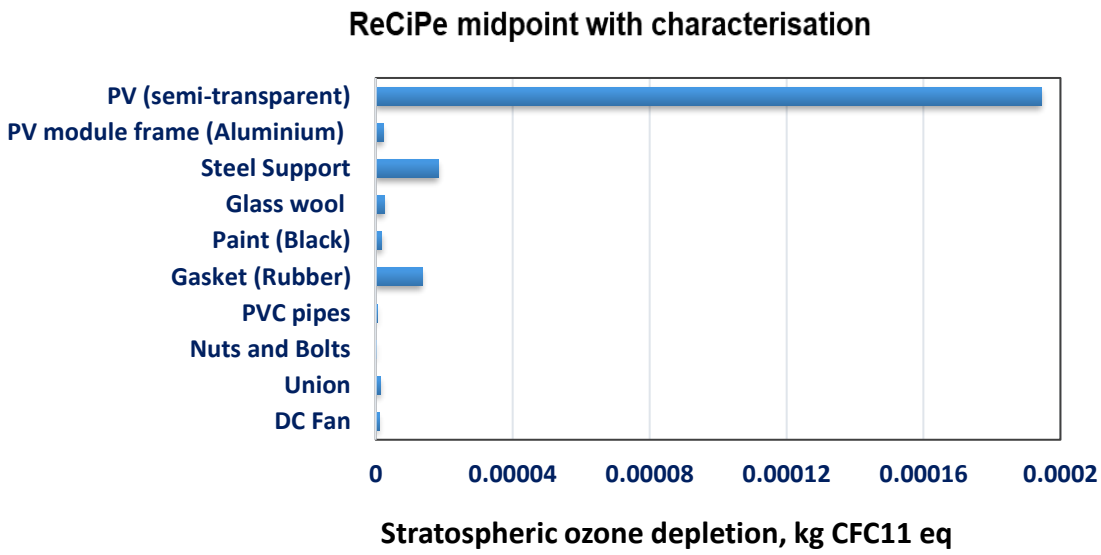

Fig. 6.8 ReCiPe midpoint with characterization according to ozone depletion

In **Fig. 6.9**, additional insights based on ReCiPe midpoint characterization are provided. The analysis focuses on categories such as human toxicity, considering both carcinogenic and non-carcinogenic effects, as well as marine, freshwater, and terrestrial ecotoxicity. Notably, PV module and steel support emerge as the components with the highest impacts across these categories, followed by the union, gasket, and aluminum frame. Interestingly, in marine and freshwater ecotoxicity, as well as human carcinogenic toxicity, components of the BiSPVT system, except for the PV module, demonstrate comparatively lower impacts. Fig. 6.9 highlights that terrestrial ecotoxicity and human non-carcinogenic toxicity generally exhibit significantly higher values compared to human carcinogenic toxicity. Specifically, PV modules demonstrate similar values for terrestrial and human non-carcinogenic toxicity, with numerical values of 249 and 248 kg 1,4-DCB, respectively. In contrast, for terrestrial ecotoxicity, PV modules exhibit impacts 1.5 times higher than steel support and 1.7 times higher than unions. Regarding human carcinogenic toxicity, PV modules show the highest values, with 111.1 kg 1,4-DCB, making them 9 times more impactful than PVC pipes and 14 times more impactful than unions.

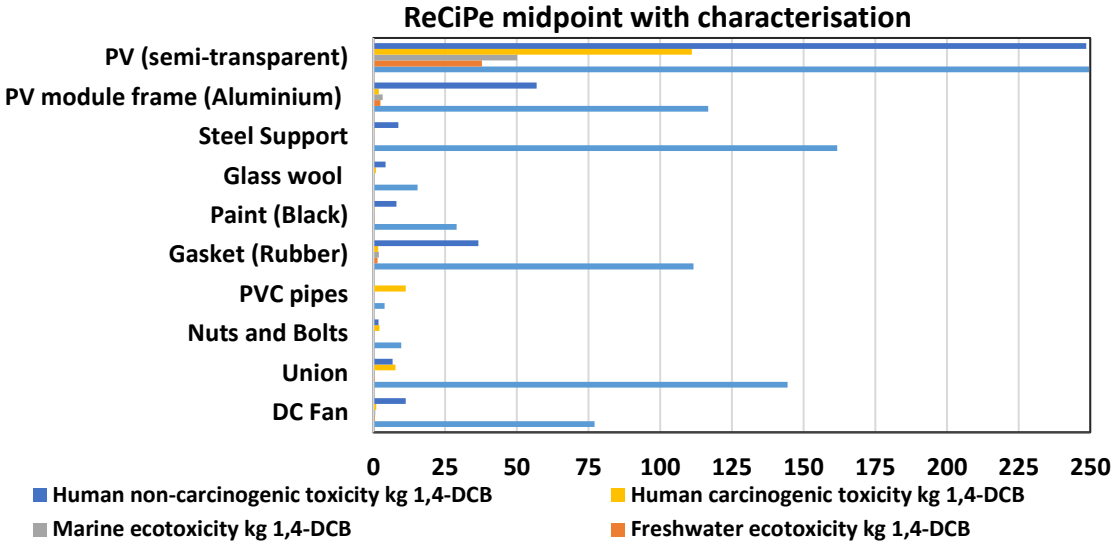

Fig. 6.9 ReCiPe midpoint with characterization according to Human carcinogenic toxicity, Human non-carcinogenic, Marine ecotoxicity ,freshwater ecotoxicity and terrestrial ecotoxicity

6.4 Contribution Analysis

Contributional analysis involves assessing the individual contributions of various components and factors to a system's overall performance and environmental impact. This analysis is crucial for identifying key areas for improvement and optimization in PVT system design and operation. **Fig. 6.10** illustrates the contribution of each component of the BiSPVT system to 18 environmental impact categories as per the ReCiPe midpoint method. The analysis reveals that the PV module accounts for an average of 72.2% of the impact, with the highest impact in the marine ecotoxicity category. The next significant contributors are the steel support and rubber gasket, with average contributions of 15.2% and 4.1%, respectively, across the 18 impact categories. Also, the steel support has the highest impact in the water consumption category.

This observation is consistent with findings reported in several LCA studies on PV and PVT systems, where PV modules are identified as the major source of environmental burden due to energy-intensive silicon processing, module fabrication, and upstream electricity consumption [168].

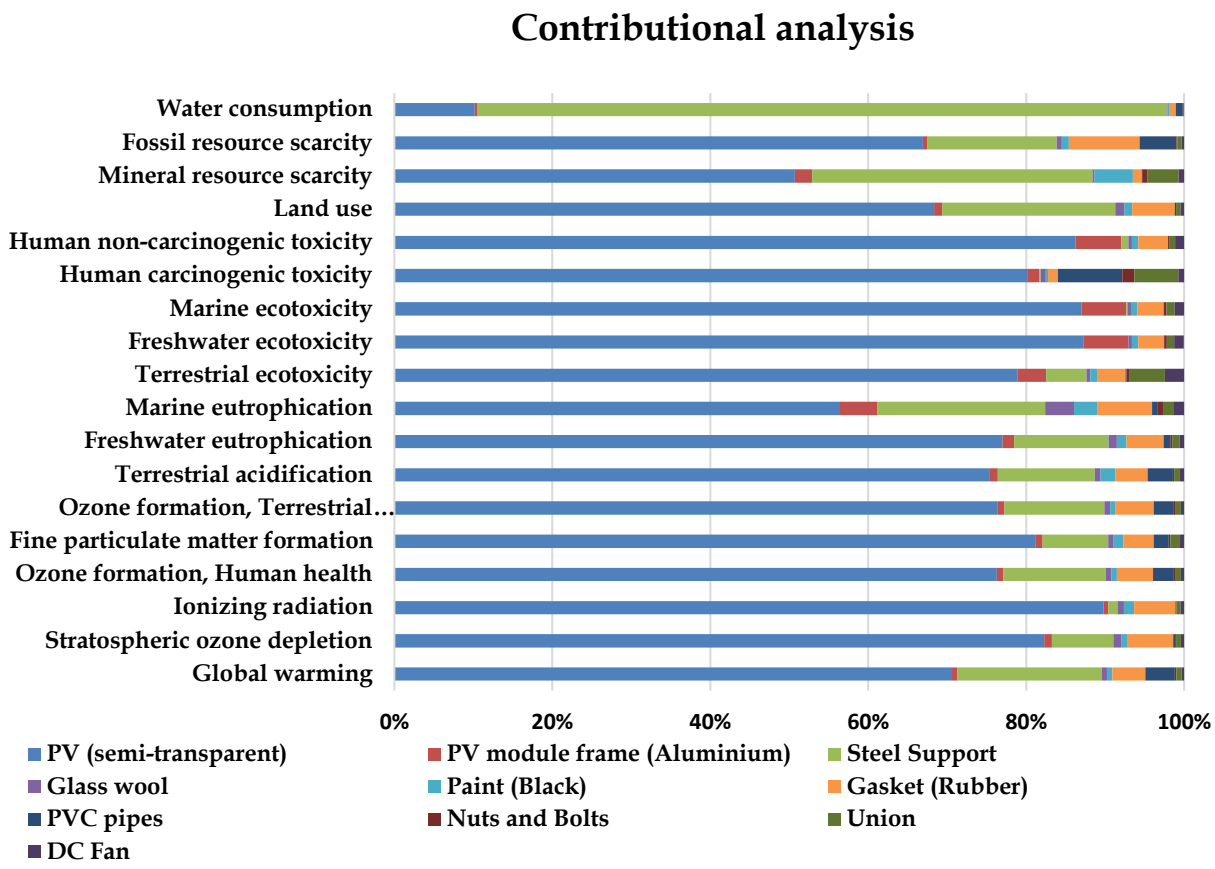

Fig. 6.10 Contribution of each component of BiSPVT system based on midpoint damage assessment

6.4.1 Discussion based on impact of each component on LCA assessment methods

The environmental impact of PV module mainly comes from the processes involved in converting silicon into single-crystal wafers and PV module, primarily using the Czochralski process [160]. Conversely, for steel having a significant impact on the environment assessment methods can be attributed to the heat inputs required for ferronickel production ("Simapro," ecoinvent). Reducing the use of steel or opting for alternative materials in PVT module manufacturing could mitigate environmental impact. As LCA results indicates in the previous section, PV module typically contribute the most to environmental impact. Analyzing the environmental profile of crystalline-silicon PV modules, [206] noted that their life cycle involves various phases, with upstream processes like raw material acquisition and manufacturing having the greatest impact. The operational phase, marked by minimal maintenance needs, contributes less to environmental impact. Recycling also emerges as a crucial aspect in minimizing environmental impact.

The component-wise environmental impact assessment also provides important insights from a circular economy perspective. By identifying the dominant contributors to the overall environmental burden, such as the photovoltaic module, steel support structure, and rubber gasket, the analysis highlights opportunities for design improvement beyond performance optimization. These findings support strategies including material substitution with lower-impact alternatives, increased use of recycled or secondary materials, and improved recyclability at end-of-life. Furthermore, the modular nature of the BiSPVT facade enables design-for-disassembly, allowing key components to be recovered, reused, or recycled, thereby reducing resource depletion and lifecycle environmental impacts. Such considerations are essential for transitioning building-integrated photovoltaic technologies from linear material use toward circular and sustainable building energy systems.

6.5 Sensitivity Analysis

Sensitivity analyses were performed to evaluate the environmental performance of the BiSPVT facade system with various PV panel technologies to identify the most environmentally friendly option. **Table 6.4** presents the environmental impacts of the BiSPVT framework for five solar module technologies: Amorphous silicon (a-Si), Copper indium selenide (CIS), multi-Si, ribbon Si, and single Si.

In this study, the sensitivity analysis results are reported using weighting, characterization and normalization, which culminate in single score impact indicators (score points/mpts) for 18 ReCiPe Midpoint impact categories. These score points quantify the severity of each impact category's contribution to the overall environmental load, with higher scores indicating greater environmental impact. These points are dimensionless and their absolute values are not particularly important. Instead, they are primarily used to compare the relative differences between various products and components [37,38].

The findings indicate that single-Si panels contribute significantly to climate change, specifically in global warming, stratospheric ozone depletion, ionizing radiation, and particulate matter formation, while a-Si panels have the lowest climate impact. Additionally, single-Si collectors are major contributors to eutrophication and ecotoxicity. Regarding human carcinogenic effects, CIS panels have the least impact, whereas single-Si panels have the highest. Multi-Si panels are predominantly responsible for water resource depletion. Overall, a-Si solar collectors demonstrate a superior environmental profile compared to the other technologies.

Table 6.4 Results on Sensitivity analysis based on different photovoltaic module technologies for the BiSPVT system.

Impact category	a-Si (mPts)	CIS (mPts)	multi-Si (mPts)	Ribbon-Si (mPts)	single-Si (mPts)
Global warming	0.0246	0.0325	0.0493	0.0415	0.0620
Stratospheric ozone depletion	0.0011	0.0016	0.0029	0.0025	0.0037
Ionizing radiation	0.0260	0.0494	0.0616	0.0524	0.0806
Ozone formation, Human health	0.0228	0.0289	0.0481	0.0420	0.0589
Fine particulate matter formation	0.0148	0.0177	0.0297	0.0257	0.0381
Ozone formation, Terrestrial ecosystems	0.0272	0.0341	0.0587	0.0514	0.0713
Terrestrial acidification	0.0187	0.0234	0.0365	0.0315	0.0445
Freshwater eutrophication	0.1223	0.2355	0.3521	0.3047	0.4503
Marine eutrophication	0.0006	0.0019	0.0055	0.0051	0.0061
Terrestrial ecotoxicity	0.0579	0.0549	0.6137	0.6041	0.6199
Freshwater ecotoxicity	0.4779	0.5882	1.2580	1.1755	1.3477
Marine ecotoxicity	0.3683	0.4503	1.0912	1.0266	1.1602
Human carcinogenic toxicity	3.7362	2.2146	3.7616	2.7892	4.1681
Human non-carcinogenic toxicity	0.0087	0.0115	0.0241	0.0225	0.0264
Land use	0.0011	0.0013	0.0021	0.0018	0.0024
Mineral resource scarcity	0.0000	0.0000	0.0000	0.0000	0.0000
Fossil resource scarcity	0.0586	0.0735	0.1137	0.0926	0.1397
Water consumption	0.0630	0.0635	0.1081	0.0836	0.1040

6.6 Summary of the chapter

The present study demonstrates the environmental and economic feasibility of implementing BiSPVT facade in mild cold weather condition of India taking into consideration four different climatic variations in Srinagar. Based on the LCA methods (GWP, ReCiPe) adopted for assessing system environmental performance by taking into account the systems components, PV module and steel structure was found to have significant environmental impact in comparison to other components. The impact of the proposed BiSPVT system per square meter of the facade, based on primary materials, resulted in 0.98 t $CO_{2,eq}/m^2$ according to the GWP 100a scenario. Sensitivity analysis showed that consideration of a-Si PV module among other PV module technologies has the lesser environmental impact

7

Conclusions and Scopes for Future Work

Chapter Outline:

CHAPTER 7: CONCLUSIONS AND SCOPES FOR FUTURE WORK

7.1 Brief summary of the investigation

The performance evaluation of a Building Integrated Semi-Transparent Photovoltaic Thermal (BiSPVT) Facade system, as detailed in the preceding chapters, was initiated with the formulation of a robust thermal modeling framework (Chapter 3). A one-dimensional, steady-state numerical model was developed in MATLAB to capture the thermal and electrical dynamics of the BiSPVT Facade installed on the south-facing vertical wall of a building in Srinagar, India. The model accounted for key physical and operational parameters, solar radiation, airflow, temperature distributions, and material properties, across different layers of the Facade, including the PV module, air channel, and absorber wall. Four distinct weather conditions (clear, hazy, hazy-cloudy, and cloudy), prevalent in Srinagar were incorporated to represent the climatic variability throughout the year.

The model incorporated multiple assumptions to simplify and capture the heat transfer interactions, such as quasi-steady-state conduction, uniform surface temperatures, and constant thermophysical properties of air. The governing energy balance equations accurately captured solar radiation absorption, convection within the air channel, and radiative losses. System specifications included 14 PV modules (each rated at 115 W), providing a total installed capacity of 1.6 kWp. The model also introduced metrics such as instantaneous thermal and electrical efficiencies, thermal load levelling (TLL), and exergy gain to assess system reliability and comfort within the building envelope. Thermal performance was analyzed in terms of outlet air temperatures and resultant indoor air temperature rise, which demonstrated effectiveness for space heating, especially during colder months.

7.1.1 Annual Energy Analysis of a Building Integrated Semi-Transparent Photovoltaic Thermal Facade

- Through simulation results under varying climatic conditions of Srinagar, this chapter quantified the system's annual energy performance. The BiSPVT system achieved an annual electrical energy gain of 121.22 kWh/m², overall thermal energy gain of 366.23 kWh/m², and a useful exergy output of 122.36 kWh/m².
- Seasonal trends demonstrated that October yielded the highest exergy (17.67 kWh/m²), attributed to clearer skies and higher solar irradiance, while June recorded the minimum (4.32 kWh/m²). The PV module exhibited a maximum efficiency of

18.9% in January and reached a peak module temperature of 33.6°C in October. The overall thermal efficiency peaked at 57.58% in January due to lower ambient temperatures and greater heat extraction for space heating.

- Notably, indoor air temperatures (T_r) showed an increase of up to 9.76°C above ambient, proving the potential of BiSPVT integration for space heating. Instantaneous efficiency analysis identified an optical efficiency of 78.3% and a heat loss coefficient of 1.422 W/m²K for the PV module. TLL values for different sky conditions were found to be around 0.41, suggesting stable indoor conditions across diurnal cycles.
- This energy modeling highlights the dual advantage of BiSPVT systems in improving PV efficiency and meeting space heating demands, validating their suitability in cold and moderately sunny regions like Srinagar.

7.1.2 Exergy, Exergoeconomic and Enviroeconomic Analysis of a Building Integrated Semi-transparent Photovoltaic/Thermal (BiSPV/T) Facade

- Annual useful exergy gain stood at 122.36 kWh/m², with the highest monthly exergy obtained in October. Energy and exergy losses were found to be inversely related to the incident solar radiation, with June and July showing lower loss rates due to higher radiation intensity and October exhibiting higher losses owing to moderate radiation coupled with ambient variations.
- An exergoeconomic assessment over a 30-year lifespan at a 4% discount rate revealed optimal values of Ren and Rex (energy and exergy loss rate ratios), demonstrating economic viability. Additionally, the system enabled annual CO_2 mitigation of 2.81 tonnes, translating to an environmental cost reduction of $40.87. The Energy Payback Time (EPBT) was estimated at 3.2 years based on thermal output and 9.8 years based on exergy gain. The Greenhouse Payback Time (GPBT) was observed to be 2.5 years.
- The uniform annualized cost (UAC) for the system was in the range of $0.031–0.20/kWh, depending on interest rates and discounting assumptions. Sensitivity analyses showed significant influence of interest rates on economic parameters like LCCE (Life Cycle Cost of Energy), EPF (Energy Production Factor), and UAC. These findings not only confirm the technical efficiency of the system but also underscore its economic and environmental feasibility.

7.1.3 Life Cycle Assessment of a Semi-Transparent Building Integrated Photovoltaic Facade

- The total GHG emissions from the system amounted to 0.98 tCO_2-eq/m^2, primarily dominated by the PV modules and the steel structure used in mounting.
- Among various PV technologies assessed, amorphous silicon (a-Si) showed the least environmental impact, supporting its preference in future installations. The CO_2 reduction of 2.81 tonnes/year aligns with the LCA results, demonstrating the potential of such systems to offset embodied emissions within a few years of operation.
- The study emphasized the need to integrate replacement cycles of building materials in LCA and EPBT assessments, a factor currently under-addressed. Doing so could further lower environmental impacts and EPBT estimates. Furthermore, validation of simulated energy outputs through experimental data was identified as a future direction to enhance robustness. Component-wise sensitivity analysis was also proposed to identify high-impact zones within the system architecture.
- Overall, the LCA results reinforce the long-term sustainability of BiSPVT Facades in cold climatic zones, presenting them as credible solutions for decarbonizing building energy consumption with quantifiable environmental benefits.

7.2 Future Scope

This study has comprehensively analysed the annual energy, exergy, exergoeconomic, and enviroeconomic performance of a Building-Integrated Semitransparent Photovoltaic Thermal (BiSPVT) facade system for cold climatic conditions, specifically for Srinagar, India. However, there remains significant scope for future enhancement and application of this research in broader contexts.

- **Extension to Transient Modelling:** The present study is based on a steady-state thermal model. Future work can incorporate transient (time-dependent) simulations to better understand the system's performance during fluctuating daily and seasonal climatic conditions.

- **Experimental Validation:** Physical testing of the BiSPVT system under real conditions can validate the numerical findings and help fine-tune model parameters, especially for temperature, irradiance, and air flow variations.

- **Application Across Diverse Climatic Zones:** The current model is location-specific to Srinagar. Expanding the study to other Indian and international climatic zones can help evaluate the adaptability and performance of the facade in varying weather conditions.
- **Material-Level Improvements:** Exploring advanced PV materials (e.g., bifacial or perovskite-based semi-transparent modules) and insulation materials may improve both electrical and thermal efficiencies.

This study serves as a foundation for these future research directions, supporting the advancement of energy-efficient, environmentally responsible building technologies.

REFERENCES

[1] Liao X, Ali ABM, Singh NSS, Baghoolizadeh M, Alam MM, Orlova T, et al. Comprehensive review of green roof and photovoltaic-green roof systems for different climates to examine the energy-saving and indoor thermal comfort. Int Commun Heat Mass Transf 2025;164:108946. https://doi.org/10.1016/j.icheatmasstransfer.2025.108946.

[2] Alshareef RS, Maghrabie HM. Building-integrated photovoltaics with energy storage systems – A comprehensive review. J Energy Storage 2025;116:115916. https://doi.org/10.1016/j.est.2025.115916.

[3] Cozzi, L., Gould, T., Bouckart, S., Crow, D., Kim, T. Y., McGlade, C., ... & Wetzel D. World energy outlook 2020 n.d.

[4] Laura Cozzi, Alex Martinos, Thomas Spencer, Víctor García Tapia, Arthur Roge led, Davide D'Ambrosio, et al. Global Energy Review 2025 2025.

[5] IEA. IEA (2022), World Energy Outlook 2022, IEA, Paris https://www.iea.org/reports/world-energy-outlook-2022, License: CC BY 4.0 (report); CC BY NC SA 4.0 (Annex A). CC BY 40 (Report); CC BY NC SA 40 (Annex A) 2022.

[6] Peng C, Huang Y, Wu Z. Building-integrated photovoltaics (BIPV) in architectural design in China. Energy Build 2011;43:3592–8. https://doi.org/10.1016/j.enbuild.2011.09.032.

[7] Parida B, Iniyan S, Goic R. A review of solar photovoltaic technologies. Renew Sustain Energy Rev 2011;15:1625–36. https://doi.org/10.1016/j.rser.2010.11.032.

[8] Jackson T, Oliver M. The viability of solar photovoltaics. Energy Policy 2000;28:983–8. https://doi.org/10.1016/S0301-4215(00)00085-9.

[9] Nilson RS, Stedman RC. Are big and small solar separate things?: The importance of scale in public support for solar energy development in upstate New York. Energy Res Soc Sci 2022;86:102449. https://doi.org/10.1016/j.erss.2021.102449.

[10] Chandel R, Chandel SS, Malik P. Perspective of new distributed grid connected roof top solar photovoltaic power generation policy interventions in India. Energy Policy 2022;168:113122. https://doi.org/10.1016/j.enpol.2022.113122.

[11] Rohankar N, Jain AK, Nangia OP, Dwivedi P. A study of existing solar power policy framework in India for viability of the solar projects perspective. Renew Sustain Energy Rev 2016;56:510–8. https://doi.org/10.1016/j.rser.2015.11.062.

[12] Kumar Kirme S, Kapse VS. A comprehensive review of residential building energy efficiency measures in India. Energy Build 2024;319:114537. https://doi.org/10.1016/j.enbuild.2024.114537.

[13] Dawn S, Tiwari PK, Goswami AK, Mishra MK. Recent developments of solar energy in India: Perspectives, strategies and future goals. Renew Sustain Energy Rev 2016;62:215–

35. https://doi.org/10.1016/j.rser.2016.04.040.

[14] Zhang T, Wang M, Yang H. A review of the energy performance and life-cycle assessment of building-integrated photovoltaic (BIPV) systems. Energies 2018;11. https://doi.org/10.3390/en11113157.

[15] Craciunescu D, Fara L, Dabija A, Sterian P. Intelligent Approach for Improvement of BIPV Systems Performance : Case Study Intelligent Approach for Improvement of BIPV Systems Performance : Case Study 2019. https://doi.org/10.1088/1757-899X/471/11/112015.

[16] Silveira FA. Design , photovoltaic solar energy and measurement artifact Design , energia solar por conversão fotovoltaica e artefato de Design , photovoltaic solar energy and measurement artifact 2020. https://doi.org/10.35522/eed.v28i3.1016.

[17] Yu G, Yang H, Yan Z, Kyeredey M. A review of designs and performance of façade-based building integrated photovoltaic-thermal (BIPVT) systems. Appl Therm Eng 2021;182:116081. https://doi.org/10.1016/j.applthermaleng.2020.116081.

[18] Regina S, Freitas T. Photovoltaic Potential in Building Façades 2018.

[19] Das D, Kalita P, Dewan A, Tanweer S. Development of a novel thermal model for a PV/T collector and its experimental analysis. Sol Energy 2019;188:631–43. https://doi.org/10.1016/j.solener.2019.06.005.

[20] Scofield JH. The Solar Spectrum the Stefan-Boltzmann Law the Planck Distribution. Opt Lasers Eng 2009;68:1–9.

[21] Ramos CAF, Alcaso AN, Cardoso AJM. Photovoltaic-thermal (PVT) technology: Review and case study. IOP Conf Ser Earth Environ Sci 2019;354. https://doi.org/10.1088/1755-1315/354/1/012048.

[22] Lamy-Mendes A, Pontinha ADR, Alves P, Santos P, Durães L. Progress in silica aerogel-containing materials for buildings' thermal insulation. Constr Build Mater 2021;286:122815. https://doi.org/10.1016/j.conbuildmat.2021.122815.

[23] Zheng N, Zhang H, Duan L, Wang X, Liu L. Energy , exergy , exergoeconomic and exergoenvironmental analysis and optimization of a novel partially covered parabolic trough photovoltaic thermal collector based on life cycle method. Renew Energy 2022;200:1573–88. https://doi.org/10.1016/j.renene.2022.10.092.

[24] Rajoria CS, Agrawal S, Tiwari GN. Overall thermal energy and exergy analysis of hybrid photovoltaic thermal array. Sol Energy 2012;86:1531–8. https://doi.org/10.1016/j.solener.2012.02.014.

[25] Wajs J, Golabek A, Bochniak R, Mikielewicz D, Gaur A, Tiwari GN, et al. Transient analysis, exergy and thermo-economic modelling of façade integrated photovoltaic/thermal solar collectors. Energy 2019;137:109–26. https://doi.org/10.1016/j.energy.2020.117255.

[26] Gaur A, Tiwari GN, Ménézo C, Al-Helal IM. Numerical and experimental studies on a Building integrated Semi-transparent Photovoltaic Thermal (BiSPVT) system: Model

validation with a prototype test setup. Energy Convers Manag 2016;129:329–43. https://doi.org/10.1016/j.enconman.2016.10.017.

[27] Park KE, Kang GH, Kim HI, Yu GJ, Kim JT. Analysis of thermal and electrical performance of semi-transparent photovoltaic (PV) module. Energy 2010;35:2681–7. https://doi.org/10.1016/j.energy.2009.07.019.

[28] Yoon JH, Shim SR, An YS, Lee KH. An experimental study on the annual surface temperature characteristics of amorphous silicon BIPV window. Energy Build 2013;62:166–75. https://doi.org/10.1016/j.enbuild.2013.01.020.

[29] Fossa M, Ménézo C, Leonardi E. Experimental natural convection on vertical surfaces for building integrated photovoltaic (BIPV) applications. Exp Therm Fluid Sci 2008;32:980–90. https://doi.org/10.1016/j.expthermflusci.2007.11.004.

[30] Gan G. Numerical determination of adequate air gaps for building-integrated photovoltaics. Sol Energy 2009;83:1253–73. https://doi.org/10.1016/j.solener.2009.02.008.

[31] Ritzen MJ, Vroon ZAEP, Rovers R, Lupíšek A, Geurts CPW. Environmental impact comparison of a ventilated and a non-ventilated building-integrated photovoltaic rooftop design in the Netherlands: Electricity output, energy payback time, and land claim. Sol Energy 2017;155:304–13. https://doi.org/10.1016/j.solener.2017.06.041.

[32] Peng J, Lu L, Yang H. An experimental study of the thermal performance of a novel photovoltaic double-skin facade in Hong Kong. Sol Energy 2013;97:293–304. https://doi.org/10.1016/j.solener.2013.08.031.

[33] Peng J, Lu L, Yang H, Han J. Investigation on the annual thermal performance of a photovoltaic wall mounted on a multi-layer façade. Appl Energy 2013;112:646–56. https://doi.org/10.1016/j.apenergy.2012.12.026.

[34] Lu L, Law KM. Overall energy performance of semi-transparent single-glazed photovoltaic (PV) window for a typical office in Hong Kong. Renew Energy 2013;49:250–4. https://doi.org/10.1016/j.renene.2012.01.021.

[35] Gao W, Moayedi H, Shahsavar A. The feasibility of genetic programming and ANFIS in prediction energetic performance of a building integrated photovoltaic thermal (BIPVT) system. Sol Energy 2019;183:293–305. https://doi.org/10.1016/j.solener.2019.03.016.

[36] Shakouri M, Ghadamian H, Noorpoor A. Quasi-dynamic energy performance analysis of building integrated photovoltaic thermal double skin façade for middle eastern climate case. Appl Therm Eng 2020;179:115724. https://doi.org/10.1016/j.applthermaleng.2020.115724.

[37] Wajs J, Golabek A, Bochniak R, Mikielewicz D. Air-cooled photovoltaic roof tile as an example of the BIPVT system e An experimental study on the energy and exergy performance. Energy 2020;197:117255. https://doi.org/10.1016/j.energy.2020.117255.

[38] Shahsavar A, Talebizadehsardari P, Arıcı M. enviroeconomic analysis of building integrated photovoltaic / thermal , earth-air heat exchanger , and hybrid systems. J

Clean Prod 2022;362:132510. https://doi.org/10.1016/j.jclepro.2022.132510.

[39] Liang R, Wang P, Zhou C, Pan Q, Riaz A, Zhang J. Thermal performance study of an active solar building façade with speci fi c PV / T hybrid modules. Energy 2020;191:116532. https://doi.org/10.1016/j.energy.2019.116532.

[40] Preet S, Sharma MK, Mathur J, Chowdhury A, Mathur S. Performance evaluation of photovoltaic double-skin facade with forced ventilation in the composite climate. J Build Eng 2020;32:101733. https://doi.org/10.1016/j.jobe.2020.101733.

[41] Salameh T, El M, Assad H, Tawalbeh M, Ghenai C, Merabet A, et al. Analysis of cooling load on commercial building in UAE climate using building integrated photovoltaic façade system. Sol Energy 2020;199:617–29. https://doi.org/10.1016/j.solener.2020.02.062.

[42] Cekon M. Climate response of a BiPV façade system enhanced with latent PCM- based thermal energy storage 2020;152:368–84. https://doi.org/10.1016/j.renene.2020.01.070.

[43] Goulart S, Mantelli S, Martins G, Campos R, Pinto G. Energy balance and performance assessment of PV systems installed at a positive-energy building (PEB) solar energy research centre 2020;212:258–74. https://doi.org/10.1016/j.solener.2020.10.080.

[44] Jois S, Ramamritham K A V. Facade solar PV potential estimation considering rooftop capacity and building code for Indian cities. Conf. Facade Sol. PV potential Estim. considering rooftop Capacit. Build. code Indian cities., IEEE; n.d. https://doi.org/p. 408-411.

[45] Shakouri M, Ghadamian H, Hoseinzadeh S, Sohani A. Multi-objective 4E analysis for a building integrated photovoltaic thermal double skin Façade system. Sol Energy 2022;233:408–20. https://doi.org/10.1016/j.solener.2022.01.036.

[46] Liang R, Guo Y, Zhao L, Gao Y. Real-time monitoring implementation of PV / T façade system based on IoT. J Build Eng 2021;41:102451. https://doi.org/10.1016/j.jobe.2021.102451.

[47] Chen M, Zhang W, Xie L, He B, Wang W, Li J, et al. Energy & Buildings Improvement of the electricity performance of bifacial PV module applied on the building envelope 2021;238. https://doi.org/10.1016/j.enbuild.2021.110849.

[48] Sharma MK, Preet S, Mathur J, Chowdhury A, Mathur S. Parametric analysis of factors affecting thermal performance of photovoltaic triple skin façade system (PV-TSF). J Build Eng 2021;40:102344. https://doi.org/10.1016/j.jobe.2021.102344.

[49] Rounis ED, Athienitis AK, Stathopoulos T. BIPV / T curtain wall systems : Design , development and testing. J Build Eng 2021;42:103019. https://doi.org/10.1016/j.jobe.2021.103019.

[50] Jalalizadeh M, Fayaz R, Delfani S, Jafari H. Dynamic simulation of a trigeneration system using an absorption cooling system and building integrated photovoltaic thermal solar collectors. J Build Eng 2021;43:102482. https://doi.org/10.1016/j.jobe.2021.102482.

[51] Alrashidi H, Issa W, Sellami N, Sundaram S, Mallick T. Thermal performance evaluation and energy saving potential of semi-transparent CdTe in Façade BIPV. Sol Energy 2022;232:84–91. https://doi.org/10.1016/j.solener.2021.12.037.

[52] Bezaatpour J, Ghiasirad H, Bezaatpour M, Ghaebi H. Towards optimal design of photovoltaic / thermal facades : Module-based assessment of thermo-electrical performance , exergy efficiency and wind loads. Appl Energy 2022;325:119785. https://doi.org/10.1016/j.apenergy.2022.119785.

[53] Ge M, Zhao Y, Xuan Z, Zhao Y, Wang S. ScienceDirect Experimental research on the performance of BIPV / T system with. Energy Reports 2022;8:454–9. https://doi.org/10.1016/j.egyr.2022.05.179.

[54] Zhang C, Ji J, Wang C, Ke W, Xie H, Yu B. Experimental and numerical studies on the thermal and electrical performance of a CdTe ventilated window integrated with vacuum glazing. Energy 2022;244:123128. https://doi.org/10.1016/j.energy.2022.123128.

[55] Sohani A, Cornaro C, Hassan M, Pierro M, Moser D, Ni S, et al. Building integrated photovoltaic / thermal technologies in Middle Eastern and North African countries : Current trends and future perspectives 2023;182. https://doi.org/10.1016/j.rser.2023.113370.

[56] Duffie JA, Beckman WA. Solar engineering of thermal processes. Fourth. New Jersey: John Wiley \& Sons; 2013.

[57] Maghrabie HM, Abdelkareem MA, Al-alami AH, Ramadan M, Mushtaha E, Wilberforce T, et al. State-of-the-Art Technologies for Building-Integrated Photovoltaic Systems 2021.

[58] Dai Y, Bai Y. Performance Improvement for Building Integrated. Energies 2021;14.

[59] Debbarma M, Sudhakar K, Baredar P. Thermal modeling, exergy analysis, performance of BIPV and BIPVT: A review. Renew Sustain Energy Rev 2017;73:1276–88. https://doi.org/10.1016/j.rser.2017.02.035.

[60] Agathokleous RA, Kalogirou SA. Double skin facades (DSF) and building integrated photovoltaics (BIPV): A review of configurations and heat transfer characteristics. Renew Energy 2016;89:743–56. https://doi.org/10.1016/j.renene.2015.12.043.

[61] Agathokleous RA, Kalogirou SA. Double skin facades (DSF) and building integrated photovoltaics (BIPV): A review of configurations and heat transfer characteristics. Renew Energy 2016;89:743–56.

[62] Ji J, Yi H, Pei G, He HF, Han CW, Luo CL. Numerical study of the use of photovoltaic-Trombe wall in residential buildings in Tibet. Proc Inst Mech Eng Part A J Power Energy 2007;221:1131–40.

[63] Bellazzi A, Belussi L, Meroni I. Estimation of the performance of a BIPV façade in working conditions through real monitoring and simulation. Energy Procedia 2018;148:479–82. https://doi.org/10.1016/j.egypro.2018.08.123.

[64] Hu Z, He W, Ji J, Hu D, Lv S, Chen H, et al. Comparative study on the annual performance of three types of building integrated photovoltaic (BIPV) Trombe wall system. Appl Energy 2017;194:81–93. https://doi.org/10.1016/j.apenergy.2017.02.018.

[65] Hu Z, He W, Hu D, Lv S, Wang L, Ji J, et al. Design , construction and performance testing of a PV blind-integrated Trombe wall module. Appl Energy 2017;203:643–56. https://doi.org/10.1016/j.apenergy.2017.06.078.

[66] Ahmed OK, Hamada KI, Salih AM. Enhancement of the performance of Photovoltaic/Trombe wall system using the porous medium: Experimental and theoretical study. Energy 2019;171:14–26.

[67] Kaiser AS, Zamora B, Mazón R, García JR, Vera F. Experimental study of cooling BIPV modules by forced convection in the air channel. Appl Energy 2014;135:88–97. https://doi.org/10.1016/j.apenergy.2014.08.079.

[68] Jie J, Hua Y, Gang P, Bin J, Wei H. Study of PV-Trombe wall assisted with DC fan. Build Environ 2007;42:3529–39.

[69] Koyunbaba BK, Yilmaz Z. The comparison of Trombe wall systems with single glass, double glass and PV panels. Renew Energy 2012;45:111–8.

[70] Irshad K, Habib K, Thirumalaiswamy N. Implementation of Photo Voltaic Trombe Wall system for developing non-air conditioned buildings. Proc - 2013 IEEE Conf Sustain Util Dev Eng Technol IEEE CSUDET 2013 2013:68–73. https://doi.org/10.1109/CSUDET.2013.6670988.

[71] Irshad K, Habib K, Thirumalaiswamy N. Energy and cost analysis of photo voltaic trombe wall system in tropical climate. Energy Procedia 2014;50:71–8. https://doi.org/10.1016/j.egypro.2014.06.009.

[72] Vats K, Tomar V, Tiwari GN. Effect of packing factor on the performance of a building integrated semitransparent photovoltaic thermal (BISPVT) system with air duct. Energy Build 2012;53:159–65. https://doi.org/10.1016/j.enbuild.2012.07.004.

[73] Peng J, Lu L, Yang H, Han J. Investigation on the annual thermal performance of a photovoltaic wall mounted on a multi-layer façade. Appl Energy 2013;112:646–56.

[74] Hu Z, He W, Ji J, Zhang S. A review on the application of Trombe wall system in buildings. Renew Sustain Energy Rev 2017;70:976–87.

[75] Xu XW, Su YX. Numerical simulation of air flow in BiPV-Trombe wall. Adv. Mater. Res., vol. 860, 2014, p. 141–5.

[76] Jovanovic J, Sun X, Stevovic S, Chen J. Energy-efficiency gain by combination of PV modules and Trombe wall in the low-energy building design. Energy Build 2017;152:568–76. https://doi.org/10.1016/j.enbuild.2017.07.073.

[77] Asefi G, Habibollahzade A, Ma T, Houshfar E, Wang R. Thermal management of building-integrated photovoltaic/thermal systems: A comprehensive review. Sol Energy 2021;216:188–210. https://doi.org/10.1016/j.solener.2021.01.005.

[78] Taffesse F, Verma A, Singh S, Tiwari GN. Periodic modeling of semi-transparent photovoltaic thermal-trombe wall (SPVT-TW). Sol Energy 2016;135:265–73. https://doi.org/10.1016/j.solener.2016.05.044.

[79] Peng J, Curcija DC, Lu L, Selkowitz SE, Yang H, Zhang W. Numerical investigation of the energy saving potential of a semi-transparent photovoltaic double-skin facade in a cool-summer Mediterranean climate. Appl Energy 2016;165:345–56. https://doi.org/10.1016/j.apenergy.2015.12.074.

[80] Tiwari A, Sodha MS, Chandra A, Joshi JC. Performance evaluation of photovoltaic thermal solar air collector for composite climate of India. Sol Energy Mater Sol Cells 2006;90:175–89. https://doi.org/10.1016/j.solmat.2005.03.002.

[81] Tiwari A, Sodha MS. Parametric study of various configurations of hybrid PV/thermal air collector: Experimental validation of theoretical model. Sol Energy Mater Sol Cells 2007;91:17–28. https://doi.org/10.1016/j.solmat.2006.06.061.

[82] Bambrook SM, Sproul AB. Maximising the energy output of a PVT air system. Sol Energy 2012;86:1857–71. https://doi.org/10.1016/j.solener.2012.02.038.

[83] Yoon J, Song J, Lee S. Practical application of building integrated photovoltaic (BIPV) system using transparent amorphous silicon thin-film PV module. Sol Energy 2011;85:723–33. https://doi.org/10.1016/j.solener.2010.12.026.

[84] Irshad K, Habib K, Thirumalaiswamy N. Performance evaluation of PV-Trombe wall for sustainable building development. Procedia Cirp 2015;26:624–9.

[85] Abu-Rub H, Iqbal A, Amin S, Abdelkadar G, Salem N, Mansoor S, et al. Feasibility analysis of solar photovoltaic array cladding on commercial towers in Doha, Qatar - a case study. Int J Sustain Energy 2010;29:76–86. https://doi.org/10.1080/14786460903406590.

[86] Aaditya G, Pillai R, Mani M. An insight into real-time performance assessment of a building integrated photovoltaic (BIPV) installation in Bangalore (India). Energy Sustain Dev 2013;17:431–7. https://doi.org/10.1016/j.esd.2013.04.007.

[87] Mishra GK, Tiwari GN, Bhatti TS. Effect of water flow on performance of building integrated semi-transparent photovoltaic thermal system: A comparative study. Sol Energy 2018;174:248–62. https://doi.org/10.1016/j.solener.2018.09.011.

[88] Yin HM, Yang DJ, Kelly G, Garant J. Design and performance of a novel building integrated PV/thermal system for energy efficiency of buildings. Sol Energy 2013;87:184–95. https://doi.org/10.1016/j.solener.2012.10.022.

[89] Chow TT, He W, Ji J. An experimental study of façade-integrated photovoltaic/water-heating system. Appl Therm Eng 2007;27:37–45. https://doi.org/10.1016/j.applthermaleng.2006.05.015.

[90] Ibrahim A, Fudholi A, Sopian K, Othman MY, Ruslan MH. Efficiencies and improvement potential of building integrated photovoltaic thermal (BIPVT) system. Energy Convers Manag 2014;77:527–34. https://doi.org/10.1016/j.enconman.2013.10.033.

[91] Ibrahim A, Fudholi A, Sopian K, Yusof M. Efficiencies and improvement potential of building integrated photovoltaic thermal (BIPVT) system. Energy Convers Manag 2014;77:527–34. https://doi.org/10.1016/j.enconman.2013.10.033.

[92] Anderson TN, Duke M, Morrison GL, Carson JK. Performance of a building integrated photovoltaic/thermal (BIPVT) solar collector. Sol Energy 2009;83:445–55. https://doi.org/10.1016/j.solener.2008.08.013.

[93] Gautam KR, Andresen GB. Performance comparison of building-integrated combined photovoltaic thermal solar collectors (BiPVT) with other building-integrated solar technologies. Sol Energy 2017;155:93–102. https://doi.org/10.1016/j.solener.2017.06.020.

[94] Kim JH, Park SH, Kang JG, Kim JT. Experimental performance of heating system with buildingintegrated PVT (BIPVT) collector. Energy Procedia 2014;48:1374–84. https://doi.org/10.1016/j.egypro.2014.02.155.

[95] Martin-Escudero K, Salazar-Herran E, Campos-Celador A, Diarce-Belloso G, Gomez-Arriaran I. Solar energy system for heating and domestic hot water supply by means of a heat pump coupled to a photovoltaic ventilated façade. Sol Energy 2019;183:453–62. https://doi.org/10.1016/j.solener.2019.03.058.

[96] Xu L, Ji J, Luo K, Li Z, Xu R, Huang S. Annual analysis of a multi-functional BIPV/T solar wall system in typical cities of China. Energy 2020;197:117098. https://doi.org/10.1016/j.energy.2020.117098.

[97] Pugsley A, Zacharopoulos A, Mondol JD, Smyth M. BIPV/T facades – A new opportunity for integrated collector-storage solar water heaters? Part 2: Physical realisation and laboratory testing. Sol Energy 2020;206:751–69. https://doi.org/10.1016/j.solener.2020.05.098.

[98] Davidsson H, Perers B. System analysis of a multifunctional PV / T hybrid solar window 2012;86:903–10. https://doi.org/10.1016/j.solener.2011.12.020.

[99] Corbin CD, Zhai ZJ. Experimental and numerical investigation on thermal and electrical performance of a building integrated photovoltaic – thermal collector system 2010;42:76–82. https://doi.org/10.1016/j.enbuild.2009.07.013.

[100] Wang Z, Zhang J, Wang Z, Yang W, Zhao X. Experimental investigation of the performance of the novel HP-BIPV / T system for use in residential buildings. Energy Build 2016;130:295–308. https://doi.org/10.1016/j.enbuild.2016.08.060.

[101] Piratheepan M, Anderson TN. Performance of a building integrated photovoltaic / thermal concentrator for facade applications. Sol Energy 2017;153:562–73. https://doi.org/10.1016/j.solener.2017.06.006.

[102] Wang J, Tian X, Ji J, Zhang C, Ke W, Yuan S. Field experimental investigation of a multifunctional curved CIGS photovoltaic / thermal (PV / T) roof system for traditional Chinese buildings. Energy Convers Manag 2022;271:116219. https://doi.org/10.1016/j.enconman.2022.116219.

[103] Peng J, Lu L, Yang H, Ma T. Comparative study of the thermal and power performances

of a semi-transparent photovoltaic façade under different ventilation modes. Appl Energy 2015;138:572–83. https://doi.org/10.1016/j.apenergy.2014.10.003.

[104] Wang M, Peng J, Li N, Lu L, Ma T, Yang H. Assessment of energy performance of semi-transparent PV insulating glass units using a validated simulation model. Energy 2016;112:538–48. https://doi.org/10.1016/j.energy.2016.06.120.

[105] Wang M, Peng J, Li N, Yang H, Wang C, Li X, et al. Comparison of energy performance between PV double skin facades and PV insulating glass units. Appl Energy 2017;194:148–60. https://doi.org/10.1016/j.apenergy.2017.03.019.

[106] Bahaj ABS, James PAB, Jentsch MF. Potential of emerging glazing technologies for highly glazed buildings in hot arid climates. Energy Build 2008;40:720–31. https://doi.org/10.1016/j.enbuild.2007.05.006.

[107] Radhi H. Energy analysis of façade-integrated photovoltaic systems applied to UAE commercial buildings. Sol Energy 2010;84:2009–21. https://doi.org/10.1016/j.solener.2010.10.002.

[108] Ng PK, Mithraratne N, Kua HW. Energy analysis of semi-transparent BIPV in Singapore buildings. Energy Build 2013;66:274–81. https://doi.org/10.1016/j.enbuild.2013.07.029.

[109] Wong PW, Shimoda Y, Nonaka M, Inoue M, Mizuno M. Semi-transparent PV: Thermal performance, power generation, daylight modelling and energy saving potential in a residential application. Renew Energy 2008;33:1024–36. https://doi.org/10.1016/j.renene.2007.06.016.

[110] Leite Didoné E, Wagner A. Semi-transparent PV windows: A study for office buildings in Brazil. Energy Build 2013;67:136–42. https://doi.org/10.1016/j.enbuild.2013.08.002.

[111] Zhang W, Lu L, Peng J, Song A. Comparison of the overall energy performance of semi-transparent photovoltaic windows and common energy-efficient windows in Hong Kong. Energy Build 2016;128:511–8. https://doi.org/10.1016/j.enbuild.2016.07.016.

[112] Chow TT, Fong KF, He W, Lin Z, Chan ALS. Performance evaluation of a PV ventilated window applying to office building of Hong Kong. Energy Build 2007;39:643–50. https://doi.org/10.1016/j.enbuild.2006.09.014.

[113] Chow TT, Qiu Z, Li C. Potential application of "see-through" solar cells in ventilated glazing in Hong Kong. Sol Energy Mater Sol Cells 2009;93:230–8. https://doi.org/10.1016/j.solmat.2008.10.002.

[114] Olivieri L, Caamaño-Martín E, Moralejo-Vázquez FJ, Martín-Chivelet N, Olivieri F, Neila-Gonzalez FJ. Energy saving potential of semi-transparent photovoltaic elements for building integration. Energy 2014;76:572–83. https://doi.org/10.1016/j.energy.2014.08.054.

[115] Liao W, Xu S. Energy performance comparison among see-through amorphous-silicon PV (photovoltaic) glazings and traditional glazings under different architectural conditions in China. Energy 2015;83:267–75. https://doi.org/10.1016/j.energy.2015.02.023.

[116] Miyazaki T, Akisawa A, Kashiwagi T. Energy savings of office buildings by the use of semi-transparent solar cells for windows. Renew Energy 2005;30:281–304. https://doi.org/10.1016/j.renene.2004.05.010.

[117] Li DHW, Lam TNT, Chan WWH, Mak AHL. Energy and cost analysis of semi-transparent photovoltaic in office buildings. Appl Energy 2009;86:722–9. https://doi.org/10.1016/j.apenergy.2008.08.009.

[118] Saidur R, Boroumandjazi G, Mekhlif S, Jameel M. Exergy analysis of solar energy applications. Renew Sustain Energy Rev 2012;16:350–6. https://doi.org/10.1016/j.rser.2011.07.162.

[119] Fujisawa T, Tani T. Annual exergy evaluation on photovoltaic-thermal hybrid collector 1997;47:135–48.

[120] Tiwari GN. Analysis of series connected photovoltaic thermal air collectors partially covered by semitransparent photovoltaic module. Sol Energy 2016;137:452–62. https://doi.org/10.1016/j.solener.2016.08.052.

[121] Azadian, Farshad & Mohd Radzi MA. A general approach toward building integrated photovoltaic systems and its implementation barriers: A revie. Renew Sustain Energy Rev 2013;22:527–38.

[122] Gholami H, Røstvik HN, Müller-Eie D. Holistic economic analysis of building integrated photovoltaics (BIPV) system: Case studies evaluation. Energy Build 2019;203. https://doi.org/10.1016/j.enbuild.2019.109461.

[123] Liu Z, Zhang Y, Zhang L, Luo Y, Wu Z, Wu J, et al. Modeling and simulation of a photovoltaic thermal-compound thermoelectric ventilator system. Appl Energy 2018;228:1887–900. https://doi.org/10.1016/j.apenergy.2018.07.006.

[124] Shittu S, Li G, Zhao X, Ma X, Akhlaghi YG, Ayodele E. Optimized high performance thermoelectric generator with combined segmented and asymmetrical legs under pulsed heat input power. J Power Sources 2019;428:53–66. https://doi.org/10.1016/j.jpowsour.2019.04.099.

[125] Chow TT, Pei G, Fong KF, Lin Z, Chan ALS, Ji J. Energy and exergy analysis of photovoltaic – thermal collector with and without glass cover. Appl Energy 2009;86:310–6. https://doi.org/10.1016/j.apenergy.2008.04.016.

[126] Rajoria CS, Agrawal S, Tiwari GN. Exergetic and enviroeconomic analysis of novel hybrid PVT array. Sol Energy 2013;88:110–9. https://doi.org/10.1016/j.solener.2012.11.018.

[127] Saadon S, Gaillard L, Menezo C, Giroux-Julien S. Exergy, exergoeconomic and enviroeconomic analysis of a building integrated semi-transparent photovoltaic/thermal (BISTPV/T) by natural ventilation. Renew Energy 2020;150:981–9. https://doi.org/10.1016/j.renene.2019.11.122.

[128] Agathokleous RA, Kalogirou SA, Karellas S. Exergy analysis of a naturally ventilated Building Integrated Photovoltaic / Thermal (BIPV / T) system. Renew Energy 2018;128:541–52. https://doi.org/10.1016/j.renene.2017.06.085.

[129] Jha P, Das B, Gupta R. Energy and exergy analysis of photovoltaic thermal air collector under climatic condition of North Eastern India. Energy Procedia 2019;158:1161–7. https://doi.org/10.1016/j.egypro.2019.01.299.

[130] Rafae O, Mohammed O. Case Studies in Thermal Engineering Energy and exergy analysis of hybrid photovoltaic thermal solar system under climatic condition of North Iraq. Case Stud Therm Eng 2021;28:101429. https://doi.org/10.1016/j.csite.2021.101429.

[131] Shahsavar A, Rajabi Y. Exergoeconomic and enviroeconomic study of an air based building integrated photovoltaic / thermal (BIPV / T) system. Energy 2018;144:877–86. https://doi.org/10.1016/j.energy.2017.12.056.

[132] Lu L, Yang HX. Environmental payback time analysis of a roof-mounted building-integrated photovoltaic (BIPV) system in Hong Kong. Appl Energy 2010;87:3625–31. https://doi.org/10.1016/j.apenergy.2010.06.011.

[133] Li Z, Zhang W, Xie L, Wang W, Tian H, Chen M, et al. Life cycle assessment of semi-transparent photovoltaic window applied on building. J Clean Prod 2021;295:126403. https://doi.org/10.1016/j.jclepro.2021.126403.

[134] Alnaser NW. First smart 8.64 kW BIPV in a building in Awali Town at Kingdom of Bahrain. Renew Sustain Energy Rev 2018;82:205–14. https://doi.org/10.1016/j.rser.2017.09.041.

[135] Wilson R, Young A. The embodied energy payback period of photovoltaic installations applied to buildings in the U.K. Build Environ 1996;31:299–305. https://doi.org/10.1016/0360-1323(95)00053-4.

[136] Nawaz, I. & Tiwari G. Embodied energy analysis of photovoltaic (PV) system based on macro- and micro-level. Energy Policy 2006;34:3144–52. https://doi.org/10.1016/j.enpol.2005.06.018.

[137] Yatim Y, Yahya MW, Tajuddin MFN, Ismail B, Sulaiman SI. Tecno-economic analysis of PV module selection for residential BIPV with net metering implementation in Malaysia. IEEE Student Conf Res Dev Inspiring Technol Humanit SCOReD 2017 - Proc 2017;2018-Janua:361–5. https://doi.org/10.1109/SCORED.2017.8305364.

[138] Agrawal, Basant & Tiwari G. Life cycle cost assessment of building integrated photovoltaic thermal (BIPVT) systems. Energy Build 2010;42:1472–81. https://doi.org/10.1016/j.enbuild.2010.03.017.

[139] Hou, Guofu & Sun, Honghang & Jiang, Ziying & Pan, Ziqiang & Wang, Yibo & Zhang, Xiaodan & Zhao, Ying & Yao Q. Life cycle assessment of grid-connected photovoltaic power generation from crystalline silicon solar modules in China. Appl Energy 2015;164. https://doi.org/10.1016/j.apenergy.2015.11.023.

[140] Yu Z, Ma W, Xie K, Lv G, Chen Z, Wu J, et al. Life cycle assessment of grid-connected power generation from metallurgical route multi-crystalline silicon photovoltaic system in China. Appl Energy 2017;185:68–81. https://doi.org/10.1016/j.apenergy.2016.10.051.

[141] Li G, Xuan Q, Pei G, Su Y, Lu Y, Ji J. Life-cycle assessment of a low-concentration PV module for building south wall integration in China. Appl Energy 2018;215:174–85. https://doi.org/10.1016/j.apenergy.2018.02.005.

[142] Kabakian V, McManus MC, Harajli H. Attributional life cycle assessment of mounted 1.8kWp monocrystalline photovoltaic system with batteries and comparison with fossil energy production system. Appl Energy 2015;154:428–37. https://doi.org/10.1016/j.apenergy.2015.04.125.

[143] Agrawal S, Tiwari GN. Exergoeconomic analysis of glazed hybrid photovoltaic thermal module air collector. Sol Energy 2012;86:2826–38. https://doi.org/10.1016/j.solener.2012.06.021.

[144] Kamthania D, Tiwari GN. Energy metrics analysis of semi-transparent hybrid PVT double pass facade considering various silicon and non-silicon based PV module Hyphen is accepted. Sol Energy 2014;100:124–40. https://doi.org/10.1016/j.solener.2013.11.015.

[145] Tiwari S, Tiwari GN. Thermal analysis of photovoltaic thermal integrated greenhouse system (PVTIGS) for heating of slurry in potable biogas plant: An experimental study. Sol Energy 2017;155:203–11. https://doi.org/10.1016/j.solener.2017.06.021.

[146] Taffesse F, Verma A, Singh S, Tiwari GN. Periodic modeling of semi-transparent photovoltaic thermal-trombe 2016;135:265–73. https://doi.org/10.1016/j.solener.2016.05.044.

[147] Tripathi R, Tiwari GN, Dwivedi VK. Energy matrices evaluation and exergoeconomic analysis of series connected N partially covered (glass to glass PV module) concentrated- photovoltaic thermal collector : At constant flow rate mode. Energy Convers Manag 2017;145:353–70. https://doi.org/10.1016/j.enconman.2017.05.012.

[148] Agrawal S, Tiwari GN. Enviroeconomic analysis and energy matrices of glazed hybrid photovoltaic thermal module air collector. Sol Energy 2013;92:139–46. https://doi.org/10.1016/j.solener.2013.02.019.

[149] Barnwal P, Tiwari GN. Life cycle energy metrics and CO2 credit analysis of a hybrid photovoltaic/thermal greenhouse dryer. Int J Low Carbon Technol 2008;3:203–20. https://doi.org/10.1093/ijlct/3.3.203.

[150] Kalogirou SA, Tripanagnostopoulos Y. Industrial application of PV/T solar energy systems. Appl Therm Eng 2007;27:1259–70. https://doi.org/10.1016/j.applthermaleng.2006.11.003.

[151] Kumar S. Thermal-economic analysis of a hybrid photovoltaic thermal (PVT) active solar distillation system: Role of carbon credit. Urban Clim 2013;5:112–24. https://doi.org/10.1016/j.uclim.2013.07.001.

[152] Kumar S, Tiwari GN. Life cycle cost analysis of single slope hybrid (PV/T) active solar still. Appl Energy 2009;86:1995–2004. https://doi.org/10.1016/j.apenergy.2009.03.005.

[153] Nayak, S., Kumar, A., Singh, A. K., & Tiwari GN. Energy matrices analysis of hybrid PVT greenhouse dryer by considering various silicon and non-silicon PV modules. Int

J Sustain Energy 2013;33:336–348.

[154] Izquierdo M, de Agustín-Camacho P. Solar heating by radiant floor: Experimental results and emission reduction obtained with a micro photovoltaic-heat pump system. Appl Energy 2015;147:297–307. https://doi.org/10.1016/j.apenergy.2015.03.007.

[155] Renno C, Petito F. Choice model for a modular configuration of a point-focus CPV/T system. Energy Build 2015;92:55–66. https://doi.org/10.1016/j.enbuild.2015.01.023.

[156] Chow TT, Ji J. Environmental life-cycle analysis of hybrid solar photovoltaic/thermal systems for use in Hong Kong. Int J Photoenergy 2012;2012. https://doi.org/10.1155/2012/101968.

[157] Agrawal S, Tiwari GN. Overall energy, exergy and carbon credit analysis by different type of hybrid photovoltaic thermal air collectors. Energy Convers Manag 2013;65:628–36. https://doi.org/10.1016/j.enconman.2012.09.020.

[158] Rajoria CS, Agrawal S, Dash AK, Tiwari GN, Sodha MS. A newer approach on cash flow diagram to investigate the effect of energy payback time and earned carbon credits on life cycle cost of different photovoltaic thermal array systems. Sol Energy 2016;124:254–67. https://doi.org/10.1016/j.solener.2015.11.034.

[159] Wang W, Liu Y, Wu X, Xu Y, Yu W, Zhao C, et al. Environmental assessments and economic performance of BAPV and BIPV systems in Shanghai. Energy Build 2016;130:98–106. https://doi.org/10.1016/j.enbuild.2016.07.066.

[160] Lamnatou C, Chemisana D. Photovoltaic/thermal (PVT) systems: A review with emphasis on environmental issues. Renew Energy 2017;105:270–87. https://doi.org/10.1016/j.renene.2016.12.009.

[161] Tripanagnostopoulos Y, Souliotis M, Battisti R, Corrado A. Performance, cost and life-cycle assessment study of hybrid PVT/AIR solar systems. Prog Photovoltaics Res Appl 2006;14:65–76. https://doi.org/10.1002/pip.634.

[162] Tripathy M, Joshi H, Panda SK. Energy payback time and life-cycle cost analysis of building integrated photovoltaic thermal system influenced by adverse effect of shadow. Appl Energy 2017;208:376–89. https://doi.org/10.1016/j.apenergy.2017.10.025.

[163] Saadon S, Gaillard L, Giroux-Julien S, Ménézo C. Simulation study of a naturally-ventilated building integrated photovoltaic/thermal (BIPV/T) envelope. Renew Energy 2016;87:517–31. https://doi.org/10.1016/j.renene.2015.10.016.

[164] Deo A, Mishra GK, Tiwari GN. A thermal periodic theory and experimental validation of building integrated semi-transparent photovoltaic thermal (BiSPVT) system. Sol Energy 2017;155:1021–32. https://doi.org/10.1016/j.solener.2017.07.013.

[165] Gupta N, Tiwari A, Tiwari GN. A thermal model of hybrid cooling systems for building integrated semitransparent photovoltaic thermal system. Sol Energy 2017;153:486–98. https://doi.org/10.1016/j.solener.2017.05.086.

[166] Lamnatou C, Smyth M, Chemisana D. Building-Integrated Photovoltaic/Thermal

(BIPVT): LCA of a façade-integrated prototype and issues about human health, ecosystems, resources. Sci Total Environ 2019;660:1576–92. https://doi.org/10.1016/j.scitotenv.2018.12.461.

[167] Bazán J, Rieradevall J, Gabarrell X, Vázquez-Rowe I. Low-carbon electricity production through the implementation of photovoltaic panels in rooftops in urban environments: A case study for three cities in Peru. Sci Total Environ 2018;622–623:1448–62. https://doi.org/10.1016/j.scitotenv.2017.12.003.

[168] Tiwari GN, Saini H, Tiwari A, Deo A, Gupta N, Saini PS. Periodic theory of building integrated photovoltaic thermal (BiPVT) system. Sol Energy 2016;125:373–80. https://doi.org/10.1016/j.solener.2015.12.028.

[169] Lin W, Ma Z, Cooper P, Sohel MI, Yang L. Thermal performance investigation and optimization of buildings with integrated phase change materials and solar photovoltaic thermal collectors. Energy Build 2016;116:562–73. https://doi.org/10.1016/j.enbuild.2016.01.041.

[170] Gholampour M, Ameri M. Energy and exergy analyses of Photovoltaic/Thermal flat transpired collectors: Experimental and theoretical study. Appl Energy 2016;164:837–56. https://doi.org/10.1016/j.apenergy.2015.12.042.

[171] Khaki M, Shahsavar A, Khanmohammadi S, Salmanzadeh M. Energy and exergy analysis and multi-objective optimization of an air based building integrated photovoltaic/thermal (BIPV/T) system. Sol Energy 2017;158:380–95. https://doi.org/10.1016/j.solener.2017.09.056.

[172] Buonomano A, Calise F, Palombo A, Vicidomini M. Adsorption chiller operation by recovering low-temperature heat from building integrated photovoltaic thermal collectors: Modelling and simulation. Energy Convers Manag 2017;149:1019–36. https://doi.org/10.1016/j.enconman.2017.05.005.

[173] Asaee SR, Nikoofard S, Ugursal VI, Beausoleil-Morrison I. Techno-economic assessment of photovoltaic (PV) and building integrated photovoltaic/thermal (BIPV/T) system retrofits in the Canadian housing stock. Energy Build 2017;152:667–79. https://doi.org/10.1016/j.enbuild.2017.06.071.

[174] Bigaila E, Athienitis AK. Modeling and simulation of a photovoltaic/thermal air collector assisting a façade integrated small scale heat pump with radiant PCM panel. Energy Build 2017;149:298–309. https://doi.org/10.1016/j.enbuild.2017.05.045.

[175] Assoa YB, Sauzedde F, Boillot B, Boddaert S. Development of a building integrated solar photovoltaic/thermal hybrid drying system. Energy 2017;128:755–67. https://doi.org/10.1016/j.energy.2017.04.062.

[176] Piratheepan M, Anderson TN. Performance of a building integrated photovoltaic/thermal concentrator for facade applications. Sol Energy 2017;153:562–73. https://doi.org/10.1016/j.solener.2017.06.006.

[177] Strobach E, Bhatia B, Yang S, Zhao L, Wang EN. High temperature annealing for structural optimization of silica aerogels in solar thermal applications. J Non Cryst Solids 2017;462:72–7. https://doi.org/10.1016/j.jnoncrysol.2017.02.009.

[178] Debbarma M, Sudhakar K, Baredar P. Thermal modeling, exergy analysis, performance of BIPV and BIPVT: A review. Renew Sustain Energy Rev 2017;73:1276–88. https://doi.org/10.1016/j.rser.2017.02.035.

[179] Moreno A, Riverola A, Chemisana D. Energetic simulation of a dielectric photovoltaic-thermal concentrator. Sol Energy 2018;169:374–85. https://doi.org/10.1016/j.solener.2018.04.037.

[180] Gupta N, Tiwari GN. Effect of water flow on building integrated semitransparent photovoltaic thermal system with heat capacity. Sustain Cities Soc 2018;39:708–18. https://doi.org/10.1016/j.scs.2018.03.008.

[181] Agathokleous RA, Kalogirou SA, Karellas S. Exergy analysis of a naturally ventilated Building Integrated Photovoltaic/Thermal (BIPV/T) system. Renew Energy 2018;128:541–52. https://doi.org/10.1016/j.renene.2017.06.085.

[182] Shahsavar A, Rajabi Y. Exergoeconomic and enviroeconomic study of an air based building integrated photovoltaic/thermal (BIPV/T) system. Energy 2018;144:877–86. https://doi.org/10.1016/j.energy.2017.12.056.

[183] Fu Y, Liu X, Yuan Z. Life-cycle assessment of multi-crystalline photovoltaic (PV) systems in China. J Clean Prod 2015;86:180–90. https://doi.org/10.1016/j.jclepro.2014.07.057.

[184] Hou G, Sun H, Jiang Z, Pan Z, Wang Y, Zhang X, et al. Life cycle assessment of grid-connected photovoltaic power generation from crystalline silicon solar modules in China. Appl Energy 2016;164:882–90. https://doi.org/10.1016/j.apenergy.2015.11.023.

[185] Alsema, E.A. & de Wild-Scholten M. Environmental Impact of Crystalline Silicon Photovoltaic Module Production. Mater Res Soc Symp Proc 2011;895. https://doi.org/10.1557/PROC-0895-G03-05.

[186] Graebig M, Bringezu S, Fenner R. Comparative analysis of environmental impacts of maize-biogas and photovoltaics on a land use basis. Sol Energy 2010;84:1255–63. https://doi.org/10.1016/j.solener.2010.04.002.

[187] Stoppato A. Life cycle assessment of photovoltaic electricity generation. Energy 2008;33:224–32. https://doi.org/10.1016/j.energy.2007.11.012.

[188] Pehnt M. Dynamic life cycle assessment (LCA) of renewable energy technologies. Renew Energy 2006;31:55–71. https://doi.org/10.1016/j.renene.2005.03.002.

[189] Perez MJR, Fthenakis V, Kim HC, Pereira AO. Façade-integrated photovoltaics: A life cycle and performance assessment case study. Prog Photovoltaics Res Appl 2012;20:975–90. https://doi.org/10.1002/pip.1167.

[190] Saygin H, Nowzari R, Mirzaei N, Aldabbagh LBY. Performance evaluation of a modified PV/T solar collector: A case study in design and analysis of experiment. Sol Energy 2017;141:210–21. https://doi.org/10.1016/j.solener.2016.11.048.

[191] Fetela R. Exergy of Heat Radiation 2016:187–92.

[192] Rosen MA, Dincer I. Exergoeconomic analysis of power plants operating on various fuels. Appl Therm Eng 2003;23:643–58. https://doi.org/10.1016/S1359-4311(02)00244-2.

[193] Junedi MM, Ludin NA, Hamid NH, Kathleen PR, Hasila J, Ahmad Affandi NA. Environmental and economic performance assessment of integrated conventional solar photovoltaic and agrophotovoltaic systems. Renew Sustain Energy Rev 2022;168:112799. https://doi.org/10.1016/j.rser.2022.112799.

[194] Antonanzas J, Arbeloa-Ibero M, Quinn JC. Comparative life cycle assessment of fixed and single axis tracking systems for photovoltaics. J Clean Prod 2019;240:118016. https://doi.org/10.1016/j.jclepro.2019.118016.

[195] Gaur A, Ménézo C, Giroux S, others. Numerical studies on thermal and electrical performance of a fully wetted absorber PVT collector with PCM as a storage medium. Renew Energy 2017;109:168–87.

[196] El Alami Y, Baghaz E, Nasrin R, Padmanaban S, Louzazni M. Numerical approach of an advanced hybrid photovoltaic thermal system based on exergy, energy, enviro-economic, and sustainability factors. Results Eng 2025;27:106342. https://doi.org/10.1016/j.rineng.2025.106342.

[197] Zou W, Yu G, Du X. Energy and exergy analysis of photovoltaic thermal collectors: Comprehensive investigation of operating parameters in different dynamic models. Renew Energy 2024;221:119710. https://doi.org/10.1016/j.renene.2023.119710.

[198] Javadijam R, Shahverdian MH, Sohani A, Sayyaadi H. A 4E Comparative Study between BIPV and BIPVT Systems in Order to Achieve Zero-Energy Building in Cold Climate. Buildings 2023;13. https://doi.org/10.3390/buildings13123028.

[199] Battisti, Riccardo & Corrado A. Evaluation of Technical Improvements of Photovoltaic Systems Through Life Cycle Assessment Methodology. Energy 2005;30:952–67. https://doi.org/10.1016/j.energy.2004.07.011.

[200] Kun-Mo Lee, Atsushi Inaba. Life Cycle Assessment. 2004.

[201] Various Authors. SimaPro database manual. n.d.

[202] simapro n.d. https://simapro.com/.

[203] Ecoinvent n.d. https://ecoinvent.org/database/.

[204] Koley S. Sustainability appraisal of arsenic mitigation policy innovations in West Bengal, India. Infrastruct Asset Manag 2022;10:17–37. https://doi.org/10.1680/jinam.21.00021.

[205] Tripanagnostopoulos Y, Souliotis M, Battisti R, Corrado A. Energy, cost and LCA results of PV and hybrid PV/T solar systems. Prog Photovoltaics Res Appl 2005;13:235–50. https://doi.org/10.1002/pip.590.

[206] Hsu DD, O'Donoughue P, Fthenakis V, Heath GA, Kim HC, Sawyer P, et al. Life Cycle Greenhouse Gas Emissions of Crystalline Silicon Photovoltaic Electricity Generation:

Systematic Review and Harmonization. J Ind Ecol 2012;16:9290. https://doi.org/10.1111/j.1530-9290.2011.00439.x.

[207] Frischknecht R, Editors NJ, Althaus H-J, Bauer C, Doka G, Dones R, et al. Implementation of Life Cycle Impact Assessment Methods. Am Midl Nat 2007;150:1–151.

[208] Goedkoop M, Spriensma R. The Eco-indicator 99 - A damage oriented method for Life Cycle Impact Assessment. Assessment 2001:144.

भारतीय प्रौद्योगिकी संस्थान गुवाहाटी
Indian Institute of Technology Guwahati

LIST OF PUBLICATIONS

Journals

1. **Hazarika, P.,** Shyam, Kalita, P., & Gaur, A. (2025). Annual Energy Analysis of a Building-Integrated Semitransparent Photovoltaic Thermal Façade. Journal of Solar Energy Engineering, 147(3), 034501.

2. **Hazarika, P.,** Shyam, Kalita, P., & Gaur, A. (2026). Exergy, exergoeconomic and enviroeconomic analysis of a building integrated semitransparent photovoltaic/thermal (BiSPV/T) facade. International Journal of Ambient Energy.

3. **Hazarika, P.,** Shyam, Kalita, P., & Gaur, A. (2025). Exergetic Analysis and Life Cycle Assessment of a Semi-Transparent Building Integrated Photovoltaic Facade. Energy and Buildings. (*Under Review*)

Conferences Papers

1. **Hazarika, P.,** Shyam, Kalita, P., & Gaur, A. (2024, July). Exergy assessment of a semi-transparent building integrated photovoltaic facade for mild weather conditions of Srinagar. In IOP Conference Series: Earth and Environmental Science (Vol. 1372, No. 1, p. 012087). IOP Publishing.

2. **Hazarika, P**., Shyam, Kalita, P., & Gaur, A. Life Cycle Assessment of a Building Integrated Semitransparent Photovoltaic Thermal system: Effect on Environment. RIC Research and Industrial Conclave - Integration 2024, 09-11 August 2024 in IIT Guwahati, India, 2024.

Book Chapters

1. Kamble, A. D., Das, S., Vijaya, Das, B., Bordoloi, U., **Hazarika, P.**, & Kalita, P. (2024). Role of Solar Energy in the Development of the Indian Economy. In Challenges and Opportunities of Distributed Renewable Power (pp. 489-535). Singapore: Springer Nature Singapore.

2. Vijaya, Banik, R. K., Shanu, K., **Hazarika, P.**, Das, B., Duarah, P., & Kalita, P. (2025). A Comprehensive Review on Advances, Challenges, and Opportunities in Lithium-Ion Batteries for Hybrid and Electric Vehicles. Battery Electric Vehicles, E-Fuel Powered Hybrids and Fuel Cell Powertrains, 377-417.